

DESIGN AND CONSTRUCTION OF A PUMPED REFRIGERANT LOOP
FOR COMMERCIAL SCALE LOW-GWP REFRIGERANT
HEAT EXCHANGER TESTING

By

A B M IMRAN CHOWDHURY

Bachelor of Science in Mechanical Engineering

Bangladesh University of Engineering and Technology

Dhaka, Bangladesh

2017

Submitted to the Faculty of the
Graduate College of the
Oklahoma State University
in partial fulfillment of
the requirements for
the Degree of
MASTER OF SCIENCE
July, 2021

DESIGN AND CONSTRUCTION OF A PUMPED REFRIGERANT LOOP
FOR COMMERCIAL SCALE LOW-GWP REFRIGERANT
HEAT EXCHANGER TESTING

Thesis Approved:

Dr. Christian K. Bach

Thesis Advisor

Dr. Craig R. Bradshaw

Dr. Khaled A. Sallam

ACKNOWLEDGEMENTS

I want to begin by showing my utmost gratitude to Almighty. Belief in him has given me strength in every step of my life. This journey to graduate life in foreign country was certainly the toughest decision I made in my academic career. I could not have done it without the unconditional love and support from my family. Specially, I want to thank my loving mother who even took care of me by being thousands of miles away.

Dr. Christian Bach has been a true mentor to me throughout the master's program. I have learnt so much from his classes and my meetings with him. It is not only academic knowledge that I gained from him, but his guidance has also helped me to grow as a human being. I will always be grateful to him for the positive impact he has on me. I am proud to have him as my advisor.

I became friend with Khurram Makhani from the first semester when Dr. Bach assigned projects to both of us. Our projects are interrelated that made our coordination so crucial. He is a great independent researcher. I have learnt a lot from him and for that I cannot thank him enough.

During the building phase of my thesis project, I got acquaintance with Aaron Bell. The construction of my setup went smooth due to the expertise I got from him. He has helped me with brazing, PVC tubing and ideas I needed during the construction. I would like to thank him for his unequivocal effort to this project. I could not have finished the project without him. I would also like to express my gratitude to Gary Thacker who has assisted my project with his electrical expertise.

I am grateful to the UGTAs who have helped me throughout the project timeline. A special thank you to Joaquin Rodriguez and Simon Devlin for their assistance with the data acquisition.

I would also like to thank the BETSRG members. They were always there when I needed their assistance. Specially I want to thank Saad Saleem and Abraham Lee who helped me on numerous occasions with their experimental knowledge and support.

I also want to acknowledge the donations from Danfoss and Warrender. Their donated equipment are at the center of my experimental setup. Their support and donations have saved a lot of time and effort from my side.

Name: A B M IMRAN CHOWDHURY

Date of Degree: JULY, 2021

Title of Study: DESIGN AND CONSTRUCTION OF A PUMPED REFRIGERANT LOOP FOR
COMMERCIAL SCALE LOW-GWP REFRIGERANT HEAT EXCHANGER
TESTING

Major Field: MECHANICAL AND AEROSPACE ENGINEERING

Abstract: A pumped refrigerant loop for refrigerant conditioning is developed to allow testing of heat exchangers using a wide range of refrigerants, including low global warming potential refrigerants. The pumped refrigerant loop can be connected to the tested heat exchanger within the OSU Psychrometric Coil Testing Facility. The pumped refrigerant loop provides refrigerant for a range of temperatures including for comfort cooling conditions at around 12°C and high temperature refrigeration applications at about 1°C. Depending on refrigerant temperature and quality, the maximum cooling capacity for the tested heat exchanger varies from 4 to 12 tons. The pumped refrigerant loop allows fine control of the flowrate within an anticipated 1% of flow and 1.5% of inlet quality to the tested heat exchanger. A secondary pumped glycol loop uses 40 kW of electric heat to control the refrigerant subcooling and quality – or alternatively can be used as an 11+_ton heat source if the tested coil is a condenser. This secondary loop can additionally be used for hydronic coil testing in the Coil Testing Facility. This thesis presents the development of a steady state model for the pumped refrigerant loop. That model is then used with specific design conditions for sizing and selection of components. This thesis additionally presents the development of other subsystems including data acquisition, control system, and safety circuit. An appendix provides numerous annotated pictures of the construction of the setup.

TABLE OF CONTENTS

Chapter	Page
I. INTRODUCTION.....	1
1.1. Background	2
1.2. Literature Review.....	2
1.3. Project Objectives	7
II. PUMPED REFRIGERANT LOOP DESIGN	8
2.1. Concept of Pumped Refrigerant Loop	8
2.2. Modes of Operations	10
III. MODEL DEVELOPMENT	15
3.1. Design Conditions and Constraints	15
3.2. Thermodynamic Model.....	17
3.3. Simulation Plan	18
IV. SELECTION OF COMPONENTS	22
4.1. Refrigerant Loop Components.....	22
4.2. Glycol Loop Components	30
V. INSTRUMENTATION, CONTROL AND SAFETY	35
5.1. Instrumentation	35
5.2. Control	39
5.3. Safety	47
VI. CONCLUSION AND FUTURE WORK	55
REFERENCES.....	57

Chapter	Page
APPENDICES	62
APPENDIX A: EES STEADY STATE MODEL	62
APPENDIX B: EXPERIMENTAL SETUP	67
APPENDIX C: REFRIGERANT FLOW DIRECTION.....	80
APPENDIX D: GLYCOL FLOW DIRECTION.....	88
APPENDIX E: SAFETY CIRCUIT AND NAMEPLATES	96

LIST OF TABLES

Table	Page
2.1. An overview of the operation modes of PRL.	10
3.1. Design conditions for tested HX.	16
3.2. Input variables for parametric study	19
3.3. Parametric table (air conditioning applications).	20
3.4. Parametric table (refrigerant applications).....	20
3.5. Ranges of variables found in parametric study.	21
4.1. Suction line sizing.....	29
4.2. Liquid line sizing.	30
4.3. Pre-evaporator in cooling mode.....	31
4.4. Pre-evaporator in heating mode (Load = 35.16 kW, Brine flow = 37.85 L/min)	31
4.5. Pressure drop calculation in glycol tube.	33
5.1. Information of pressure transducer.	36
5.2. Information of the three RTDs.....	36
5.3. Information of mass flow meter for both refrigerant and glycol.	37
5.4. cRIO pinout of PRL including measurement type and name.	38
5.5. Functions of blocks in the Modelica model	40
5.6. Characteristic properties of pump.	41
5.7. Performance parameter of PI controller for quality in dynamic model	45
5.8. Performance parameter of PI controller for mass flow rate.....	46
5.9. Specification of time delay relay.	47
5.10. Specification of DOM.....	48

Table	Page
5.11. Specification of bypass timer.....	48
5.12. Specification of relays.....	49
5.13. Low pressure cutout specifications.....	49
5.14. High pressure cutout specifications.....	49
5.15. Temperature switch specifications.....	50
5.16. Glycol flow switch specifications.....	50
5.17. Refrigerant flow switches.....	50
5.18. Abbreviation of the safety devices.....	53

LIST OF FIGURES

Figure	Page
2.1. Log(P)-h diagram with vapor compression refrigeration cycle (left), PRL (right).....	9
2.2. Schematic diagram of PRL containing both hydronic and refrigerant tested HX.	11
2.3. PRL in cooling mode (inactive components are shaded).....	12
2.4. PRL in heating mode (inactive components are shaded).....	13
2.5. PRL in hydronic mode (inactive components are shaded).....	14
3.1. Illustration of PRL processes in log(P)-h diagram.....	17
4.1. Illustration of design capacity selection.....	23
4.2. Cascade heat exchanger selection process.	25
4.3. Refrigerant pump curve for rotational speed of 1500 rpm.....	27
4.4. Illustration of the correction curve from Hydraulic institute.	27
4.5. Suction line capacities for R410A for different L copper tube diameters in inches.	29
4.6. Glycol pump curve compared with the system curve at maximum 3600 rpm.....	34
5.1. Pumped refrigerant loop model.	40
5.2. Quality vs time for different controller gains.....	45
5.3. Mass flow rate vs time for different controller gains.....	46
5.4. Safety circuit.....	52
A.1. Graphical user interface of the model.	65
A.2. The dynamic p-h diagram in the EES model.	66
B.1. North side view of the setup.....	67
B.2. South side view of the setup.....	68
B.3. East side view of the setup.....	69

Figure	Page
B.4. West side view of the setup.....	70
B.5. Pump subframe.....	71
B.6. Each corner of the pump subframe is vertically supported two 2" by 2" natural rubbers.....	72
B.7. Refrigerant pump mounted on two pieces of unistrut that are part of the pump subframe	72
B.8. Glycol pump mounted on two pieces of unistrut that are part of the pump subframe	73
B.9. HX attached to the Unistrut of the structure with aluminum bar and rubber on both sides ...	74
B.10. Heater mounted on the structure with a vertical unistrut	75
B 11. Glycol filter mounted on the railing of the mezzanine in top of the wind tunnel	76
B.12. Refrigerant strainer mounted with clamp on a unistrut.....	77
B.13. Refrigerant mass flow meter mounted with clamps	78
B.14. Transmitter of the mass flow meter mounted on the structure	78
B.15. Glycol expansion tank mounted on the structure with bracket	79
C.1. Flow direction to the inlet of the pre-evaporator.....	80
C.2. Flow from the pre-evaporator to the cascade condenser through intermediate valve.	81
C.3. Flow from the pre-evaporator to the condenser and the bypass.....	82
C.4. Flow to the inlet of the cascade condenser.....	83
C.5. Flow from the cascade condenser to the strainer.....	84
C.6. Flow from the strainer to the pump.....	85
C.7. Flow from pump to mass flow meter with pressure relief in between.	86
C.8. Flow to and from the mass flow meter.....	87
E.1. Safety circuit.....	96
E.2. Refrigerant pump's nameplate.	97
E.3. Refrigerant motor's nameplate.....	97
E.4. Glycols pump nameplate.	98
E.5. Glycol motor nameplate.	98

Figure	Page
E.6. Mass flow meter nameplate.....	99
E.7. Mass flow transmitter nameplate.....	99
E.8. Heater nameplate.....	100
E.9. Pre-evaporator nameplate.....	101
E.10. Cascade condenser nameplate.....	102

ABBREVIATIONS

CFC	Chlorofluorocarbon
DX	Direct Expansion
DOM	Delay on Make
EES	Engineering Equation Solver
GFS	Glycol Flow Switch
GWP	Global Warming Potential
HCFC	Hydrochlorofluorocarbon
HFC	Hydrofluorocarbon
HGBC	Hot Gas Bypass Chiller
HMX	Heat and Mass Heat Exchanger
HX	Heat Exchanger
LV	LabVIEW input
OSU	Oklahoma State University
PI	Proportional Integral
PID	Proportional Integral Derivative
PRL	Pumped Refrigerant Loop
RFS	Refrigerant Flow Switch
RTD	Resistance Temperature Detector
SCR	Silicon Controlled Rectifier
TEWI	Total Equivalent Warming Impact
UN	United Nations
VFD	Variable Frequency Drive
VI	Virtual Instrument

CHAPTER I

INTRODUCTION

Heating, ventilation and air conditioning system or HVAC is responsible to condition the indoor air temperature and humidity. Air can be conditioned by more than one way including evaporative cooling, vapor compression or absorption. Systems using vapor compression cycles are the prominent ones where refrigerants are used to control the air properties. Initially, Chlorofluorocarbon (CFC) refrigerants were used in this kind of system, but these refrigerants were found to deplete the ozone layer. CFC were replaced by Hydrochlorofluorocarbon (HCFC) and Hydrofluorocarbon (HFC). These refrigerants have high global warming potential (GWP), responsible for getting the environment warmer. A movement of environmental conservatist groups has been urging for reducing the usage of HFCs. In response, the Montreal protocol (UNEP, 2020) was adopted as an international agreement. It requires that HFC need to be reduced by 85% from 2019 to late 2040s. Alternative refrigerants with low GWP including Carbon dioxide, ammonia, and R152a should be tested. Also, due to worldwide use of vapor compression system in HVAC, energy efficiency of this cycle is an important topic of concern which can save a lot of energy. Heat exchangers (HXs) are a key component that can reduce the energy consumption of HVAC systems. To test HXs and refrigerants and evaluate their performance, a large project is underway in Oklahoma State University to build a research facility “The Psychometric Coil Testing Facility”.

1.1 Background

The psychometric coil testing facility will enable OSU to test heat exchangers having a capacity of up to 20 tons and will also have a wide range of operating conditions. It will also allow to evaluate the performance of the more recent low GWP refrigerants. The facility has a closed loop air circulation system which consists of two sections. The conditioning sections utilizes different components like humidifier, heater, conditioning coils and blowers. This section creates an air flow with properties that are needed for a particular test. The test section includes inlet and outlet temperature and humidity measurements and allows to mount heat exchangers with a face area of up to 7 ft by 8 ft.

The tested HX will be connected to pumped refrigerant loop (PRL) rather than a regular vapor compression cycle because, unlike the PRL, a regular refrigeration cycle is limited to one refrigerant. In a vapor compression refrigeration cycle, various oils are used in the compressor for different refrigerants. The oil needs to be flushed out when refrigerant is changed. Also, one compressor is not suitable for variety of refrigerants. It makes the use of different refrigerants unpractical and costly. The pumped refrigerant loop will make it possible to cost-effectively conduct experiments with numerous refrigerants including the low GWP refrigerants. The PRL is the focus of this thesis. The PRL will consist of two loops i.e., a refrigerant loop, and a glycol loop. A hot gas bypass chiller provides cooling capacity to the PRL.

1.2 Literature Review

Over the years numerous studies have been carried out to investigate the heat exchanger performance and environmentally friendly refrigerants. Researchers have been employing varying methods in their experiments. A striking similarity among many of these experiments is the adoption of pumped refrigerant loop for substantial control. The pumped loop, this thesis trying to implement```` is also for the same purpose which is ease of operation, but the application and scale

of the setup will be commercial. To support commercial scale testing of heat exchangers of varying kinds with a capacity up to 20 tons and possible future environmentally friendly refrigerants, the pumped loop is designed to be very flexible and robust. This section will briefly discuss literature on some of the low-GWP refrigerants and applications involving pumped loops.

1.2.1 Refrigerants with Reduced Environmental Impact

The performance of low GWP refrigerants is measured based on their heat transfer, pressure drop, flammability, volumetric efficiency and energy consumption. Jacob *et al.* (2019) investigated the local heat transfer coefficients and pressure drop of R450A relative to R134a. R450A is a zeotropic mixture of R134a and R1234ze (42/58% by mass) which is nonflammable. In primary refrigerant loop, they used positive displacement pump, cooler and evaporator to condition the refrigerant. The heat transfer coefficient was 5% lower than R134a and pressure drop was 8% higher. Longo *et al.* (2019) experimented on the boiling heat transfer coefficient and frictional pressure drop of two low GWP refrigerants: R1234ze(Z) and R1233zd(E). They used a variable speed pump to circulate the refrigerant. The boiling heat transfer was higher and frictional pressure drop was lower for R1234ze(Z) than R1233zd(E). Yu *et al.* (2021) investigated 34 refrigerant mixtures to find alternative of R410A which have low GWP and mild flammability. Four of the mixtures, found close to the performance of R410A are R32/R1123/R161/R131I (20/40/10/30), R1123/R161/R131I (65/5/30), R1123/R152a/R131I (65/5/30) and R1123/R1234ze(E)/R131I (65/5/30). It was mentioned that further experiment are necessary to establish their applicability. Mateu-Royo *et al.* (2021) provided a comparative analysis of low GWP refrigerants; R1234ze(E) and R515B to replace R134a. R1234ze(E) and R515B have around 25% lower heating capacity than R134a due to reduced latent heat of vaporization and suction density. These refrigerants can reduce total equivalent warming impact (TEWI) by 15% compared to R134a. TEWI is an index to compare the global warming effects of alternative conditioning systems. R515B meets better safety regulations as it is nonflammable. Llopis *et al.* (2019) experimentally evaluated the alternatives of R404A for

commercial refrigeration system. These substitute refrigerants are R454C, R459B, R457A and R455A as R404A. It is found that these low GWP refrigerants provide reduced charge and energy consumption. Cabello *et al.* (2021) experimentally analyzed the energy consumption of low GWP blend R468A compared to R404A in a commercial refrigerant plant. R468A exhibits an increase in compressor discharge temperature, larger operation time and similar energy consumption.

The pumped refrigerant loop will facilitate performance test of refrigerants and heat exchangers and will help to validate any claims related to refrigerants by vigorous experiments in combination with the psychometric coil testing facility.

1.2.2 Application of Pumped Loop

Pumped loops have unique advantages in various research and measurement applications, including testing numerous heat exchangers and various refrigerants. Some examples of their applications are presented in this subsection.

Several studies had been completed on evaporators and/or condensers using pumped loops. Some of these studies focused on oil retention in microchannel type evaporators and condensers and their effects on heat transfer rate and pressure drop. Yatim *et al.* (2016) experimented on a microchannel condenser with refrigerants R410A and R134a to investigate oil retention in the tested heat exchangers. They developed a pump-boiler loop type setup for this experiment. The three-systems setup included one main refrigeration loop. A variable speed gear pump was used to pump refrigerant through the loop allowing for precise refrigerant flow control. Cremaschi *et al.* (2018) conducted a similar experiment on evaporators of air-source heat pump systems. They measured the effects of oil retention on evaporator heat transfer capacity and refrigerant side pressure drop. The same pump-boiler type closed loop refrigeration system as in Yatim *et al.* (2016) experiment was utilized.

Pumped loops also have been used for frosting experiments. Lee *et al.* (2010) experimented on the air-side heat transfer characteristics of flat plate finned-tube heat exchangers under frosting conditions. They used a duct-like test section for the air flow. To create frost on heat exchangers, ethylene glycol-water mixture was used as secondary fluid. The mixture was circulated through the loop by a magnetic gear pump. Hrnjak *et al.* (2017) investigated the effect of louver angle on the performance of micro channel heat exchangers with serpentine fins and flat tubes during periodic frosting conditions. Their topics of interest were air side pressure drop and over all heat transfer coefficient. They used a pumped loop to pump the ethyl alcohol (refrigerant) and a wind tunnel with desired air flow.

Huang *et al.* (2020) conducted a research on the thermal and hydraulic characteristics of a bare tube heat exchangers under dry and wet air-side conditions. The water loop of the heat exchangers includes gear pump with variable speed. The wind tunnel was closed loop containing air handling unit to control the air temperature and humidity. Yi *et al.* (2020) tried to increase heat transfer by experimenting on a detachable plate type film heat and mass exchanger (HMX) using lithium bromide and water as working fluid. Two conditions were explored, generator-condenser condition and absorber-evaporator condition. They also utilized pumped loop to evaluate the performance. Hu *et al.* (2020) did similar kind of experiment on absorption heat exchanger. The HX consists of a multi section absorption heat transformer and a plate HX. Similarly, they pumped the working fluid. Redo *et al.* (2020) tried to improve the flow distribution of two-phase flow in vertical header with dual compartment of micro channel heat exchangers. To create the desired condition of real air conditioning unit, they utilized a magnetically driven centrifugal pump, control valve. Bell and Groll (2011) experimentally analyzed the effects of particulate fouling on hybrid heat exchangers and air side pressure drop of a hybrid dry cooler. Their setup included a wind tunnel for air flow and a pumped water loop to supply water to the tested heat exchanger. Bell and Groll (2011) tested on both plate-fin HX and micro channel heat exchanger.

Pumped loops have also been used in experiments for generation of model validation data. Lee *et al.* (2003) developed a program to analyze a fin and tube evaporator containing zeotropic mixture refrigerant with air maldistribution. They used a secondary pumped cooling water loop including pump, bypass loop, and motor driven micro valve to control the subcooling of the refrigerant in the main loop at the inlet of the distributor. Li and Hrnjak (2021) brought up the issue of maldistribution in parallel channel of plate heat exchangers. They validate their numerical analysis of single-phase flow distribution in brazed plate heat exchangers. Their setup consisted of two water loops; hot side, cold side and single-phase water closed loop. All loops were run by separate centrifugal pumps. Sarfraz (2020) at Oklahoma State University experimented on fin-and-tube heat exchangers for single phase and two-phase flow. He developed two models, Xfin model and Fin discretized model to account cross fin conduction. The facility used to validate the models, consists of air and refrigerant sides. The air side consists of a psychometric chamber in which the air is conditioned with desired properties. The chamber is comprised of heaters, humidifier, and cooling coil with other necessary equipment. The refrigerant loop designed by Saleem *et al.* (2020) consists of refrigerant pump, heat pump to provide cooling capacity and hot water loop to provide quality control at inlet of tested heat exchanger.

The secondary refrigeration loop (SL) is getting popular in commercial and industrial applications. Kruse (2000) showed that energy consumption can be reduced by using CO₂ as secondary refrigerant. Kauffeld (2008) studied the supermarket refrigeration and made a comparison between indirect distributed cascade and two stage refrigeration system. The SL showed improved efficiency compared to direct expansion (DX) system in Kauffeld's study. According to Delventura *et al.* (2007), the refrigerant emissions are one sixth of direct expansion (DX) system.

Kazachki and Hinde (2006) showed that SL system has two advantages over DX system: short liquid refrigerant supply line and short vapor refrigerant return line. They also compared the energy consumption of DX and SL system in the USA for different climates. It was shown that annual

energy consumption of SL systems is lower than for DX systems by 6.6 to 8.2%. A comparison study can be done on the PRL and vapor compression cycle to investigate the energy consumption, efficiency and future prospect of pumped loop in HVAC applications.

1.3 Project Objectives

The objective of the thesis is to design and construct a pumped loop as an alternative to the vapor compression cycle to connect the tested heat exchanger in the psychometric coil testing facility. Initially, a model needs to be developed for the PRL. This model will be developed based on some specific testing criteria. Key variables would be identified, and their range would be measured for all possible experimental conditions. The components will be sized and selected for the construction to begin. Data acquisition and control need to be implemented along with safety features.

CHAPTER II

PUMPED REFRIGERANT LOOP DESIGN

The main feature of the pumped refrigerant loop is the absence of the compressor. A centrifugal pump will replace the compressor. Due to the nonexistent compressor, the pumped loop will not be an independent cycle. The loop depends on other cycles or loop for providing cooling capacity. The following sections will describe the concept of the pumped refrigerant loop and different ways to utilize the design.

2.1 Concept of Pumped Refrigerant Loop

The main objective of the pumped refrigerant loop is to replicate the inlet conditions of the evaporator of a vapor compression refrigeration cycle. The reason is that the tested heat exchanger or the refrigerants will end up in a refrigerant system which incorporates vapor compression cycle. PRL presents an easy way of testing with wide range of refrigerants. The operating conditions for the loops design are adopted from AHRI Standard 540 (AHRI, 2015). Based on the standards evaporator dew point temperature, superheat and quality at inlet, the other components - condenser, pre-evaporator and pump were incorporated into the model. Although the model is based on evaporator condition, the condenser capacity dictates other parameters. Figure 2.1 on next page shows the comparison between the p-h diagram of an actual compression cycle and the pumped refrigerant loop.

In Figure 2.1 (left), it shows the p-h diagram of a vapor compression cycle. State point 1 is the inlet and state point 2 is the outlet of evaporator (tested coil/ HX). In the pumped loop in Figure 2.1

(right) these two state points remain constant and are equivalent to the state points 1 & 2 in pumped loop. A pump is used between state points 4 & 5 to compensate for system pressure drop.

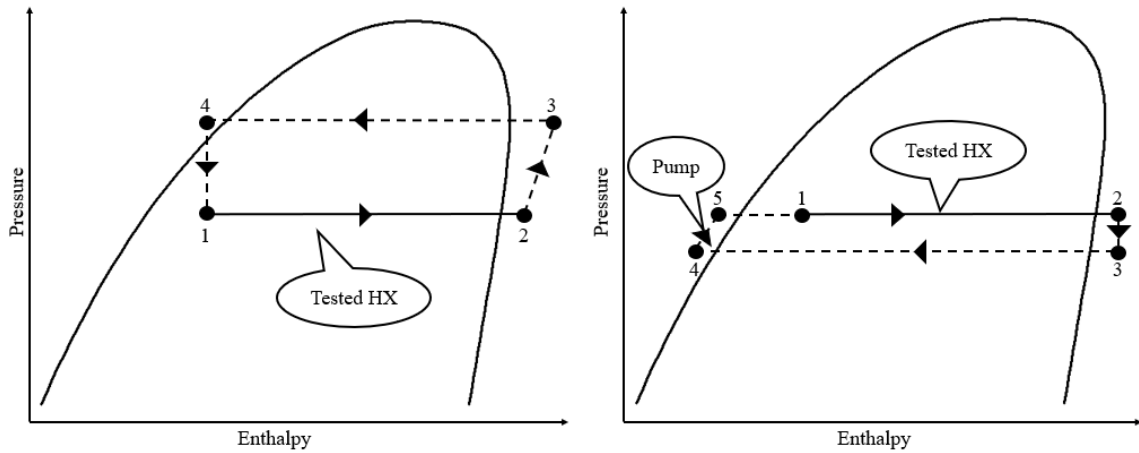


Figure 2.1: Log(P)-h diagram with vapor compression refrigeration cycle (left), PRL (right).

In a regular vapor compression cycle, refrigerant gets vaporized by heat addition in evaporator. Single phase vapor is then compressed in compressor. As a result, pressure and temperature increases and vapor refrigerant release this heat in condenser and convert to liquid. In the expansion valve, the pressure is reduced, and liquid refrigerant enters the two-phase region. This is an independent cycle where the work is done by compressor.

In the pumped loop, the evaporator works same as compression cycle but after that the single-phase vapor enters the condenser instead of a compressor. Refrigerant condenses to liquid in the condenser which is also the evaporator for hot gas bypass chiller. The condenser in pumped loop is on the lower pressure side opposite to the condenser of compression cycle. The liquid single-phase refrigerant is then pumped by the pump to desired higher pressure. A pre-evaporator is used in the pumped refrigerant loop to control the inlet quality of refrigerant to the evaporator. The pre-evaporator provides heating capacity to the pumped refrigerant loop. Another pumped loop which contains glycol is attached to the Pre-evaporator on the other side. This loop contains a pump and a heater which heats the glycol to a desired temperature. This glycol passes through the evaporator and transfers heat to the refrigerant. The rotational speed of the pump and the heat input in heater

is controlled to have control over the heat transfer to the refrigerant so that it has the desired inlet properties before the refrigerant enters the tested coil/ HX.

2.2 Modes of Operations

The pumped loop is mainly designed keeping in mind the cooling mode (the tested HX will act as an evaporator) because the design process is the most critical for this mode, but the mode of the tested HX can be changed based on the type of experiments conducted. The loop can also run in heating mode (the tested HX will act as a condenser). Due to the current circumstances another mode is added to the experimental setup at present. The tested HX that is present in the wind tunnel when writing this paper is a hydronic HX. To accommodate the tested HX the glycol loop is extended, and it included the tested HX in the loop. Figure 2.2 shows a schematic diagram of the pumped refrigerant loop. Figure 2.3, Figure 2.4 and Figure 2.5 show the schematic diagram of the PRL in different operation modes. An overview is given in Table 2.1 to describe their operation briefly.

Table 2.1: An overview of the operation modes of PRL.

Figures	Modes	Overview
Figure 2.3	Cooling mode	Heater heats up glycol. Glycol transfers heat to refrigerant through pre-evaporator controlling quality at inlet of tested HX. After tested HX, refrigerant vapor gets condensed in cascade condenser with the help of chiller. Condensed refrigerant is pumped back to pre-evaporator.
Figure 2.4	Heating mode	Glycol loop operates same way as cooling mode. In refrigerant loop, pre-evaporator functions as evaporator and tested HX acts as condenser. The cascade condenser sits idle and bypassed by refrigerant.
Figure 2.5	Hydronic mode	Hydronic HX is connected to Glycol loop through valve 2 and 3. Without the presence of refrigerant tested HX, Pre-evaporator is connected to condenser through valve 6 and valve 7.

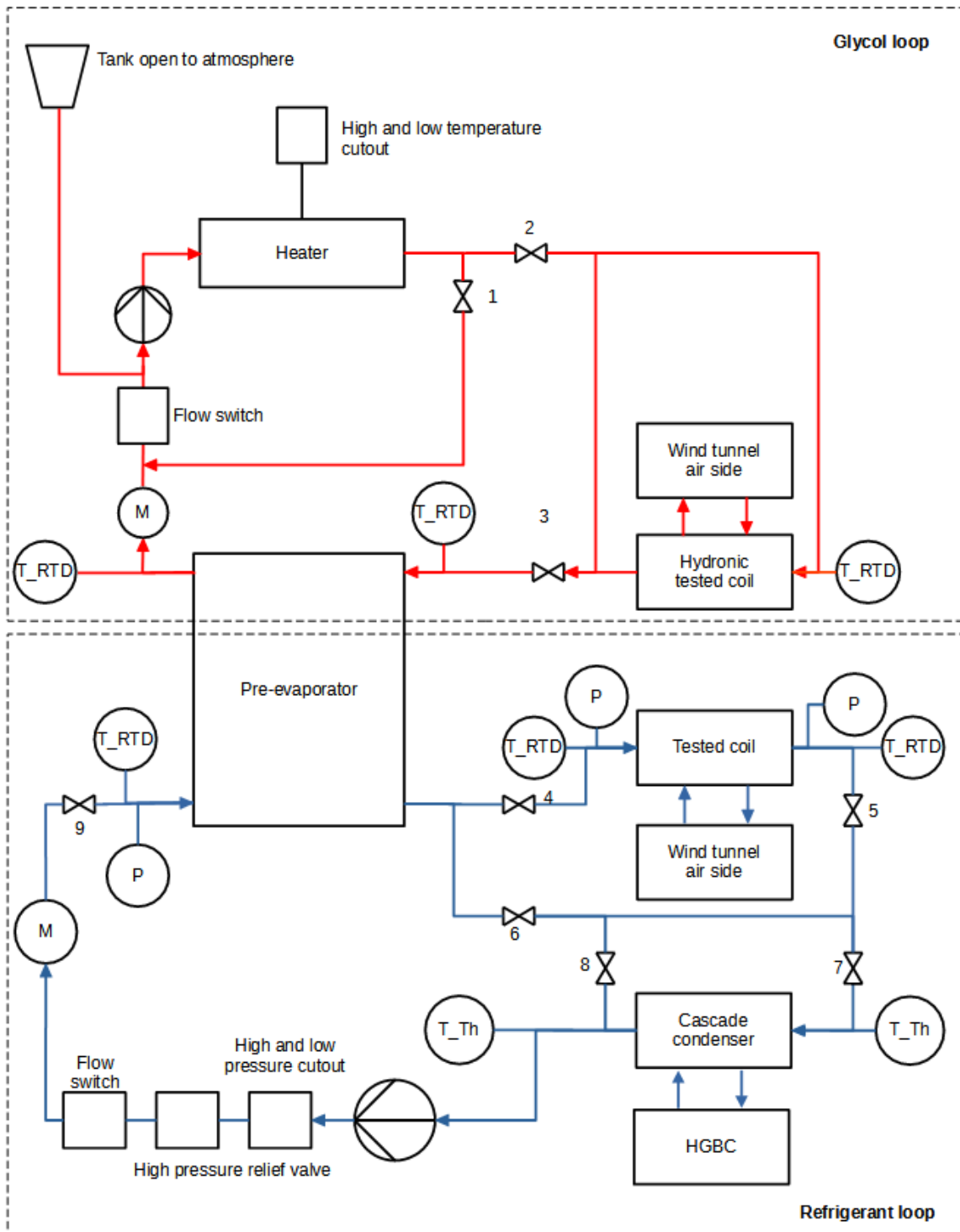


Figure 2.2: Schematic diagram of PRL containing both hydronic and refrigerant tested HX.

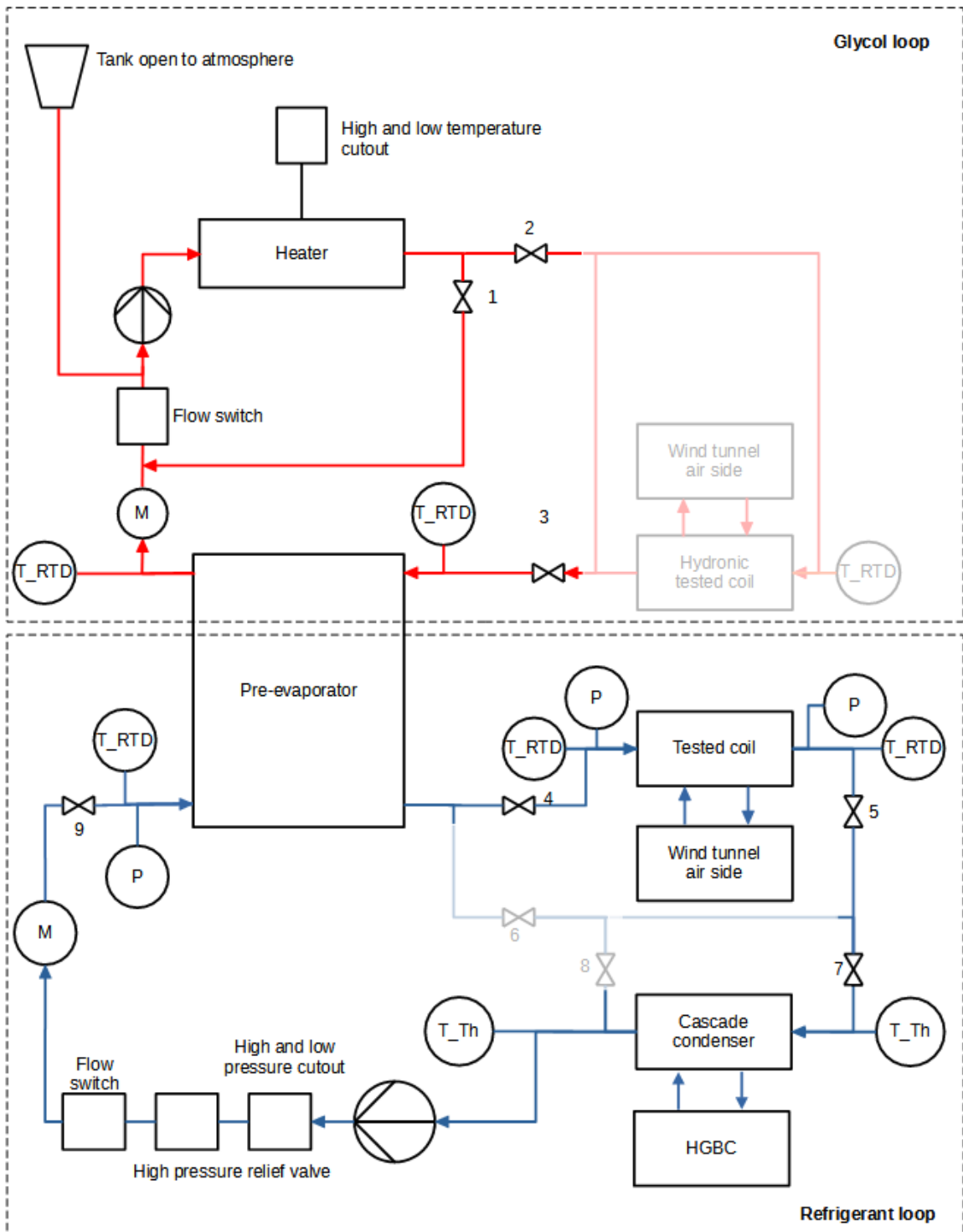


Figure 2.3: PRL in cooling mode (inactive components are shaded).

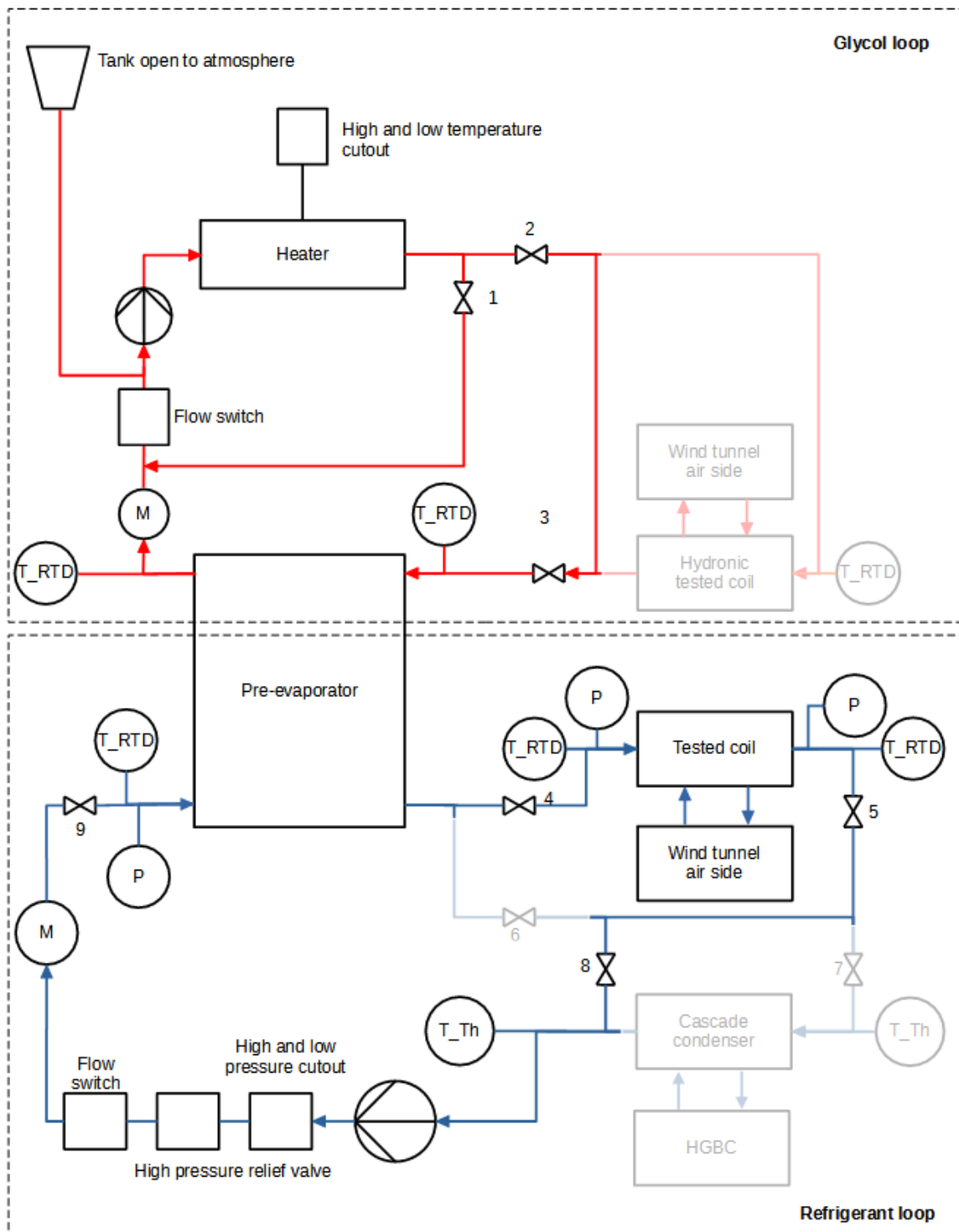


Figure 2.4: PRL in heating mode (inactive components are shaded).

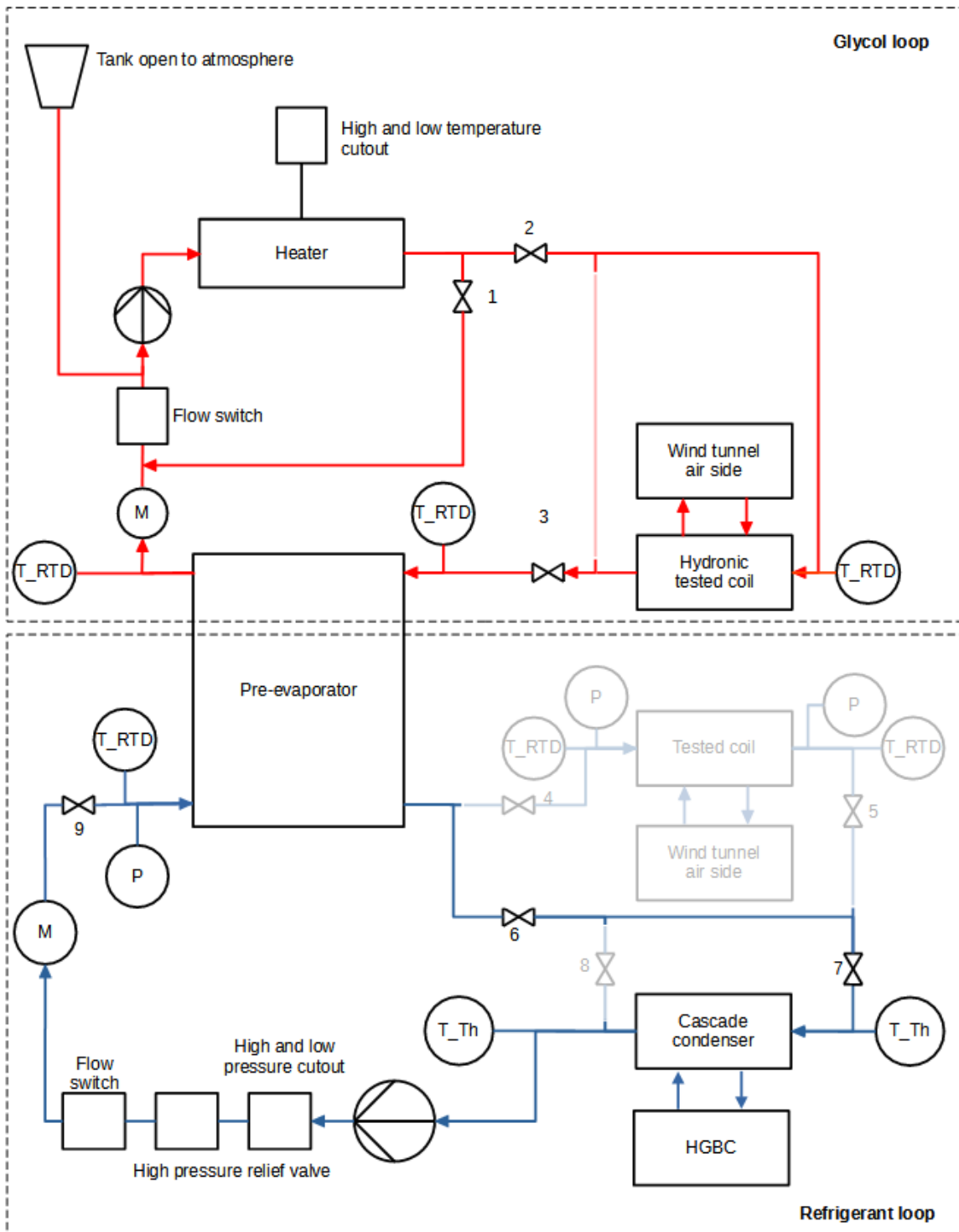


Figure 2.5: PRL in hydronic mode (inactive components are shaded).

CHAPTER III

MODEL DEVELOPMENT

The purpose of developing a thermodynamic model is to determine the size and the capacity of the components needed to build the setup. A model has been developed in Engineering Equation Solver (EES), Klein (2020). EES was chosen because of its readily available access to thermodynamic properties of numerous working fluids. The model development process followed certain steps. A design condition was chosen at first. There is no specific standard for refrigerant testing conditions like AHRI Standard 210/240 (AHRI, 2017) for performance rating of unitary air conditioning equipment and air source heat pump equipment. AHRI Standard 540 (AHRI, 2015) for performance rating of positive displacement compressors was picked for refrigerant testing as it provides standardized conditions of refrigerants like suction dew point temperature, discharge dew point temperature, subcooling, superheating etc. These properties act as references upon which the model was developed. The next step was to identify design constraints as it is a dependent loop. Following step is the actual development of the model which follows properties of refrigerants from one state point to the next. A simulation plan was conducted to identify the range of key variables for the purpose of component sizing.

3.1 Design Conditions and Constraints

Two rated conditions have been identified from AHRI Standard 540 (AHRI, 2015) for the cooling mode of HX which can be seen from Table 3.1. The evaporator dew point temperature represents

the temperature of the tested HX. Though there is no compressor in the setup, compressor discharge dew point temperature and subcooling from the table help to identify the inlet state point of evaporator.

Table 3.1: Design conditions for tested HX.

Design Conditions	Evaporator Dew Point Temperature (°C)	Superheat Temperature (°C)	Compressor Discharge Dew Point Temperature (°C)	Subcooling (K)
1 - air conditioning applications	7.2	18	54.4	8.3
2 - refrigerant applications	-6.7	4.4	48.9	0

One design constraint is pressure drop in evaporator. As no data is available of the kind of heat exchangers for testing, a pressure drop of 10 psi was assumed (Bowling, 2019) in evaporator to make the model simple. A subcooling of 5 K was fixed when the refrigerant condenses in cascade condenser. As the pumped loop is not an independent loop, it depends on Hot Gas Bypass Chiller (HGBC), Makhani (2020) to provide the cooling capacity when the PRL is running on cooling mode (tested HX acting as evaporator). The capacity from the HGBC needs to be adjusted manually to satisfy the cooling needs for the PRL.

For the two conditions above, if the tested HX is in cooling mode, some assumptions were made based on the lab environment and heat transfer. The temperature for lab chilled water is assumed as 70°F/21.1°C. To have a temperature difference of at least 10°C, the dew point temperature in cascade Condenser (HGBC) is assumed as 32°C as it was the closest condensing temperature tabulated in the rating conditions of the compressor in HGBC. As the saturation temperature in Condenser (PRL) is 7.2/-6.7°C, the temperature in evaporator (HGBC) is assumed -3/-18°C respectively (to keep around 10°C temperature difference).

By an iterative method between EES model and Hexact (Danfoss, 2018) the capacities were determined. When PRL is in cooling mode, the capacity found for the design condition 1 was 58.2 kw and for design condition 2 the capacity was found to be 32.5 kw. The capacity determination process will be discussed in detail in section 4.1.1. Heating mode was not considered for capacity calculation because it depends on the air side flow condition and the heater in glycol loop. The heater at present has a capacity of 40 kW. So, the maximum capacity can be obtained in heating mode (tested HX acting as condenser) is 40 kW and the pump power input.

3.2 Thermodynamic Model

The thermodynamic model revolves around the state point properties of refrigerants in the loop. The model is based on the given design condition provided in section 3.1. It also considers the design constraints needed for calculation. The PH diagram of PRL model is showed in Figure 3.1.

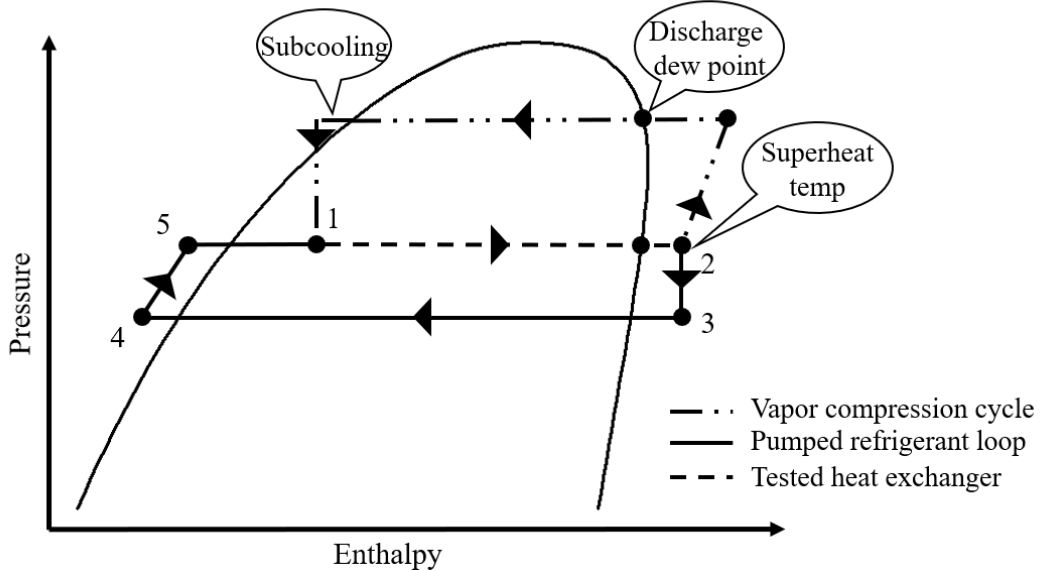


Figure 3.1: Illustration of PRL processes in log(P)-h diagram.

The evaporator dew point temperature from Table 3.1 is set as the dew point temperature for the test coil. Pressure in test coil is identified from the dew point temperature and quality of 1 (saturated vapor). The state point 2 is set to be the superheat temperature from the same table. 10 psi of

pressure drop was fixed in the test coil between state point 1 and 2 as the test coil model as per assumption. There is no pressure drop assumed from state point 2 to state point 3 as we did not have any data about the length of the pipe from test coil outlet to condenser inlet. Also, the inlet and outlet of condenser have zero pressure drop because the condenser has very low pressure drop. To identify state point 4, the dew point temperature was first calculated from the pressure of state point 3 and assuming quality of saturated vapor or liquid and then 5 K of subcooling was implemented. State point 4 to 5 represents the inlet and outlet of pump. A centrifugal pump of 90% efficiency was considered here. State point 1 is in two-phase region.

The state point 1 was calculated by assuming an ideal vapor compression cycle by considering the discharge dew point temperature and subcooling from Table 3.1. All the parameters in Table 3.1 was used to find the outlet point of the imaginary expansion valve of the ideal refrigeration cycle which is the inlet of the test coil or state point 1.

3.3 Simulation Plan

The purpose of the simulation plan was to observe the system by factoring in the conditions discussed before and by considering varieties of existing refrigerants in use that might be used as working fluid or their analogous newer more environmentally friendly refrigerants for future experiments so that the components in system can be sized properly. The variables were identified for the simulation plan and then a parametric study was conducted.

3.3.1 Input Variables and Parametric Study

Among the variables that were considered as inputs for parametric study are refrigerant, evaporator dew point temperature, superheated vapor temperature at outlet of tested HX and condenser capacity for both cooling and heating mode. These inputs are shown in Table 3.2.

Table 3.2: Input variables for parametric study

Variable name	Values
Refrigerants	R410A, R404A, R407C, R134a, R502, R22, R744
Evaporator dew point temperature	7.2 °C, -6.7 °C
Evaporator outlet temperature	18 °C, 4.4 °C
Condenser capacity	58.2 kW, 32.5 kW

3.3.2 Parametric Study and Analysis

A parametric study and analysis are used for component sizing. The study allowed to understand behavior of the variables under investigation. Their range of change under different circumstances would be used for component selection. The variables investigated in the parametric study are mass flow rate of the refrigerants, quality at inlet of the tested HX, high and low pressure in pumped loop, condenser dew point temperature and outlet temperature, capacity of tested coil and heat addition required for pre-evaporator because these variables are needed for measuring the components. The refrigerants were simulated for the two conditions listed in the Table 3.2. The results are listed in Table 3.3 and Table 3.4.

Table 3.3: Parametric table (air conditioning applications).

Refrigerant	Condenser dew point temp [°C]	Refrigerant mass flow rate [kg]	Quality [-]	High pressure [bar]	Low pressure [bar]	Test coil capacity [kW]	Heat addition in Pre-evaporator [kW]
R410A	7.02	0.25	0.3	10.95	9.22	39.75	18.42
R404A	6.95	0.33	0.36	8.47	7.45	36.24	21.92
R407C	6.91	0.25	0.27	6.85	5.83	40.94	17.24
R134a	6.76	0.28	0.26	4.74	3.72	40.74	17.44
R502	6.93	0.38	0.31	8.09	7.06	38.12	20.04
R22	6.91	0.27	0.23	7.22	6.2	43.06	15.71
R744	7.2	0.20	0.40	43.01	41.98	38.45	19.72

Table 3.4: Parametric table (refrigerant applications).

Refrigerant	Condenser dew point temp [°C]	Refrigerant mass flow rate [kg]	Quality [-]	High pressure [bar]	Low pressure [bar]	Test coil capacity [kW]	Heat addition in Pre-evaporator [kW]
R410A	-6.96	0.11	0.39	7.38	6.35	15.66	10.75
R404A	-7.044	0.14	0.47	5.79	4.77	13.62	12.79
R407C	-7.12	0.11	0.36	4.59	3.56	16.14	10.05
R134a	-7.34	0.12	0.35	3.25	2.23	15.96	10.23
R502	-7.07	0.16	0.42	5.6	4.57	14.19	11.59
R22	-7.11	0.12	0.31	4.95	3.93	17.34	8.86
R744	-6.7	0.12	0.40	30.1	29.06	19.11	13.37

The ranges that are observed for different output variables are tabulated in Table 3.5. These ranges will allow us to select refrigerant pump, heater, glycol pump, piping material and other.

Table 3.5: Ranges of variables found in parametric study.

Variables	Range of value
Mass flow rate (kg/s)	0.11 ~ 0.38
Quality at inlet (-)	0.23 ~ 0.47
Pressure (bar)	2.23 ~ 10.95
Heat addition in pre-evaporator (kW)	8.86 ~ 21.92

CHAPTER IV

SELECTION OF COMPONENTS

The pumped refrigerant loop consists of two dependent pumped loops: a refrigerant loop and a glycol loop. The component selection for both loops will be discussed in this section.

4.1 Refrigerant Loop Components

The major components in the refrigerant loop are tested HX, condenser, refrigerant pump, pipe and pre-evaporator. The pre-evaporator will be discussed in the glycol loop selection as it is a common component in both loops.

4.1.1 Cascade Heat Exchanger

The cascade heat exchanger acts as a condenser in the pumped refrigerant loop. A heat exchanger was selected from Danfoss (2021) using Hexact (Danfoss, 2018). Hexact has 3 different modes to choose a heat exchanger and test it for performance. It suggests micro plate heat exchanger and brazed plate heat exchanger. Micro plate heat exchanger would be used for the heat transfer from HGBC to PRL loop. The process of heat exchanger selection and capacity measurement for the design conditions went on hand in hand by an iterative method between the EES models of both PRL and HGBC with Hexact. In HGBC model, a condenser dew point temperature (HGBC) of almost 32°C was assumed to keep almost 10 K difference with the campus chilled water temperature as the chilled water temperature was around 21°C in the worst case. The chilled water temperature also changes depending on the season. Then, the evaporator dew point temperature of the HGBC was changed

iteratively to find the design capacity and the cascade heat exchanger for pumped loop. Figure 4.1 shows the process of how the design capacity is found when the heat transfer between refrigerants from PRL and HGBC matches the compressor capacity of the HGBC.

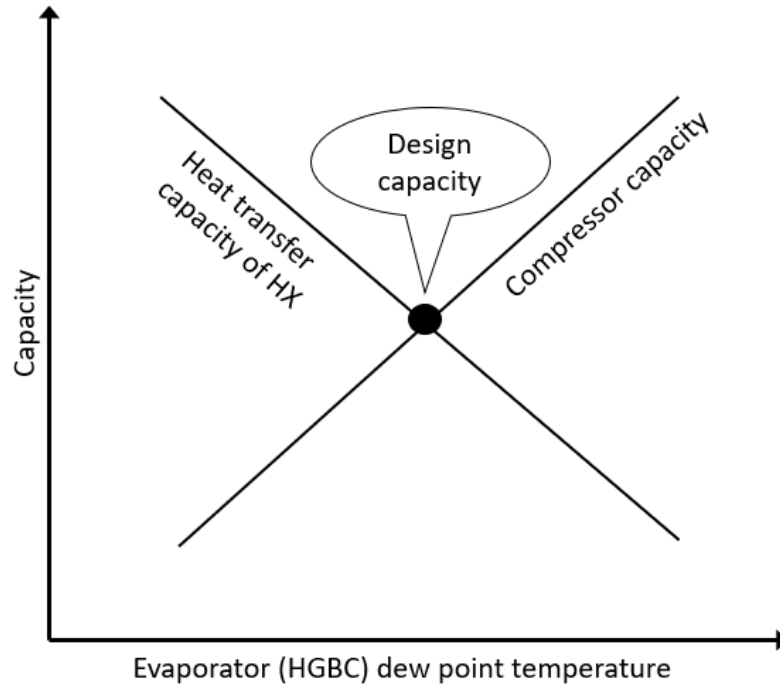


Figure 4.1: Illustration of design capacity selection.

In HGBC if the evaporator dew point increases, the compressor capacity increases but it reduces the heat transfer from condenser (PRL) to evaporator (HGBC) as the temperature difference decreases thus providing less cooling capacity to PRL. By this iterative method, the design cooling capacity was defined, and heat exchangers was selected. The whole selection process is shown in the flow chart, Figure 4.2.

One example will make the process clear to understand. For design condition 2, the evaporator dew point temperature is -6.7°C . As there is no pressure drop between the evaporator and the condenser in PRL, the condenser dew point temperature also should to be the same. On the HGBC side, at the beginning of the iteration process, an evaporator (HGBC) temperature of 23°C was assumed. The

EES model for HGBC provides a capacity of 26.42 kW. This chiller capacity is used in the PRL model in EES to find out the following parameters:

- Inlet quality for evaporator,
- Inlet temperature for condenser,
- Superheating on evaporator side,
- Subcooling on condenser side, and
- Maximum pressure drops in both sides.

These data along with the capacity provided by HGBC, refrigerants on both PRL and HGBC side, and dew point temperature during condensing in PRL and evaporating in HGBC are then used in Hexact. Hexact then provides the data of the condensing temperature in PRL. If the temperature matches the condenser design temperature of $-6.7\text{ }^{\circ}\text{C}$ within $\pm 0.01\%$, then the capacity would be selected but in this case the temperature found was $-11.96\text{ }^{\circ}\text{C}$. The evaporator (HGBC) temperature was increased, and the process was repeated. When an evaporator (HGBC) temperature of $-17.8\text{ }^{\circ}\text{C}$ was assumed, $-6.7\text{ }^{\circ}\text{C}$ was found for the PRL condenser. The capacity found for this case was 32.5 kw.

The process for finding a suitable heat exchanger for condensing is similar. The information from the EES models used as input in the design mode of Hexact. After processing the data, Hexact suggests one or more heat exchanger with specific plate number. In performance mode, the plate number can be changed to reduce or increase the pressure drop. From the performance mode, the inlet temperature, dew point temperature, outlet temperature and mass flowrate for both evaporator (HGBC) and condenser (PRL) were identified which then compared with the same parameters from the EES models. If the parameters do not match within 0.01%, the process is repeated till all the parameters match. C118L-E heat exchanger with 70 plate was selected as the cascade condenser as

it satisfied all conditions and variables. The theory of the process is showed graphically in Figure 4.2.

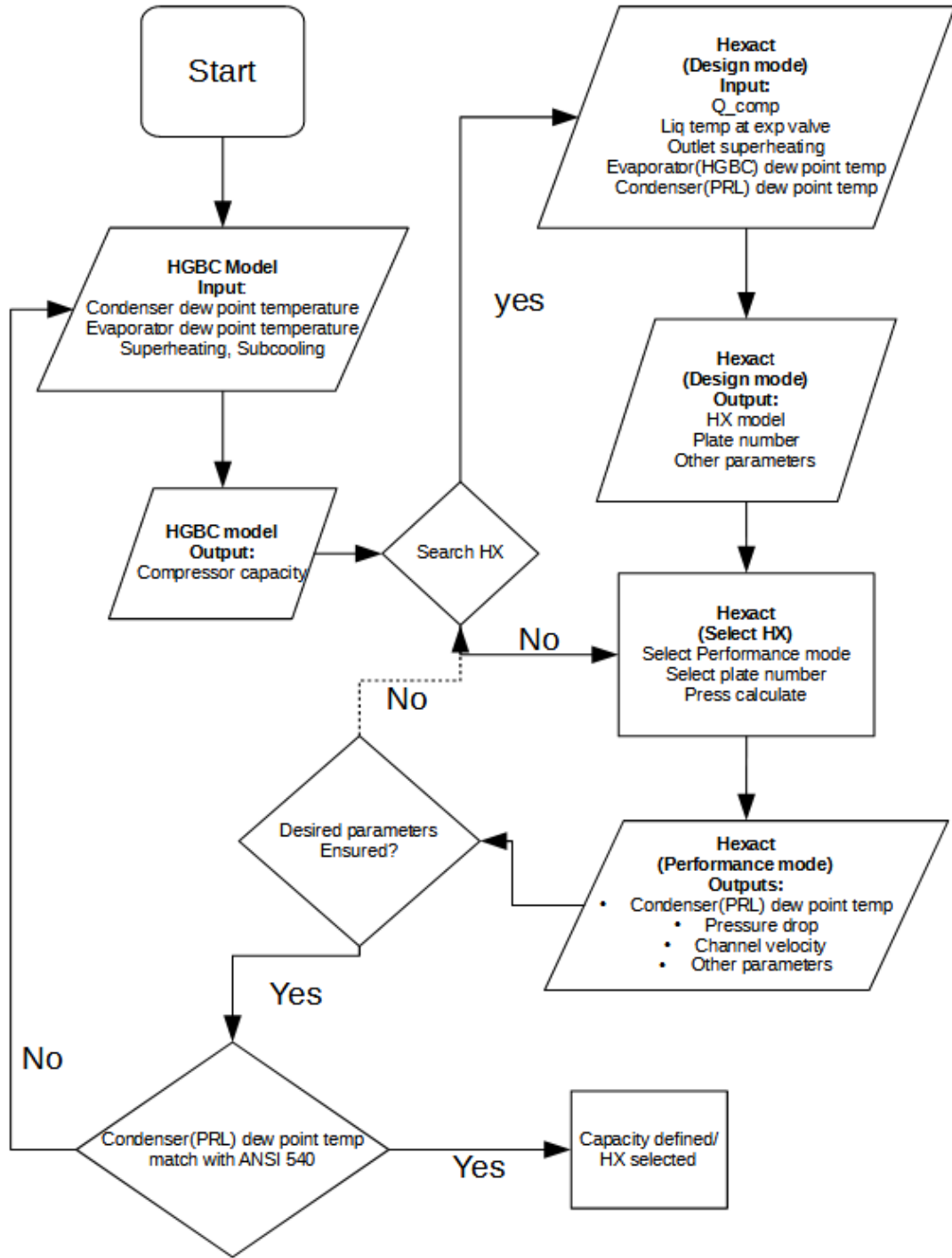


Figure 4.2: Cascade heat exchanger selection process.

4.1.2 Refrigerant Pump

Various parameters were needed to choose a pump that can have a wide performance range for wide range of refrigerants. As experiments will occur on two design conditions, both conditions were utilized to find the critical values. Different parameters with the range are provided below:

- Differential pressure head at inlet and exit: 15 psi
- Inlet pressure at pump: 47.34 psi to 610 psi
- Volumetric flow rate: 1.1 to 8.95 GPM
- Specific gravity: 0.8 to 1.5
- Temperature range: -20°C to 60°C
- Minimum net positive suction head: 9.98 ft

A regenerative turbine pump was selected based on the parameters because of its tolerance to low net positive suction head. In this case, WMTA6-LN-2S from Warrender (2021a) was the selected pump. Several pump curves were attained for the pump and the curve with lowest rotational speed found (1500 rpm) is shown in Figure 4.3. All the selected refrigerants flowrate was compared with the provided pump curve to ensure that the pump is compatible with the refrigerants for the specific design conditions. From Figure 4.3 it can be said that the required speed of the pump would be much lower to match the system required speed for the refrigerants. Two VFDs from ABB (ABB, 2021) have been obtained to control the speed of the pumps. The model number of the drives is model: ACH580). Another important aspect to be mentioned is the provided pump curve is for water circulation. So, the compatibility of the pump can be questioned with the refrigerants. Two factors are always considered when selecting a pump for any applications; specific gravity and viscosity. Specific gravity does not directly impact the pump performance. In case of centrifugal pump or regenerative turbine pump, the head and the flow are not influenced by specific gravity. Specific gravity is a term related to the weight of the fluid and it affects the work done by the pump. So, fluid of different specific gravity will require motors with different powers to handle the load, but the head and flow should remain same.

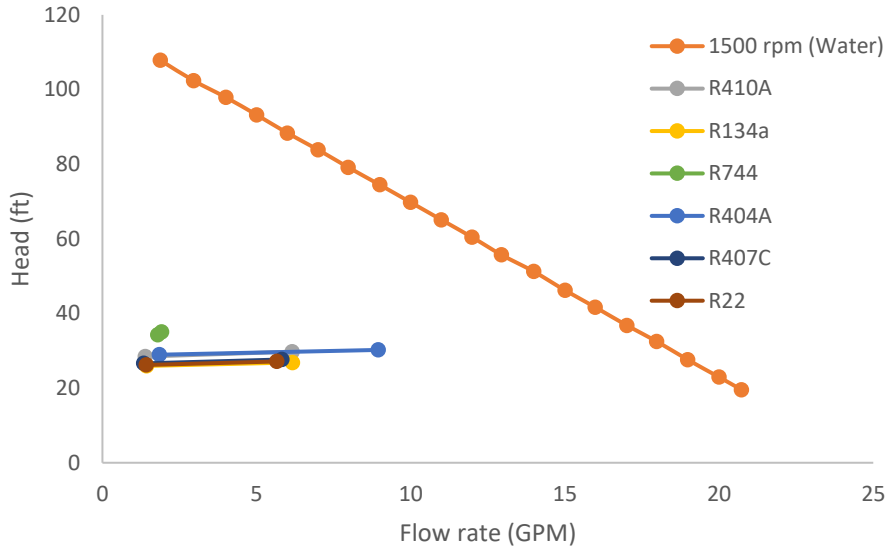


Figure 4.3: Refrigerant pump curve for rotational speed of 1500 rpm. With permission from Warrender (2021b)

For fluid viscosity, it is a completely different scenario. Viscosity affects the pump performance critically. The Hydraulic institute has published a correction chart for the pump performance (Hydraulic Institute, 2000)). An illustration of the correction curve is shown in Figure 4.4.

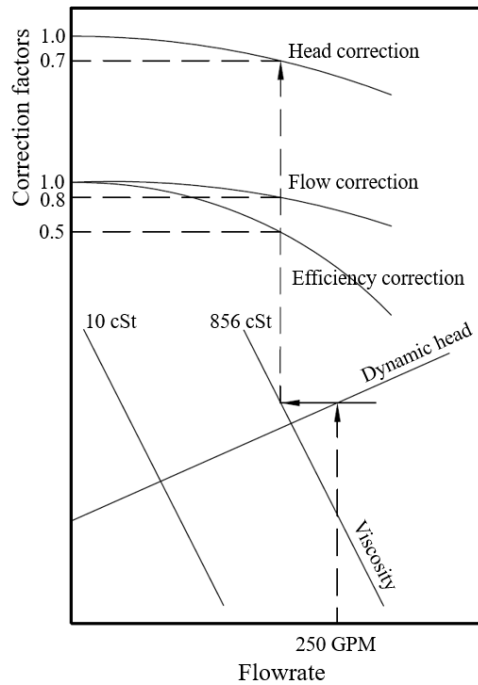


Figure 4.4: Illustration of the correction curve from Hydraulic institute.

The Figure 4.4 shows the correction factors of the flow, head and efficiency of a fluid of 856 cSt kinematic viscosity with a dynamic head and flow rate. All the refrigerants considered in the simulation study has kinematic viscosity under 0.3 cSt for the temperature range considered. It can be safely said that the correction factor of those refrigerants will be 1. So, a pump curve of water as a working fluid can be used without any modification in the applications considered in this thesis.

As various refrigerants will run through pump refrigeration loop, choosing o-ring is very important as one material might not be compatible with the variety of refrigerants. Polychloroprene is considered for this case. Polychloroprene exhibits good chemical stability and maintains flexibility over a temperature range from -35°F to 225°F. An o-ring compound of polychloroprene from Parker Hannifin is chosen whose model is C0873-70.

Based on the specifications of the pump, a motor from Techtop is chosen. The model number is GX3-AL-TF-184TC-2-B-D-5. It delivers a shaft power of 3 HP rated at 1750 rpm and can be operated with a power frequency of 60 Hz. The maximum rpm is 3510 rpm. The motor has a 15:1 turndown ratio at constant torque, corresponding to a minimum speed of 234 rpm.

4.1.3 Refrigerant Piping

Copper was chosen as the piping material for refrigerant. Pipe dimensions were selected based on the ASHRAE Handbook - Refrigeration, (ASHRAE, 2018). Two piping dimensions were chosen for suction lines and liquid lines. No discharge line was selected due to the absence of a compressor. In the ASHRAE refrigeration handbook, suction or discharge capacity is determined based on condenser saturated temperature of 105°F/40°C. Assuming condenser saturated temperature of 40°C and considering air conditioning as it provides larger capacity, the cooling capacity was determined for all the refrigerants considered in this paper. In ASHRAE handbook – Refrigeration, different line sizes are provided for different capacity in suction, discharge and liquid line for various refrigerants. A plot from the table is shown in Figure 4.5.

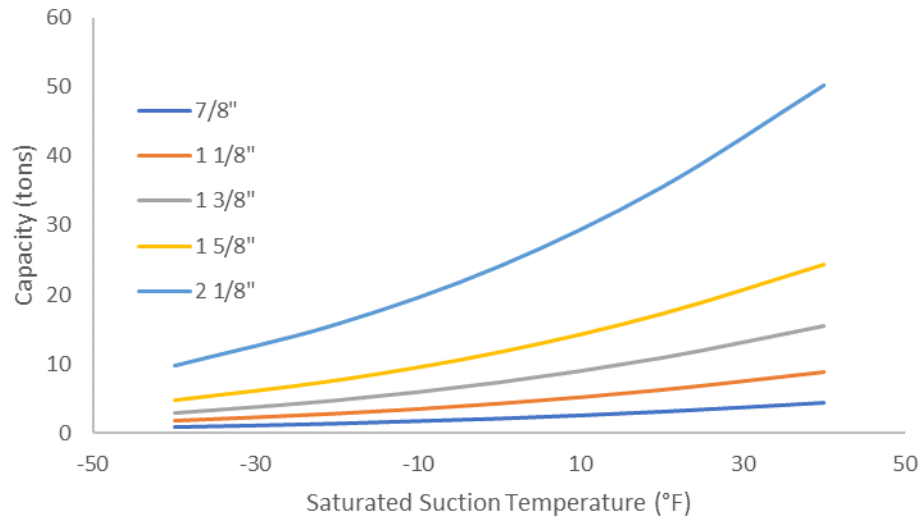


Figure 4.5: Suction line capacities for R410A for different L copper tube diameters in inches.

The maximum saturated suction temperature provided is 40°F/4.44°C but the saturation temperature for this experiment is 7.2°C. So, capacity was extrapolated for 7.2°C, assuming a capacity just over the capacity found from the extrapolation and taking the corresponding line size as the required suction line size. 1 5/8” copper pipe was chosen for the setup as it satisfies all scenarios. Table 4.1 shows the minimum pipe diameter needed for each refrigerant.

Table 4.1: Suction line sizing

Refrigerant	Mass flow rate (kg/s)	Capacity (kW)	Capacity (Tons)	Outer Diameter (in)
R410A	0.25	39.35	11.2	1 3/8
R134a	0.28	40.61	11.55	1 5/8
R22	0.27	43.07	12.25	1 5/8
R404A	0.33	35.68	10.15	1 5/8
R407C	0.25	38.73	11.02	1 5/8

In the ASHRAE 2018 Refrigeration – Handbook, the section for basic piping principles in chapter 1 provides a guideline for the liquid line velocity. The guideline suggests keeping the liquid line velocities below 300 fpm to minimize or prevent liquid hammering and over 100 fpm preventing

reverse flow. To adhere to those limits, 5/8” copper pipe was chosen. For all the refrigerants, the velocity was calculated. Some crossed the limit of 300 fpm. Then, 7/8” was chosen as the new diameter which satisfies the velocity limit. Table 4.2 shows the velocity for the refrigerants.

Table 4.2: Liquid line sizing.

Refrigerant	Mass flow rate (kg/s)	Outer Diameter (in)	Velocity (in/min)	Velocity (fpm)
R410A	0.25	7/8	1312	109.3
R134a	0.28	7/8	1454	121.1
R22	0.27	7/8	1430	119.2
R404A	0.33	7/8	1712	142.7
407C	0.25	7/8	1310	109.1

4.2 Glycol Loop Components

Glycol loop contains the pre-evaporator, glycol pump, heater and other minor components. The sizing of the components is described in order in this section.

4.2.1 Pre-evaporator

The function of the Pre-evaporator changes based on the mode the of the experiment (cooling mode or heating mode). In cooling mode, the pre-evaporator functions as a heat exchanger which transfers heat to the refrigerant from glycol to have desired properties before a refrigerant enters the tested HX which is acting as evaporator. In heating mode, it acts solely as evaporator. First, the capacity for the pre-evaporator was determined for both design conditions keeping in mind the mode of operations. During cooling mode, for design condition 1, the saturated temperature for the evaporator is 45°F/7.2°C. So, the glycol inlet temperature was assumed 70°F/21.11°C. The volumetric flow rate for glycol was assumed 2 GPM per ton of pre-evaporator capacity. During heating mode, glycol temperature at inlet of pre-evaporator was assumed 10°C more than the refrigerant outlet temperature of pre-evaporator which can reach 85 °C. For this case, the volumetric flow rate for glycol was assumed 1 GPM per ton of pre-evaporator capacity. This information is shown in Table 4.3 and Table 4.4.

Table 4.3: Pre-evaporator in cooling mode.

Refrigerant	Load (kW)	Liquid temp at Exp valve (°C)	Evaporating temp (°C)	Outlet quality (-)	Brine inlet temp (°F / °C)	Brine Volumetric flow rate (L/min)
R410A	18.38	2.16	9.36	0.3	70 / 21.11	39.57
	13.22	-18.09	-5.96	0.4		28.46
R134a	17.34	2.25	12.21	0.26		37.33
	12.64	-11.66	0.39	0.35		27.21
R32	14.97	2.26	9.38	0.24		32.23
	10.8	-11.65	-3.69	0.32		23.25
R404A	21.87	-3.87	6.2	0.36		47.09
	15.72	-12.19	-2.94	0.47		33.85
R407C	17.35	-3.87	6.2	0.27		37.35
	12.44	-18.09	-5.96	0.36		26.78
R744	7.6	-9.93	-4.18	0.21		16.36
	8.56	-14.93	-9.09	0.24		18.42

Table 4.4: Pre-evaporator in heating mode (Load = 35.16 kW, Brine flow = 37.85 L/min)

Refrigerant	Liq temp at Exp valve (°C)	Evaporating temp (°C)	Outlet temp (°C)	Superheating (K)	Brine inlet temp (°C)	Brine outlet temp (°C)
R410A	46.25	54.3	84.57	30.27	94.57	76.2
	44.05	51	84.12	33.12	94.12	75.75
R134a	46.2	54.3	68.91	14.61	78.91	60.68
	43.99	48.8	65.55	16.75	75.55	57.35
R32	36.81	44.8	84.77	39.97	94.77	76.4
	30.1	34.8	81.42	46.62	91.42	73.08
R404A	46.27	54.3	69.65	15.35	79.65	61.42
	44.06	48.8	65.13	16.33	75.13	56.94
R407C	46.22	54.3	77.5	23.2	87.5	69.19
	43.91	48.8	75.74	26.94	85.74	67.45
R744	10.12	14.9	43.01	28.11	53.01	34.99
	10.12	14.9	48.16	33.26	58.16	40.11

This information was used in Hexact and a micro plate heat exchanger (model: C62L-E) with 70 plates were selected.

4.2.2 Heater

An inline circulation heater was essential to provide the necessary heat for the pre-evaporator. It is observed that the pre-evaporator needs maximum of 21.87 kW or 6.2 tons of heating capacity during cooling mode from Table 4.3 and in heating mode the maximum heating capacity required is 35.16 kW or 10 tons. A 40 kW Chromalox heater was chosen. Model number of the heater is NWHSRG-06-040P-E1, 480 Volts 3 phase. The heating element in the heater has a INCOLOY sheathing. A J type thermocouple in a thermowell is used to keep track of the temperature and prevent overheating.

4.2.3 Silicon Controlled Rectifier (SCR)

A Silicon controlled rectifier is needed to control the heating capacity of the heater. An SCR from WATLOW DIN-A-MITE was chosen. The model number of the SCR is DC20-48S0-H000. The power circuit has 3 phase and 2 controlled legs with 480 VAC. It's cooled by natural convection meaning it doesn't have any cooling fan. Line and load voltage of the SCR is 480 VAC which is the same voltage in our lab. The input control signal is 4 to 30 mA. The SCR has alarm option for open heater and shorted SCR.

4.2.4 Glycol Piping

In the lab, we have abundance of 1 5/8" Copper pipe. Also, during heating mode glycol temperature can go up to 95°C. Copper can withstand this temperature. It was decided that the setup will use the existing copper pipe in the setup.

4.2.5 Glycol Pump

A centrifugal pump was selected for pumping glycol from Grundfos (2021). The model number is CRN1-7U-EGJG-EHQQE. It was already available in the lab and was laying unused. The pressure drop was calculated and the result was compared with the pump curve to determine if the pump is compatible with the system and operations. The highest and lowest flow rate for Glycol is 47.09 L/min and 16.36 L/min. The pressure drop was calculated for these flow rates in pipe. The pressure

drop in pipe was calculated using a formula from Copper Tube Handbook (CDA-Publication, 2010) which is

$$\Delta P = \frac{4.5Q^{1.85}}{C^{1.85}d^{4.87}} \quad (1)$$

where,

P = friction loss, psi per linear foot

Q = flow, GPM.

D = average I.D., in inches

C = constant, 150.

The K value for 90° bend was assumed as 0.75. The calculation is shown in Table 4.5 and compared on the pump curve.

Table 4.5: Pressure drop calculation in glycol tube.

Flow rate (L/min)	Flow rate (GPM)	Velocity (ft/s)	Length of tube (ft)	Pressure drops in tube (psi)	Number of 90° bend	Pressure drop in bend (psi)	Total pressure drop (psi)	Head (ft)
47.09	12.44	1.25	30	0.19	14	0.36	0.54	1.25
16.36	4.32	0.78	30	0.03	14	0.04	0.07	0.16

The system pressure loss is compared with pump curve (Grundfos, 2013) in Figure 4.6. The system needs more pressure loss to be able to be compatible with the pump. I have introduced couple of valves to increase pressure loss in the system.

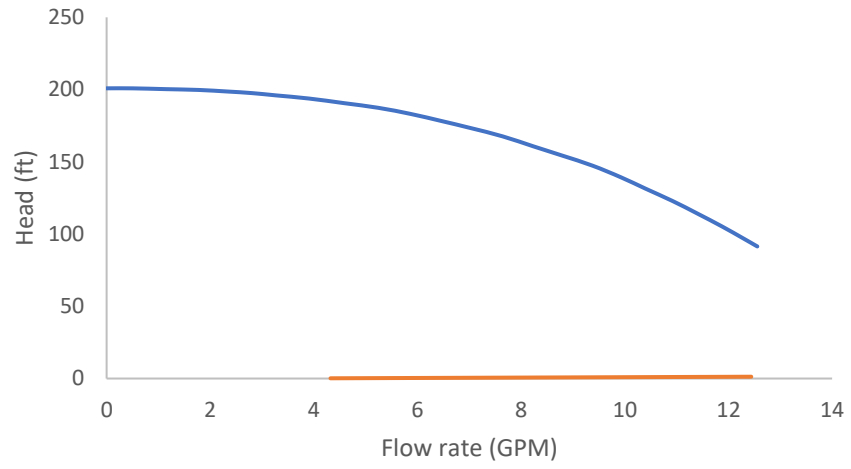


Figure 4.6: Glycol pump curve compared with the system curve at maximum 3600 rpm.

CHAPTER V

INSTRUMENTATION, CONTROL AND SAFETY

After the component selection the next step is to determine the instruments needed for data acquisition, implementation of control system of the key variables and ensuring safety of the equipment and user. This chapter will describe these processes and equipment in detail.

5.1 Instrumentation

Required measurements include temperature, pressure and mass flow rate, at different locations. Required accuracy also depends on the location. RTDs are mainly for very accurate temperature measurement. These are situated at inlet and outlet of both glycol and refrigerant side of the Pre-evaporator as we need to measure the heat transfer precisely. Another RTD is installed after the tested HX. All the pressure sensors are situated in the refrigerant line. These sensors are installed at inlet and exit of the Pre-evaporator and after the tested HX. Both RTDs and pressure transducer combined will help to pinpoint the state point location of the refrigerant in property diagram. The temperature measurement is not as critical for the condenser for that reason, two thermocouples have been used at inlet and outlet of the condenser. One mass flow meter is situated after the refrigerant pump in refrigerant loop to measure the refrigerant flow rate and another flow meter is situated in the glycol loop after glycol pump to measure the flow rate of glycol. The location of these instruments is shown in Figure 2.2. Table 5.1, Table 5.2 and Table 5.3 shows the specifications of the instruments.

Table 5.1: Information of pressure transducer.

Item	Item Specification
Model	206110CPG2M11028NN
Pressure Range	0 to 250 PSIG
Accuracy	± 0.325 PSI
Output	4 to 20 mA
Excitation	24 VAC
Location	Inlet of Pre-evaporator and inlet-outlet of tested HX
Manufacturer	Setra

Table 5.2: Information of the three RTDs.

Item	Item Specification
Models	1: R3T192L684-009(3/4)-8D06,307 2: R3T192L684-007(3/4)-8D04,305 3: R3T192L684-006-8D04-15-T3006-2
Type	100-ohm Platinum
Range	-50 to 200°C
Accuracy	$-50 \pm 0.185^\circ\text{C}$, $0 \pm 0.1^\circ\text{C}$, $100 \pm 0.27^\circ\text{C}$, $200 \pm 0.44^\circ\text{C}$
Description	1: 3/8 inch Diameter Steel Sheath (length 9 3/4 inches), Sheath Bend - 90 Degrees, Hot Leg Length - 7 3/4 inches, Temperature Coefficient - 0.00392 ohms per Degree 2: 1/4 inch Diameter Steel Sheath (length 7 3/4 inches), Sheath Bend - 90 Degrees, Hot Leg Length - 5 3/4 inches, Temperature Coefficient - 0.00392 ohms per Degree 3: 3/8 inch Diameter Steel Sheath (length 6 inches), Temperature Coefficient - 0.00392 ohms per Degree
Location	1: inlet and outlet of Pre-evaporator on glycol loop 2: inlet of Pre-evaporator on refrigerant loop 3: inlet and outlet of tested HX
Manufacturer	Pyromation
Supplier	Atech

Table 5.3: Information of mass flow meter for both refrigerant and glycol.

Item	Item Specification
Model	CMF050M320NRAAEZZZ
Nominal flow rate	151 lb/min - 249 lb/min
Accuracy	$\pm 0.25\%$ to $\pm 0.05\%$
Output	4 to 20 mA
Location	at inlet of refrigerant pump and glycol pump

Data Acquisition System

The data acquisition is a National Instruments (NI) Compact RIO (cRIO). A detailed discussion about the DAQ can be found in Kinenhole (2019).

Table 5.4: cRIO pinout of PRL including measurement type and name.

Indicator or Control Name	Electrical Signal	Chassis #	Module Model # & Type	Module Slot #	Channel Names	Pinout Code	Breakout Box
PRL-RL Test Coil Outlet Pressure	4-20 mA	NI 9035	NI 9208 Current Input	3	6	AI-9035-3-6	A
PRL-RL Test Coil Inlet Pressure	4-20 mA	NI 9035	NI 9208 Current Input	3	7	AI-9035-3-7	A
PRL-RL Pre-Evaporator Inlet Pressure	4-20 mA	NI 9035	NI 9208 Current Input	3	5	AI-9035-3-5	A
PRL-RL Evaporator Inlet Temperature	RTD	NI 9145 (2)	NI 9226 Temperature Input	7	4	RTD-91452-7-4	
PRL-GL Pre-Evaporator Outlet Temperature	RTD	NI 9145 (2)	NI 9226 Temperature Input	7	3	RTD-91452-7-2	
PRL-GL Pre-Evaporator Inlet Temperature	RTD	NI 9145 (2)	NI 9226 Temperature Input	7	2	RTD-91452-7-3	
PRL - Heater Switch	0-24 VDC	NI 9035	NI 9476 Digital Input	8	11 (Zip Terminal - 12)		
PRL - RL Pump Switch (1)	0-24 VDC	NI 9035	NI 9476 Digital Input	8	12 (Zip Terminal - 13)		
PRL - GL Pump Switch (2)	0-24 VDC	NI 9035	NI 9476 Digital Input	8	13 (Zip Terminal - 14)		
PRL-RL Condenser Inlet	TC	NI 9145 (1)	NI 9214 Temperature Input	3	13	TC-91451-3-13	A
PRL-RL Condenser Outlet	TC	NI 9145 (1)	NI 9214 Temperature Input	3	14	TC-91451-3-14	A
PRL- Test Coil Outlet Temperature	RTD	NI 9145 (2)	NI 9226 Temperature Input	7	6	RTD-91452-7-6	
PRL- Test Coil Inlet Temperature	RTD	NI 9145 (2)	NI 9226 Temperature Input	7	5	RTD-91452-7-5	
Flow Meter For refrigerant loop	4-20 mA	NI 9035	NI 9208 Current Input	4	1	AI-9035-4-1	A
Flow Meter for Glycol loop	4-20 mA	NI 9035	NI 9208 Current Input	4	0	AI-9035-4-0	A

5.2 Control

Two PI controllers have been assigned to control the inlet quality of refrigerants at inlet of the tested HX and the refrigerant flowrate. A dynamic model was created using Modelica (1997), an object-oriented language, in combination with TIL (2019) library to observe the behavior of the control system before implementing on the experimental setup. In the model the heat transfer coefficients are tuned by using the steady state simulation developed in EES. The model was developed by building blocks representative of each component in the PRL with specifications taken from the real world equipment considered for building the PRL and then, connecting those blocks. R410A was considered as the refrigerant and design condition 1 – “air conditioning” was taken as the only design choice for this model. The state properties of the working fluids are taken directly from the EES model. A brief description of the development of those blocks and the model is provided in this subsection. Figure 5.1 shows the GUI of the model and Table 5.5 provides the functions of specific blocks.

HGBC boundary: Boundary models determine the conditions at the boundary of a system. The conditions are determined by the following variables: enthalpy or temperature, mass fraction, mole fraction or relative humidity, pressure, mass flow rate or volume flow rate. In an overdetermined boundary, mass flow rate (or volume flow rate) and pressure are given at once. Therefore, the system needs an opposite boundary (undetermined boundary), with free mass flow rate (or volume flow rate) and pressure. The boundary at the inlet and outlet of cascade condenser from HGBC side are configured considering the parameters to reach steady state. The overdetermined boundary at inlet was configured for inlet temperature (-3.08°C), inlet mass fraction of {1} which means gas or liquid in pure forms, inlet pressure (724.5 kPa) and mass flowrate (-0.2991 kg/s). The negative sign before mass flowrate means it is flowing out of the boundary. The underdetermined boundary contains the outlet temperature (8.1°C) and outlet mass fraction {1}.

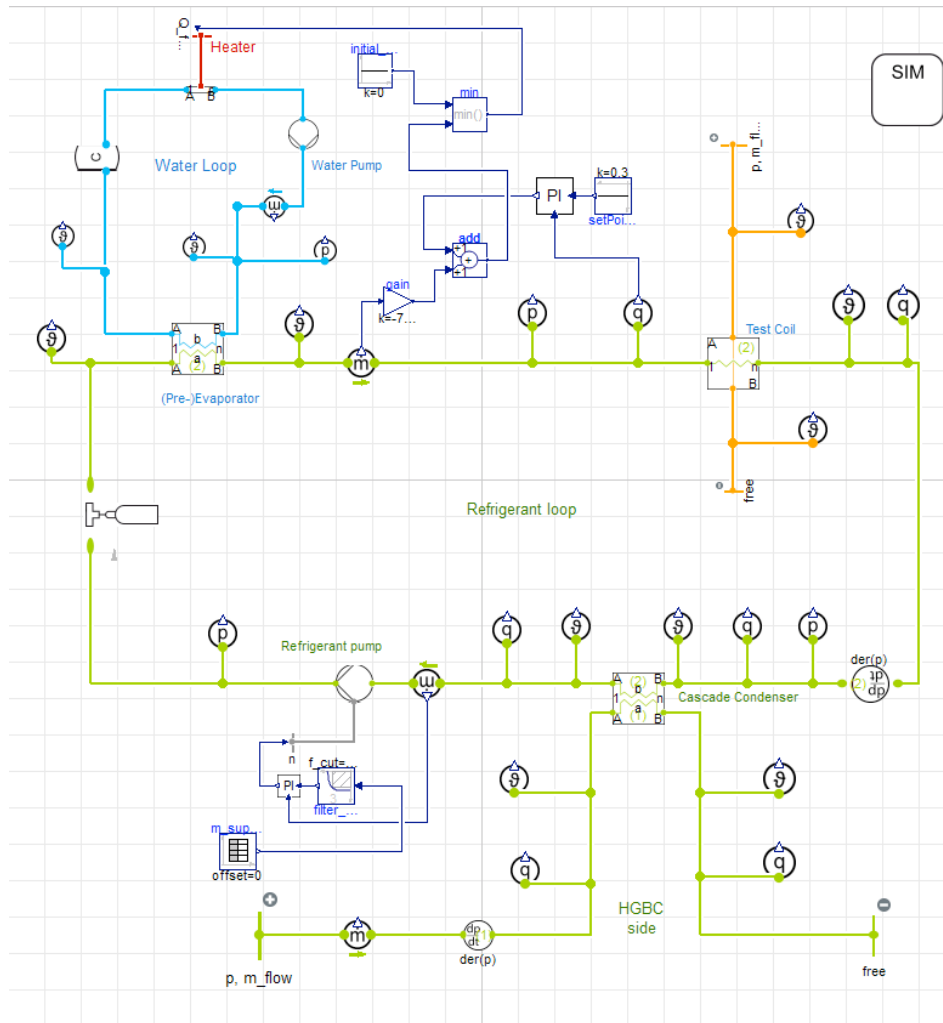














Figure 5.1: Pumped refrigerant loop model.

Table 5.5: Functions of blocks in the Modelica model

	Pressure sensor		Capacitor-variable volume, constant capacity
	Quality sensor		PI controller
	Temperature sensor		Filling station
	Mass flow meter		Tabulated setpoint at specific times
	Sim-Defines substances used in systems		Low pass, high pass, band pass and band stop filters
	Pressure state model-defines a pressure level		Generate constant signal of type real

Cascade condenser: A D118L-E cascade condenser from Danfoss was chosen using Hexact (Danfoss, 2018) for the physical experiment. The plate number was chosen to be 50. Geometrical property of the cascade condenser in the model was adjusted as per available data provided by Hexact. Internal geometrical data is not shared by the manufacturer, so the default parameters were used. 10 segments were used as a compromise for discretizing the heat exchanger. For heat transfer mode, a constant heat transfer coefficient model ($\alpha = 2,500 \text{ W/m}^2\text{-K}$) was chosen for both refrigerant at evaporating (HGBC) and condensing (PRL) side randomly as R410A. Pressure drop is neglected in the dynamic model. Steel is considered as wall material as D118L-E is made of steel and heat conduction model is chosen as geometry-based conduction.

Refrigerant pump: The pump was configured based on the pump WMTA 49 from Warrender (Warrender, 2021a) for the physical experiment. Table 5.6 shows the characteristic property of the pump determined from the pump performance curve.

Table 5.6: Characteristic properties of pump.

Pump characteristics at nominal speed	Value	Units
Nominal speed	20	Hz
Pressure at volumetric flow = 0	385.4	kPa
Volumetric flow rate at 0 pressure drop	0.00092	m ³ /s
Nominal efficiency	0.93	-
Nominal pressure	138.9	kPa
Nominal temperature	20	°C

Test coil: An aluminum micro channel heat exchanger (MCHE) from Danfoss was chosen as test coil. The selected model is D1900-C. The reason behind choosing this model was to have 40 kW capacity across test coil to achieve the desired steady state. This MCHE can provide that specific heat capacity at air inlet and test coil temperature difference of 10 K and at 2.5 m/s air velocity. 5.1 kg/s of air flow (and density = 1.2041 kg/m³) was assumed. The cross-sectional area of D1900-C (length = 1324 mm and height = 1274 mm) provides 2.5 m/s of air flow for 5.1 kg/s of air. Fin

thickness of 1 mm and fin pitch of 1.1 mm was provided from manufacturer data (Danfoss, 2019a). Fin side pressure drop was assumed zero to simplify the calculation. TIL provides a number of heat transfer models. An overall heat transfer coefficient ($\alpha = 19,000 \text{ W/m}^2\text{-K}$) was used to match the parameters from EES. Aluminum was chosen as the material for tube and fins. A nominal pressure drops of 70 kPa was set according to EES model. Heat conduction mode is geometry based for tube. Constant fin efficiency (100%) is used as the efficiency model for fin as this this is the only model provided by TIL. The Chang and Wang (default) heat transfer model was used for fin side heat transfer.

Air side boundary: The air side boundary includes moist air source and moist air sink. These are analogous to overdetermined and underdetermined boundary from refrigerant side. The source temperature was chosen as 19.36°C as the inlet temperature of refrigerant at inlet of test coil is 9.36°C and in test coil section it is already mentioned that the temperature difference between air inlet and test coil inlet should be 10 K. Atmospheric pressure was considered with an air flowrate of 5.1 kg/s mentioned in test coil section. The temperature at sink is set at 14°C which is chosen at random as it does not affect the model's performance.

Pre-evaporator: D55-EU from Danfoss was used as pre-evaporator. Geometry and wall material were chosen based on the product data sheet (Danfoss, 2019b). Other than length (466 mm) and width (50 mm), every geometrical property is kept at default due to lack of information. The heat transfer models for both refrigerant and glycol in (pre-)evaporator were chosen based on the reasons described in previous heat exchangers ($\alpha = 19,000 \text{ W/m}^2\text{-K}$). 34.5 kPa of pressure drop is considered from EES. Temporary inlet and outlet conditions are defined by overdetermined and underdetermined boundary for both refrigerant and glycol side with parameters from EES model.

Glycol pump: A Grundfos CRN1-7 A-FGJ-G-E-HQQE pump was selected for the experiment. The pump curve (Grundfos, 2013) was digitized and converted into a third order polynomial fit. The pressure difference is 385.4 kPa for volumetric flow of zero and $3.21 \text{ m}^3/\text{hr}$ (0.92 l/s) for zero

head. The nominal speed, efficiency, and temperature are 20 Hz, 93% and 20°C relatively. According to the steady state model, the glycol flow rate is 40 L/min.

Heater: The heater is a combination of a heat boundary and a tube. The heat boundary releases 18.38 kW capacity to the tube as required to achieve the steady state. For the tube, a 6" (152.4 mm) inner diameter and length of 32" (812.8 mm) galvanized steel pipe were set according to the data provided from the heater manufacturer (Chromalox, 2021). Tube side heat transfer coefficient of glycol is assumed 2,000 (W/m²-K). At first, pressure drop was assumed to be 180 kPa to get the desired result with frequency of pump being 50 Hz. Though it resulted in desired properties of refrigerant, but glycol temperature got reduced from steady state. To match the inlet glycol temperature to 21°C from steady state model, the pressure drop was reduced to 30 kPa and pump frequency was reduced to 20 Hz.

Hydraulic capacitor: A hydraulic capacitor is variable volume device with constant capacity (kg/Pa). In a closed liquid loop, Modelica requires a hydraulic capacitor, or the simulation fails because when the loop runs, even small increases in temperature lead to very high pressures as component internal volume, and as a result fluid density, are fixed. To allow for density changes with temperature, a hydraulic capacitor is used. A total mass of 3.55 kg and filling rate of 0.01 kg/s were determined.

After developing the individual component blocks, they were connected and tested. At first, the model was not providing the data that was expected as per EES model. The pressure wasn't enough in the system. Later, it was figured out that there was not enough charge in the system. So, a filling station was introduced in the refrigerant loop. A fixed mass 3.55 kg of refrigerant in the system was needed to get desired steady state. Then, two PI controller are set for the control of mass flowrate of the refrigerant in the refrigerant loop and quality at inlet of the test coil.

The output of each controller is calculated as

$$y = e \cdot K_p + e \cdot K_i, \quad (2)$$

where, e = error, K_p = proportional gain and K_i = integral gain.

5.2.1 Quality Control

The quality at inlet of the tested HX is controlled by controlling the heat input from the heater in glycol loop. The PI controller will control the silicon controlled rectifiers (SCR) which will control the heating element in the heater. The gains of the PI controller were determined in dynamic model in Modelica.

Gains of PI controllers for quality at the test coil inlet were tried to be tuned with the Ziegler and Nichols (1942) method and Skogestad (2004) method but neither tuning method provided satisfactory results. The gains were changed by trial-and-error. The set point was changed from 0.01 to 0.3 at 3,500s after the model started simulation. The simulation was given some time and a small quality to stabilize before the set point was changed. Controller performance in terms of rise time, settling time, % peak overshoot (PO), integral error (IAE) is shown for different integral gains. Rise time means the time a desired variable takes to reach within $\pm 1\%$ of the setpoint or final value. Settling time is the time needed for the desired output to enter and remain within $\pm 1\%$ of the final value. % peak overshoot or maximum overshoot is the ratio of the peak value to the final value. IAE is the integrated error which accounts for the error made over the period of the settling time.

Figure 5.2 shows the behavior of quality for different gains. When the proportional gain is 1 and the integral gain is 200, it shows the least settling time. Table 5.7 shows how the gains handle disturbance. All the gains showed similar performance to minimize disturbance.

Table 5.7: Performance parameter of PI controller for quality in dynamic model

Case number	K_p	K_i	Setpoint				Disturbance	
			Rise time	Settling time	PO	IAE	Peak	IAE
1	1	100	1130	2422	2.65	203.83	0.52	52.46
2	1	200	628	2262	18.33	156.17	0.52	54.31
3	2000	100	1142	2390	2.33	199.09	0.52	52.38
4	20000	100	1324	2460	NA	186.11	0.52	51.85

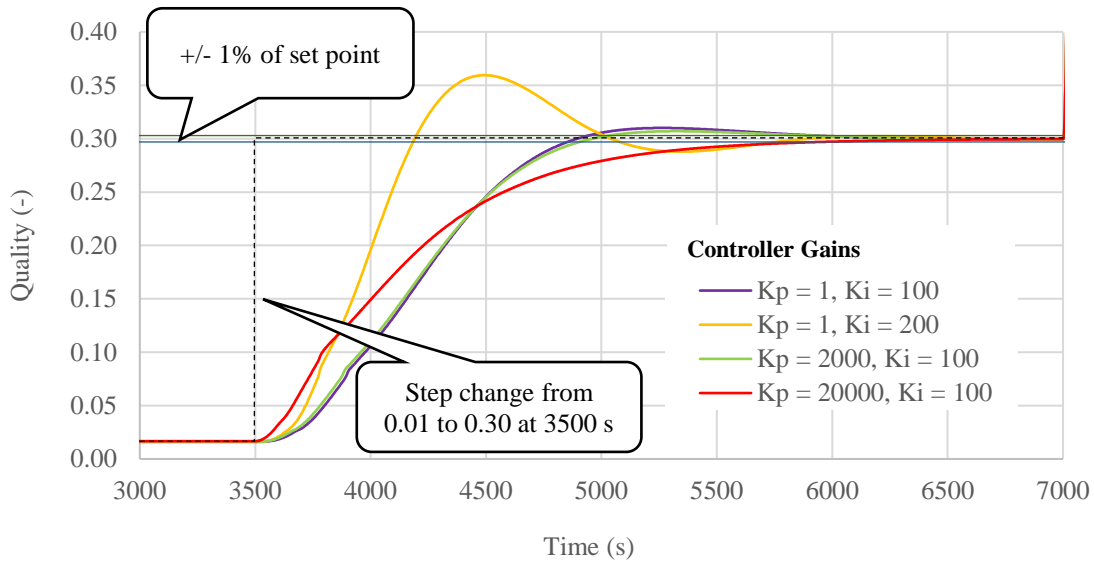


Figure 5.2: Quality vs time for different controller gains.

5.2.2 Refrigerant Flowrate Control

Another PI controller is used to control the refrigerant flow rate by adjusting the speed of the refrigerant pump.

Different types of tuning methods were considered for tuning the PI controller. Ziegler-Nichols and Skogestad's methods were among those. The tuning methods failed to achieve steady state, possibly because the model lacks a delay time which these tuning methods include in their assumptions. The gains were changed by trial and error method to get to steady state with small settling time and reasonable overshoot. The setpoint went through step change from 0.2 to 0.25 at 1000s. With a proportional gain of 0.5 and integral gain of 50, the system reacted as critically damped. When both

the proportional gain and integral gain were increased by a factor of 2, a faster way to reach setpoint was achieved with a peak. The performance parameters are shown in Table 3. Figure 3 shows the mass flow rate changes with time due to different gains. The set point was changed at 1000th second. The figure shows simulation time from 990th second. Case 2 showed better performance.

Table 5.8: Performance parameter of PI controller for mass flow rate.

Case Number	K_p	K_i	Performance parameter			
			Rise time (s)	Settling time (s)	PO	IAE
1	0.5	50	10	90	NA	0.32
2	1	100	8	24	2.65	0.28

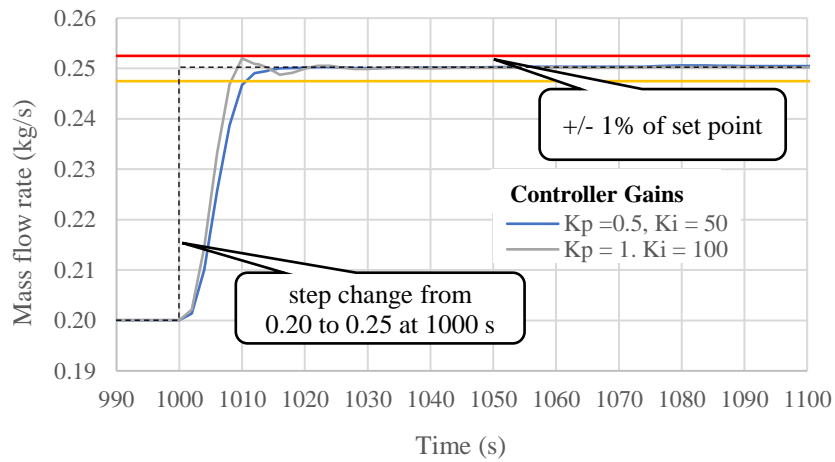


Figure 5.3: Mass flow rate vs time for different controller gains.

5.3 Safety

A safety circuit has been designed that ensures a complete shutdown of all equipment in case of any equipment malfunction like when the pumps stop working or heater is providing excessive heat to the loop . It is equipped with different kinds of electronics and switches to perform the necessary tasks. Before going into the operational details of the circuit, a brief description of the equipment is given to understand their function in the circuit.

5.3.1 Safety Circuit Devices

The safety circuit contains contact relays, time delay relays, mechanical switches like flow switch, off delay, delay on make, bypass timer.

Time Delay Relay

The function of a time delay relay is to provide electricity to certain equipment for a designated period even after its input signal is terminated. This is very important for PRL; after the heater gets turned off, both pumps need to operate for a limited time to circulate the working fluids, dissipating the heat from the water heater. I have used Macromatic TE-8861U for this function. Its specifications are shown in Table 5.9.

Table 5.9: Specification of time delay relay.

Item	Item specifications
Make and Model	Macromatic TE-8816U
Contact form	SPDT
Current rating	15 A
Voltage rating	12 to 240 V
Mounting type	DIN rail

Delay on Make (DOM)

The function of delay on make is to close circuits after a certain period of time when it gets power. During operation, some switches frequently open and close due to the behavior of the operation, causing the electronics to fail. The delay timer is set in a way that it will wait for the operation to get stable before it allows to pass current. When DOM gets power, the delay timer will start

counting. In the meantime, if it loses power, the timer will start again after it gets the power. Table 5.10 shows the specification of the device.

Table 5.10: Specification of DOM.

Item	Item specifications
Make	ICM
Model	ICM102
Time delay	1.8 to 600 sec
Control Volts	18 to 240 V
Contact ratings	1.5 A
Voltage	18 to 240 V
Temp. Rating	-40 to 167 F
Mounting type	DIN rail

Bypass timer

A bypass timer bypasses the current for a period of time fixed by the user. In operation, for some reason the switches remain open but there is need for current to pass through to the rest of the circuit. Bypass timer bypasses the current around the GFS and RFS switches for a limited session.

Table 5.11 shows the specifications of the bypass timer.

Table 5.11: Specification of bypass timer.

Item	Item specifications
Make	ICM
Model	ICM175
Time delay	10 to 1000 sec
Control Volts	18 to 240 V
Contact ratings	1 A
Voltage	18 to 240 V
Mounting type	DIN rail

Relays

I have used couple of relays to close the contacts for the refrigerant pump, glycol pump and the heater when the safety is ensured. Their specifications are given in Table 5.12.

Table 5.12: Specification of relays.

Item	Item specifications
Make and Model	Eaton D3RF2T
Contact type	DPDT
Control Volts	24 V AC
Contact rating	10 A
Terminal style	8 pin
Maximum switching Voltage	300 V
Temperature Rating	-40 to 185 °F
Mounting type	DIN rail

High- and Low-Pressure Cutout

A pressure cutout is a switch which produces analog signal based on the pressure it senses. I have used two pressure cutouts for detecting high and low pressure, The information is given in Table 5.13 and Table 5.14

Table 5.13: Low pressure cutout specifications.

Item	Item specifications
Model	P20BB-1C
Manufacturer	Johnson Controls
Switch type	SPST
Switch action	Opens at low pressure
Range	7 to 150 PSI
Reset	Manual
Connection	Sweat

Table 5.14: High pressure cutout specifications.

Item	Item specifications
Model	P70KA-1C
Manufacturer	Johnson Controls
Switch type	4 Wire, 2 Circuit
Switch action	Opens at high pressure
Range	50 to 500 PSI
Reset	Manual
Connection	Flare

Temperature Controller

I have used a PID temperature controller as a high and low temperature switch in safety circuit. It has a dual relay output which acts as switch. It contains 9 terminals. 3 terminals are used to take data from RTDs or thermocouple. 4 terminals are used for relays and 2 terminals for power. Table 5.15 shows the specifications.

Table 5.15: Temperature switch specifications.

Item	Item specifications
Make and Model	Novus - 9103000102
Type	Single loop PID and ON/OFF
Thermocouples	J, K, T and Pt100 input
Power Supply	12 to 24 Vdc/ 24 VAC
Operating temperature	0 to 60°C, 20 to 80% RH

Flow switches

I have used two flow switches for the two loops. Their specifications are given in Table 5.16 and Table 5.17.

Table 5.16: Glycol flow switch specifications.

Item	Item specifications
Brand	Gems Sensors & Controls
Series	FS-380
Sensor type	Piston
Flow setting	1 GPM
Flow range	0 to 1 GPM
Port size	1/2 in NPT male
Switch type	SPST
Maximum Pressure	1500 PSI

Table 5.17: Refrigerant flow switches.

Item	Item specifications
Brand	Gems Sensors & Controls
Series	FS-380
Sensor type	Piston
Flow setting	0.5 GPM
Flow range	0 to 1 GPM

Item	Item specifications
Port size	1/2 in NPT male
Switch type	SPST
Maximum Pressure	1500 PSI

5.3.2 Safety Circuit

The safety circuit is a 24 VAC circuit, powered by 480 V transformer. The safety circuit is shown in Figure 5.4 and the abbreviation of the equipment is shown in Table 5.18.

An emergency stop button allows manual shut down of both HGBC and PRL. Another emergency switch named PRL activation is also used only to shut down the PRL individually. There are some safety switches connected in series starting from node 1 in Figure 5.4. Among the switches, there are temperature switches, pressure switches from both PRL-HGBC, and flow switches from HGBC. High and low temperature switches functionally provided by the Novus temperature controller which is connected by a J-type thermocouple to the heater. The high-and low-pressure switches are located after the refrigerant pump in the setup. The node 9 comes after the series connection of the switches. R1 relay is connected to node 9. R1 is a compressor relay which works as a contact to the compressor of the HGBC. From node 9, two more connections are made with the heater relay and with S terminal of the off delay. Node 2 works as a hot terminal to off delay. A2 from off delay connects to ground. Node 13 works as the hot terminal for the rest of the circuit. Both R4 and R5 are connected to node 13 through the flow switches. These relays act as switches for the heater relay, R2 and R3. R2 is a glycol pump relay and R 3 is refrigerant pump relay. These relays work as contact which power the pumps. From node 13 another circuit bypasses the switches from R4 and R5 by bypass timer and connects R2 and R3 through LV switches. LV is a digital on/off relay controlled from LabVIEW.

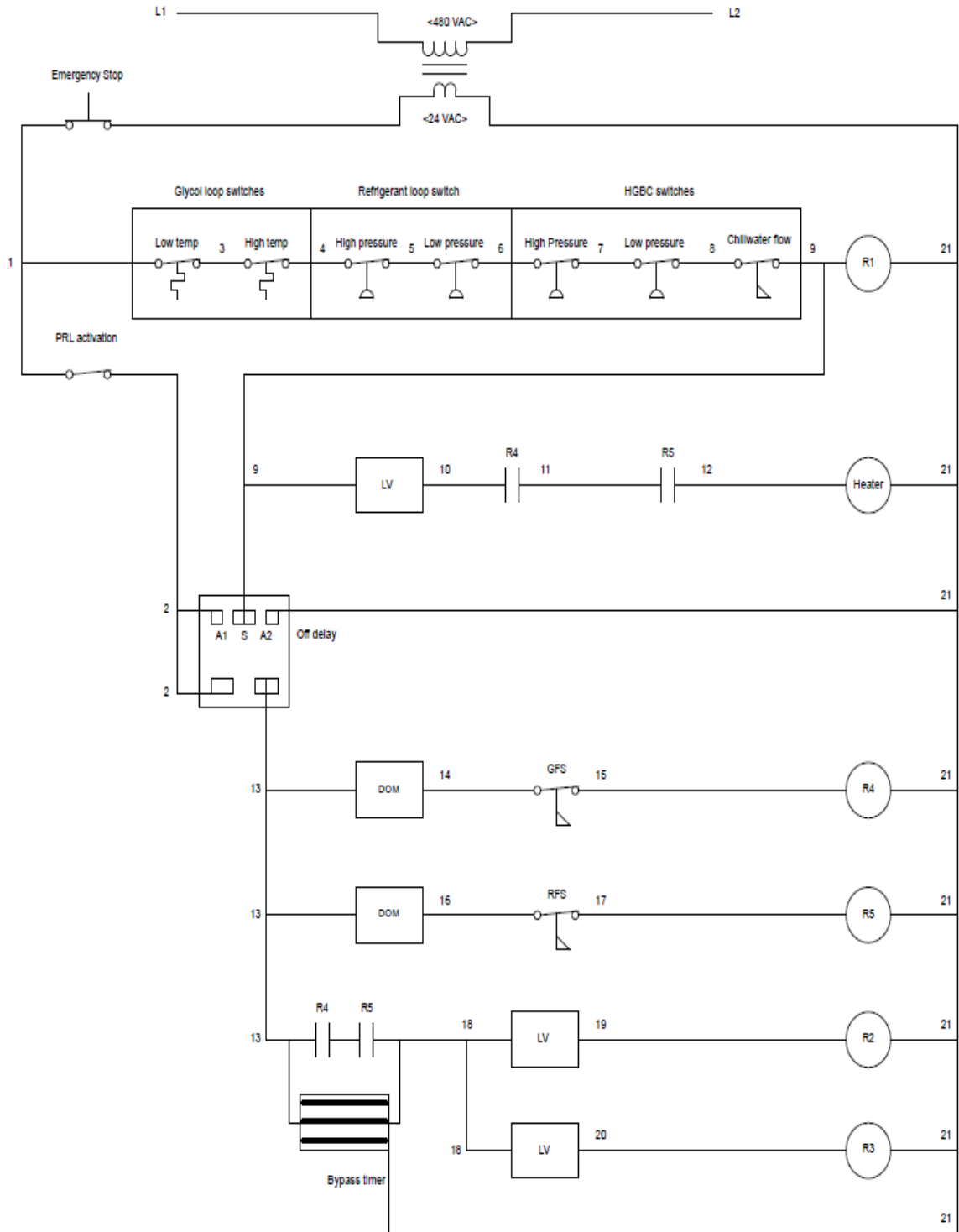


Figure 5.4: Safety circuit.

Table 5.18: Abbreviation of the safety devices.

DOM: Delay on make	R1: Compressor relay & contact	R4: Glycol flow switch relay
GFS: Glycol flow switch	R2: Glycol pump relay & contact	R5: Refrigerant flow switch
LV: LabVIEW relay output	R3: Refrigerant pump relay & contact	RFS: Refrigerant flow switch

5.3.3 Operational Sequence

The safety circuit follows two operational sequences based on the needs of the user and the state of the PRL equipment.

(a) Starting Sequence

If cutout switches from Glycol-Refrigerant and HGBC loop are closed, Relay R1 will be energized given that the chilled water flow switch is closed. When the off delay gets a signal in S, it will energize node 13. The Bypass timer will bypass the remaining safeties to energize relays R2 & R3 at first. When Glycol and refrigerant flow meet the requirement, GFS and RFS will close, energizing relay R4 & R5. DOMs are used to prevent cycling of contactors or relays that otherwise may be caused by fluttering flow switches. R4 and R5 together will energize the contactor coil for the heater contactor.

(b) Off sequence

The Safety circuit turns itself off whenever an anomaly is detected by tis sensor on the circuit. There are 4 ways the safety circuit turns off the setup which would be described in order in this section.

(1) If any of the cutout switches open, the signal to the off delay cease to exist. The heater coil gets turned off instantly. Off delay will stop passing current to node 13 after a specific time, deenergizing all relays downstream – in effect this allows to remove stored heat from the electric heater prior to shutting down the pumps.

(2) When the glycol pump is turned off or trips for some reason or glycol flow is below the critical limit or LV2 switches open, GFS will trip turning off R4 immediately thus opening all R4

switches in the circuit deenergizing heater, R2 (glycol pump) & R3 (refrigerant pump). The refrigerant pump follows the same procedure.

(3) The heater can only be turned off from LabVIEW or manually, if all the relative safety switches are closed.

(4) The PRL activation switch can turn off the safety circuit and terminate any kind of operation in the setup. Another function of the activation switch is to reset the safety circuit. If the pumps are switched off, the bypass timers will eventually run out. Therefore a dedicated activation switch is included which allows resetting the bypass timers without having to restart the HGBC compressor.

CHAPTER VI

CONCLUSION AND FUTURE WORK

The pumped refrigerant loop project went through several stages in the development process. A steady state model was developed with two design conditions, air conditioning applications and refrigerant applications. For these conditions, the supporting HGBC provides a cooling capacity of 58.2 kW or 16.5 tons for air conditioning applications and 32.5 kW or 9.24 tons for refrigerant applications. A parametric study with widely used refrigerants including R410A, R134a, R407C, R404A, and R744 was conducted. This resulted in ranges of the variables necessary to size and select the components. The refrigerant mass flow rate was found to vary from 0.11 kg/s to 0.38 kg/s. The maximum pressure found was to be 43 bar (620 psi). The maximum required heating capacity to reach the desired refrigerant quality inlet condition to the tested heat exchanger is 21.92 kW (6.2 bar).

Two heat exchangers were selected, one as cascade condenser and the second as pre-evaporator for quality control. One pump each was selected for the refrigerant and the glycol loop. A glycol heater as well as pipes for both loops were selected. According to the model and selected components, the pumped refrigerant loop can reach a capacity of 43 kW (12 tons) during cooling mode and 40 kW (11 tons) during heating mode. A dynamic model in Modelica was developed to investigate the control system with two PI controllers, one for quality at inlet of the tested heat exchanger and the other for mass flow rate of the refrigerant. A safety circuit was built to enforce a startup sequence and to prevent unsafe conditions if components or control software malfunctions – protecting personnel and equipment. The construction of the setup is close to nearing completion.

Future work required for a pumped refrigerant loop is includes:

- A 9 wire transmitter needs to be installed for the mass flow meter in the refrigerant loop. There is a dysfunctional 9 wire transmitter in the 047 room that may be repairable.
- The VFDs for both pumps and the SCR for the heater needs to be connected to the equipment and the DAQ and programmed for operations.
- The glycol loop needs to be leak tested.
- Completion of airside instrumentation of the OSU Psychrometric Coil Testing Facility, including air sample trees, psychrometers, and debugging of the code-tester instrumentation.
- Testing and commissioning of the glycol loop with the hydronic tested HX, including refrigerant to air energy balance evaluation, needs to be completed.
- The HGBC needs to be operational for the commissioning of the refrigerant loop.
- Installation of a refrigerant to air heat exchanger as tested coil in the coil testing facility.
- Commissioning of the refrigerant loop along with glycol loop in both cooling and heating mode.
- The expansion tank in the glycol loop needs to be replaced as the tank limits the operational temperature to below the applicability of boiler code. To enable higher temperatures, the system should be modified to provide pressure using elevation head.

REFERENCES

- ABB (2021). Electrical or Electronic manufacturer. Zürich, Switzerland.
- AHRI (2017). AHRI Standard 210/240. "Performance Rating of Unitary Air-conditioning & Air-source Heat Pump Equipment", Air Conditioning and Refrigeration Institute (AHRI), Arlington, VA, USA.
- AHRI (2015). AHRI Standard 540. "Performance rating of positive displacement refrigerant compressors and compressor units". Air Conditioning and Refrigeration Institute (AHRI), Arlington, VA, USA.
- Hydraulic Institute (2000). ANSI/HI 2000 edition pump standards. The Institute, Parsippany, N.J, USA.
- ASHRAE (2018). "ASHARE Handbook - Refrigeration (I-P)", American Society of Heating, Refrigeration and Air-Conditioning Engineers. Atlanta, GA, USA.
- Bell, I. and E. Groll (2011). "Experimental Analysis of the Effects of Particulate Fouling on Heat Exchanger Heat Transfer and Air-Side Pressure Drop for a Hybrid Dry Cooler." Heat Transfer Engineering 32: 264-271.
- Bell, I. H. and E. A. Groll (2011). "Air-side particulate fouling of microchannel heat exchangers: Experimental comparison of air-side pressure drop and heat transfer with plate-fin heat exchanger." Applied Thermal Engineering 31(5): 742-749.
- Bowling, K. (2019). "Commercial heat exchanger pressure drop", Email communication.
- Cabello, R., D. Sánchez, R. Llopis, L. Nebot-Andrés and D. Calleja-Anta (2021). "Energy evaluation of a low temperature commercial refrigeration plant working with the new low-GWP blend R468A as drop-in of R404A." International Journal of Refrigeration 127: 1-11.

CDA-Publication (2010). Copper Tube Handbook, Copper Development Association Inc, New York, NY, USA.

Chromalox (2021). Catalog,"Clean water and oil applications". Pittsburgh, PA, USA.

Cremaschi, L., A. S. Yatim and S. K. Mulgurthi (2018). "Experimental study of oil retention in microchannel type evaporators of air-source heat pump systems." International Journal of Refrigeration 91: 158-166.

Danfoss (2018). Danfoss Hexact 5: Heat Exchanger design software. Version 5.5.5.

Danfoss (2019a). Data sheet, Micro Channel Heat Exchanger, D1100-C MCHE Condenser. Retrieved from Danfoss website. URL:<https://assets.danfoss.com/documents/73247/-AI133486416389en-000601.pdf>.

Danfoss (2019b). Data sheet, Micro Channel Heat Exchanger, D55-EU MCHE Condenser. Retrieved from Danfoss website. URL: <https://assets.danfoss.com/documents/73378/-AI133986416027en-020401.pdf>.

Danfoss (2021). HVAC equipment manufacturer. Nordborg, Denmark.

Delventura, R., C. L. Evans and I. Richter (2007). "Secondary loop systems for the supermarket industry."

Grundfos (2013). Grundfos Data Booklet, CRN1-7 A-FGJ-G-E-HQQE. Retrieved from Grundfos website. URL: https://www.lenntech.com/uploads/grundfos/96516403/Grundfos_CRN-1-7-A-FGJ-G-E-HQQE.pdf.

Grundfos (2021). Pump manufacturer. Bjerringbro, Denmark.

Hrnjak, P., P. Zhang and C. Rennels (2017). "Effect of louver angle on performance of heat exchanger with serpentine fins and flat tubes in frosting: Importance of experiments in periodic frosting." International Journal of Refrigeration 84: 321-335.

Hu, J., X. Xie and Y. Jiang (2020). "Design and experimental study of a second type absorption heat exchanger." International Journal of Refrigeration 118: 50-60.

- Huang, Z., J. Ling, D. Bacellar, Y. Hwang, V. Aute and R. Radermacher (2020). "Airside thermal and hydraulic characteristics of compact bare tube heat exchanger under dry and wet conditions." International Journal of Refrigeration 110: 295-307.
- Jacob, T. A., E. P. Matty and B. M. Fronk (2019). "Experimental investigation of in-tube condensation of low GWP refrigerant R450A using a fiber optic distributed temperature sensor." International Journal of Refrigeration 103: 274-286.
- Kauffeld, M. (2008). "Trends and perspectives for supermarket refrigeration systems; Trends und Perspektiven fuer Supermarkt-Kaelteanlagen." Germany.
- Kazachki, G. S. and D. K. Hinde (2006). "Secondary Coolant Systems for Supermarkets." Ashrae Journal 48(9): 34-36,38,40,42-44,46.
- Kincheloe, M. C. (2019). Design and construction of a psychrometric testing facility for commercial scale heat exchanger coils. Department of Mechanical and Aerospace Engineering, Oklahoma State University. Master of Science.
- Klein, S. A. (2020). EES: Engineering equation solver, Academic Professional Version 10.835-3D.
- Kruse, H. (2000). "Refrigerant use in Europe." Ashrae Journal 42: 16-18+21.
- Lee, J., Y.-C. Kwon and M. H. Kim (2003). "An improved method for analyzing a fin and tube evaporator containing a zeotropic mixture refrigerant with air mal-distribution." International Journal of Refrigeration 26(6): 707-720.
- Lee, M., Y. Kim, H. Lee and Y. Kim (2010). "Air-side heat transfer characteristics of flat plate finned-tube heat exchangers with large fin pitches under frosting conditions." International Journal of Heat and Mass Transfer 53(13): 2655-2661.
- Li, W. and P. Hrnjak (2021). "Single-phase flow distribution in plate heat exchangers: Experiments and models." International Journal of Refrigeration 126: 45-56.
- Llopis, R., D. Calleja-Anta, D. Sánchez, L. Nebot-Andrés, J. Catalán-Gil and R. Cabello (2019). "R-454C, R-459B, R-457A and R-455A as low-GWP replacements of R-404A: Experimental evaluation and optimization." International Journal of Refrigeration 106: 133-143.

Longo, G. A., S. Mancin, G. Righetti and C. Zilio (2019). "Boiling of the new low-GWP refrigerants R1234ze(Z) and R1233zd(E) inside a small commercial brazed plate heat exchanger." International Journal of Refrigeration 104: 376-385.

Makhani, K. K. (2020). Design, Simulation, and Construction of a Hot-Gas Bypass Chiller for a Commercial Scale Psychrometric Coil Testing Facility. Department of Mechanical and Aerospace Engineering, Oklahoma State University. Master of Science.

Mateu-Royo, C., A. Mota-Babiloni, J. Navarro-Esbrí and Á. Barragán-Cervera (2021). "Comparative analysis of HFO-1234ze(E) and R-515B as low GWP alternatives to HFC-134a in moderately high temperature heat pumps." International Journal of Refrigeration 124: 197-206.

Modelica (1997). An object oriented language, Modelica Association Project.

Redo, M. A., J. Jeong, S. Yamaguchi, K. Saito and H. Kim (2020). "Characterization and improvement of flow distribution in a vertical dual-compartment header of a microchannel heat exchanger." International Journal of Refrigeration 116: 36-48.

Saad Yatim, A., P. Shashikant Deokar and L. Cremaschi (2016). "Oil retention in a microchannel type condenser and its effects on heat transfer rate performance and on the pressure drop." Science and Technology for the Built Environment 23(1): 166-180.

Saleem, S., O. Sarfraz, C. R. Bradshaw and C. K. Bach (2020). "Development of novel experimental infrastructure for collection of high-fidelity experimental data for refrigerant to air heat exchangers." International Journal of Refrigeration **114**: 189-200.

Sarfraz, O. (2020). "Development and Validation of a Reduced Order Fin-And-Tube Heat Exchanger Model". Oklahoma State University. 27737643: 202.

TIL (2019). Software package for the simulation of thermal systems, TLK-Thermo GmbH.

UNEP (2020). Handbook for the Montreal Protocol on Substances that Deplete the Ozone Layer, Ozone Secretariat.

Warrender (2021). Regenerative Turbine Pump Manufacturer. Wood Dale, IL, USA.

Warrender (2021b). Pump Curve. Personal communication. Received permission: 4/22/2021.

Yi, Y., T. Hu, X. Xie and Y. Jiang (2020). "Experimental assessment of a detachable plate falling film heat and mass exchanger couple using lithium bromide and water as working fluids." International Journal of Refrigeration 113: 219-227.

Yu, B., H. Ouyang, J. Shi, W. Liu and J. Chen (2021). "Evaluation of low-GWP and mildly flammable mixtures as new alternatives for R410A in air-conditioning and heat pump system." International Journal of Refrigeration 121: 95-104.

APPENDICES

APPENDIX A

EES STEADY STATE MODEL

\$UnitSystem SI MASS DEG bar C kJ

"Conditions"

//R\$='R410A'

//T_evap_sat= 7.2 [C]

//T_gas_return=18 [C]

//T_comp_discharge=54.4 [C]

//DELTAT_subcooled_cyc=8.3 [C]

DELTAP=10[psi]*convert(psi,bar)

//DELTAP_evap=0.8055*convert(psi,bar)

//DELTAP_pump=14.85*convert(psi,bar)

DELTAP_pump=15*convert(psi,bar)

DELTAT_subcooled=5 [C]

//Q_cond=20*3.516 [kW]

"Working fluid in refrigerant loop"

"Compressor Suction Dew Point Temperature"

"Compressor Return gas Temperature"

"Compressor Discharge Temperature"

"Actual Vapor Compression Cycle"

"Pressure drop or gain(psi) in tested coil-fixed"

"Pressure drop or gain(bar) in tested coil-fixed"

"Pressure drop or gain(psi) in pump-fixed"

"Pressure drop or gain(bar) in pump-fixed"

"subcooling for pumped loop cycle"

"Cascade condenser capacity"

"State 1: Leaving the evaporator"

P_1=pressure(R\$,T=T_evap_sat,x=1)

"Pressure of saturated vapor at compressor
suction Dew Point temperature"

h=enthalpy(R\$,T=T_evap_sat,x=1)

T[1]=T_gas_return

"Evaporator outlet temperature"

P[1]=P_1

"Evaporator outlet pressure"

h[1]=enthalpy(R\$,T=T[1],P=P[1])

"Evaporator outlet enthalpy"

s[1]=entropy(R\$,T=T[1],P=P[1])

"Evaporator outlet entropy"

"State 2 : Entering the cascade condenser (Just pressure drop of 15 psi) "

$P[2]=P[1]$ "Condenser inlet pressure"
 $h[2]=h[1]$ "Condenser inlet enthalpy"
 $s[2]=\text{entropy}(R,\mathbf{h}=h[2],\mathbf{P}=P[2])$ "Condenser inlet entropy"
 $T[2]=\text{temperature}(R,\mathbf{P}=P[2],\mathbf{h}=h[2])$ "Condenser inlet temperature"
 $T_{\text{dew_cond}}=\text{temperature}(R,\mathbf{P}=P[2],\mathbf{x}=1)$ "Condenser dew point temperature"
 $h_{\text{dew_cond}}=\text{enthalpy}(R,\mathbf{P}=P[2],\mathbf{x}=1)$ "Condenser dew point enthalpy"

"State 3 : Leaving condenser and entering pump"

$P[3]=P[2]$ "Condenser outlet pressure - assumed no pressure drop"
 $T_{\text{cond}}=\text{temperature}(R,\mathbf{P}=P[3],\mathbf{x}=0)$
 $T[3]=T_{\text{cond}}-\text{DELTAT}_{\text{subcooled}}$ "Condenser outlet temperature"
 $h[3]=\text{enthalpy}(R,\mathbf{P}=P[3],\mathbf{T}=T[3])$ "Condenser outlet enthalpy"
 $s[3]=\text{entropy}(R,\mathbf{T}=T[3],\mathbf{P}=P[3])$ "Condenser outlet entropy"

"State 4: leaving the pump and entry into heater"

$s_{\text{id_4}}=s[3]$ "Ideal entropy at outlet of pump"
 $P[4]=P[3]+\text{DELTAP}_{\text{pump}}$ "Pump outlet pressure"
 $h_{\text{id_4}}=\text{enthalpy}(R,\mathbf{P}=P[4],\mathbf{s}=s_{\text{id_4}})$ "Ideal enthalpy at outlet of pump"
 $\text{eta}=.9$ "Pump efficiency"
 $\text{eta}=(h_{\text{id_4}}-h[3])/(h[4]-h[3])$ " $h[4]$ - pump outlet enthalpy"
 $T[4]=\text{temperature}(R,\mathbf{P}=P[4],\mathbf{h}=h[4])$ "Pump outlet temperature"
 $s[4]=\text{entropy}(R,\mathbf{P}=P[4],\mathbf{h}=h[4])$ "Pump outlet entropy"

"State 5: Entering the Evaporator"

"In actual vapor compression cycle - These equations help to identify the properties of the refrigerants at inlet of the tested coil"

$P_2=\text{pressure}(R,\mathbf{T}=T_{\text{comp_discharge}},\mathbf{x}=1)$
 $T_3=\text{temperature}(R,\mathbf{P}=P_2,\mathbf{x}=0)-\text{DELTAT}_{\text{subcooled_cyc}}$

T_prevalve= **temperature**(R\$,P=P_2,h=h[4])

h[5]=**enthalpy**(R\$,T=T_3,P=P_2)

"Evaporator inlet enthalpy"

s[5]=**entropy**(R\$,h=h[5],P=P[1])

"Evaporator inlet entropy"

P[5]=P[1]+DELTAP

"Evaporator inlet pressure"

x=**quality**(R\$,h=h[5],P=P[5])

"Evaporator inlet quality"

T[5]=**temperature**(R\$,h=h[5],P=P[5])

"Evaporator inlet temperature"

"Capacity"

Q_cond=m_dot*(h[2]-h[3])

"This equation determines the mass flow rate"

Q_heater=m_dot*(h[5]-h[4])

"Capacity gained from pre-evaporator"

Q_evap=m_dot*(h[1]-h[5])

"Capacity gained in tested HX"

"Plot"

"PH plot - dynamic plot which changes with the refrigerants and the conditions"

Pc=**p_crit**(R\$)

P_do[1]= 0.99*Pc

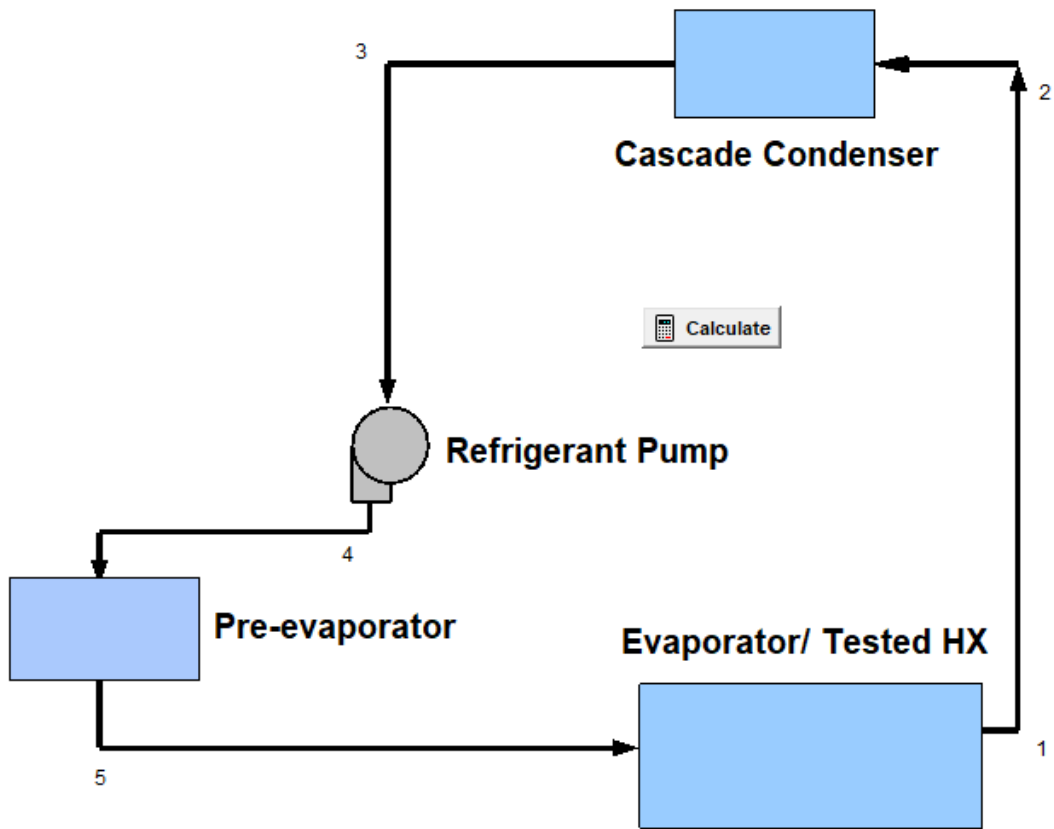
Duplicate i=2,91

P_do[i]=0.95*P_do[i-1]

h_l[i]=**enthalpy**(R\$,P=P_do[i],x=0)

h_g[i]=**enthalpy**(R\$,P=P_do[i],x=1)

End



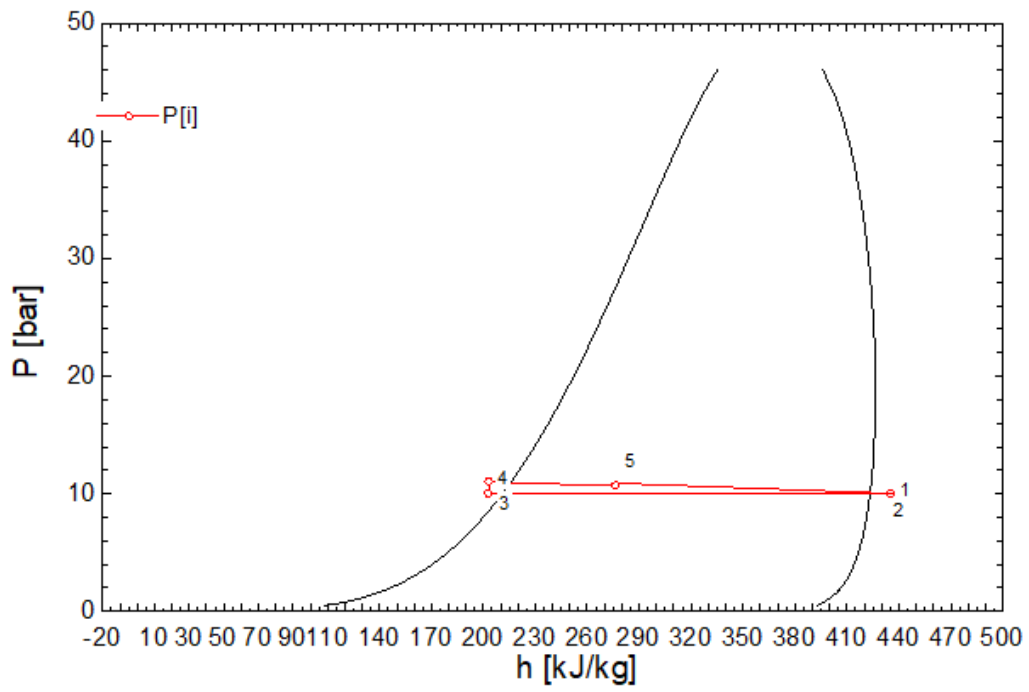
Input Variables

R\$= R410A	$T_{\text{evap,sat}} = 7.2$ [C]
	$T_{\text{gas,return}} = 18$ [C]
	$T_{\text{comp,discharge}} = 54.4$ [C]
	$\Delta T_{\text{subcooled,oyc}} = 8.3$ [C]
	$Q_{\text{cond}} = 58.2$ [kW]

Output Variables

$Q_{\text{evap}} = 39.79$ [kW]	$\dot{m} = 0.2504$ [kg/s]
$Q_{\text{heater}} = 18.38$ [kW]	$x = 0.2975$ [-]

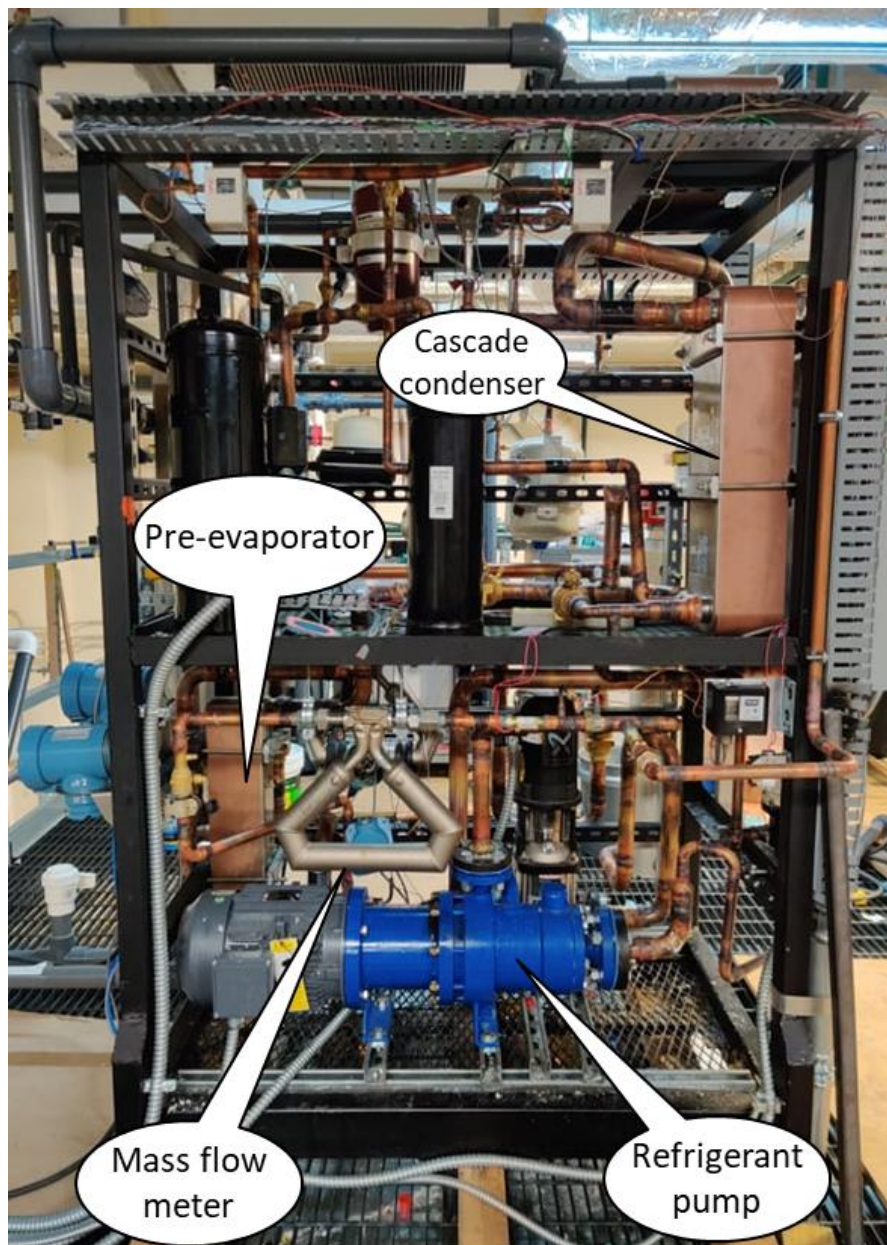
A.1: Graphical user interface of the model.



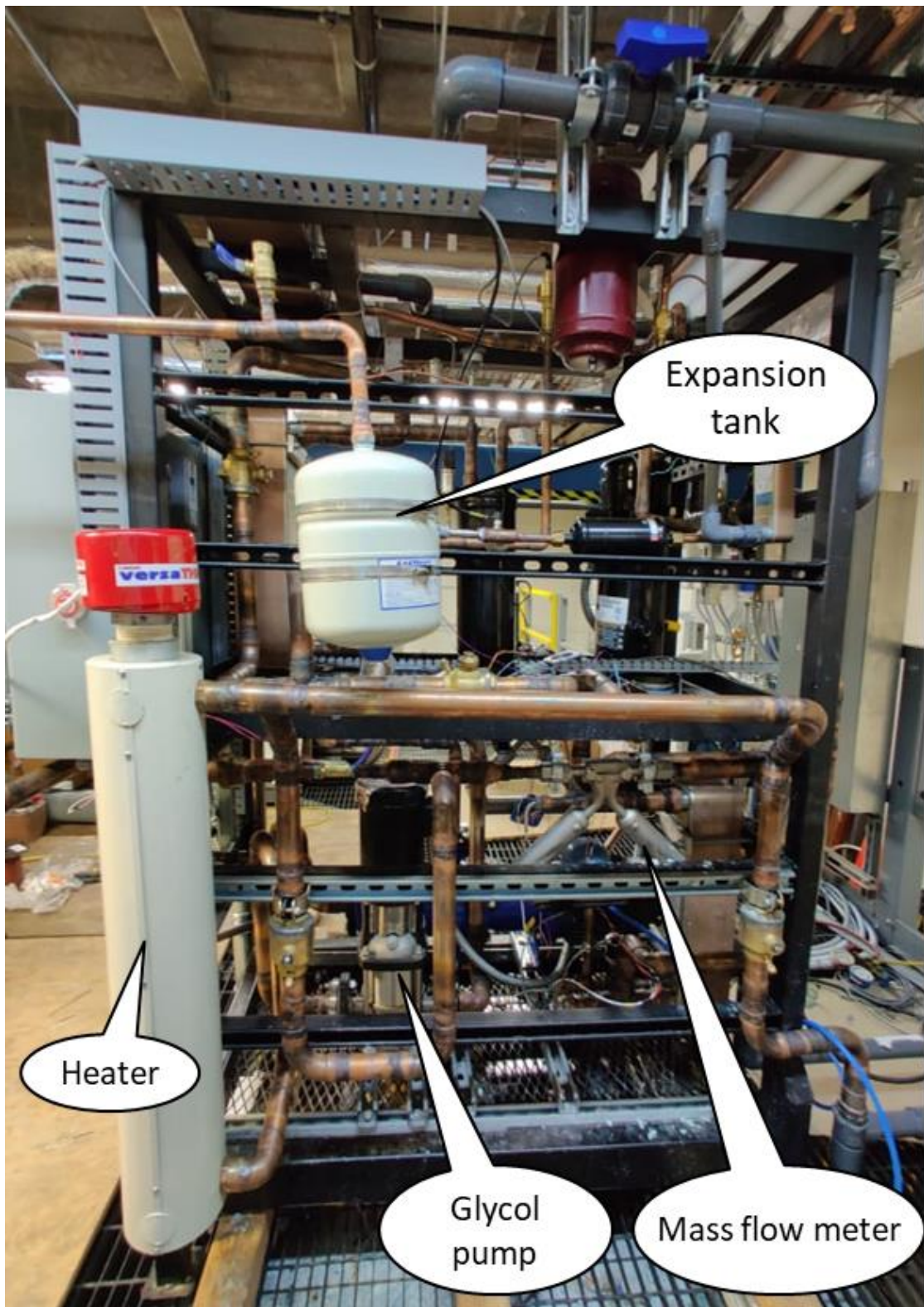
A.2: The dynamic p-h diagram in the EES model.

APPENDIX B

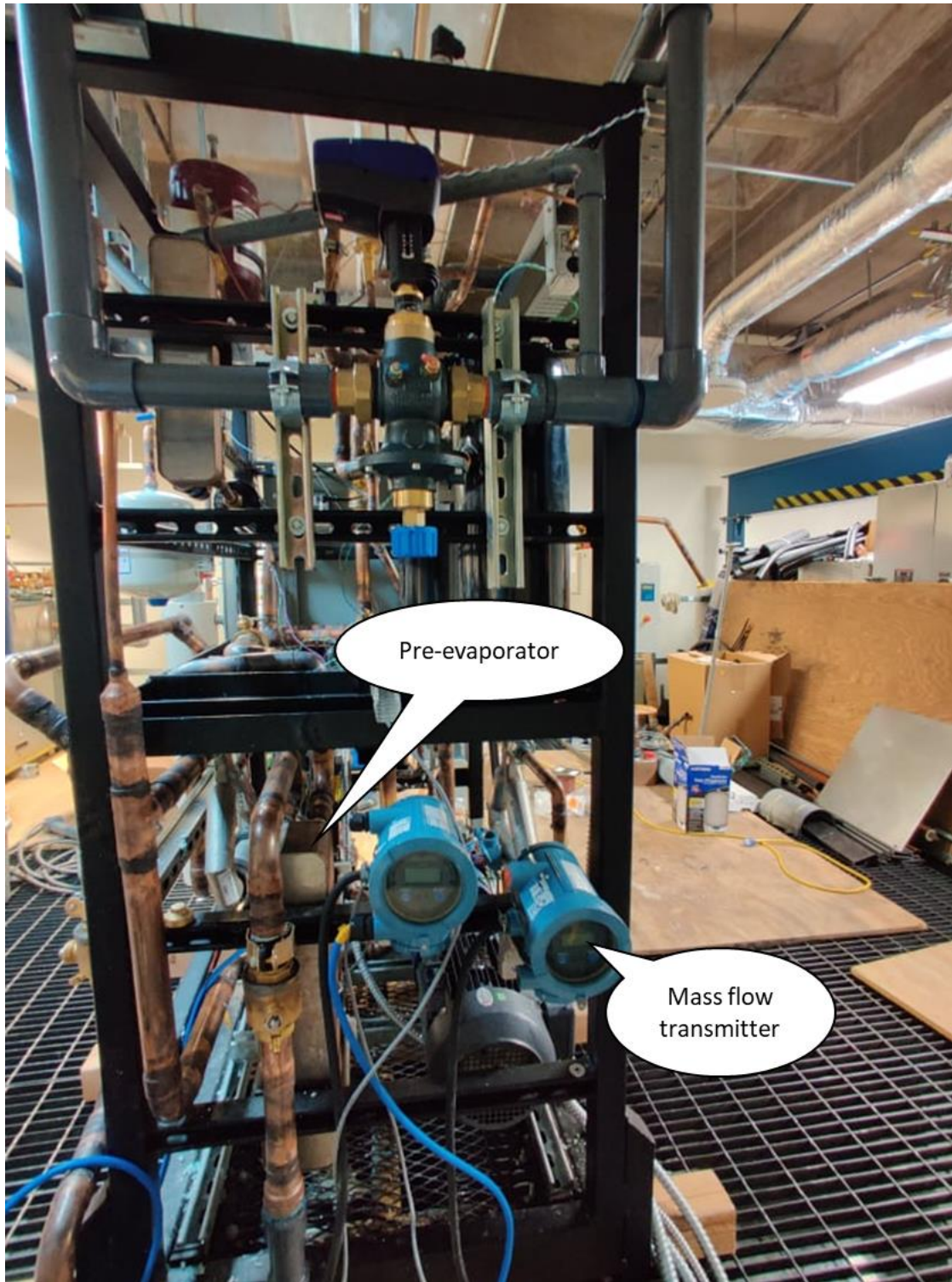
EXPERPERIMENTAL SETUP



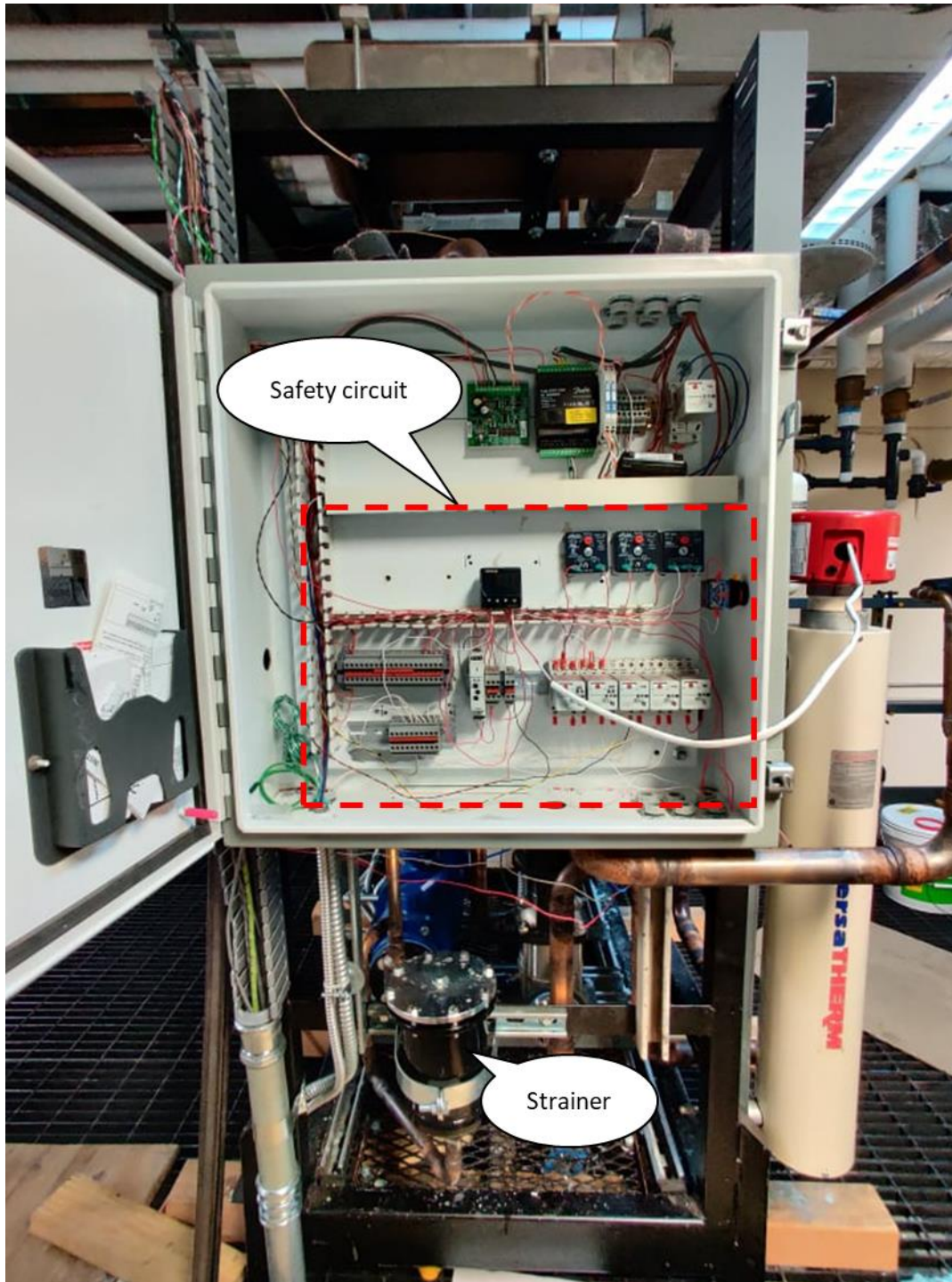
B.1: North side view of the setup.



B.2: South side view of the setup.



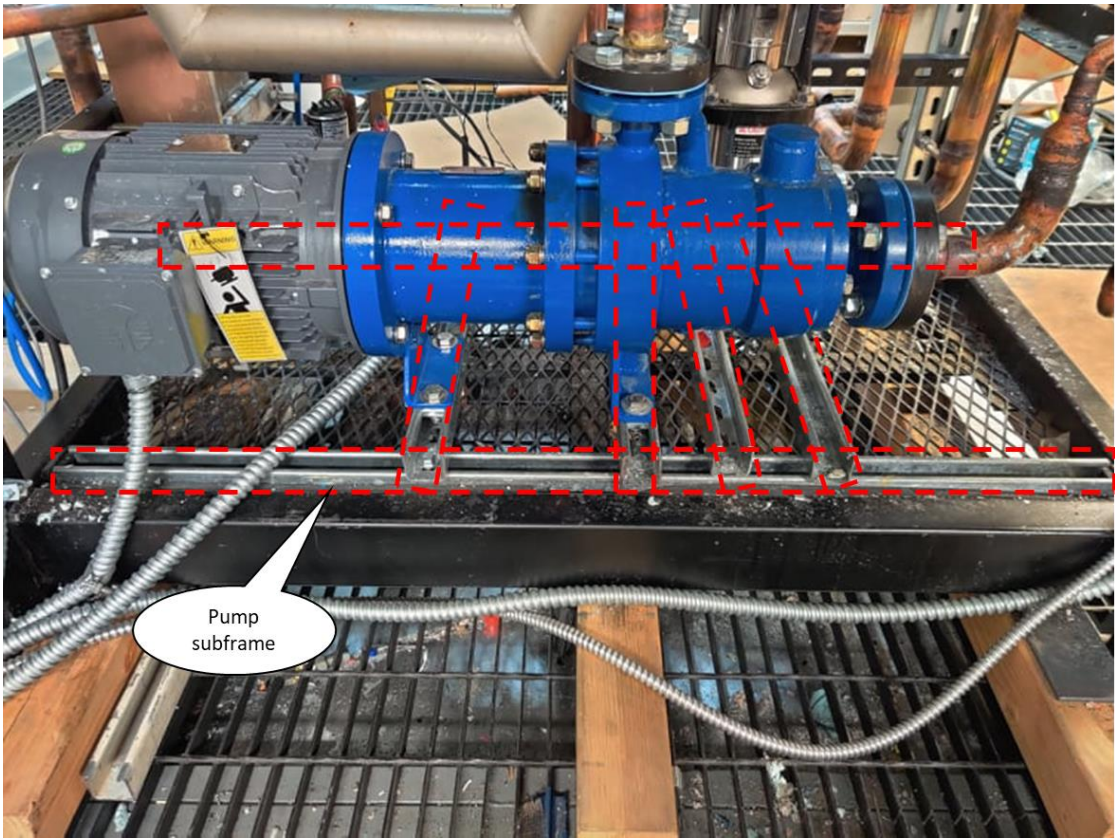
B.3: East side view of the setup.



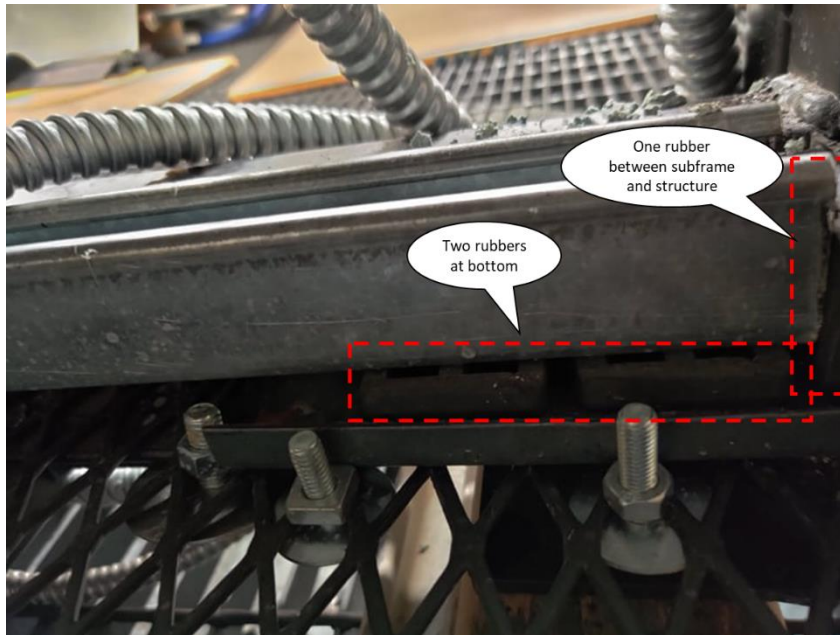
Safety circuit

Strainer

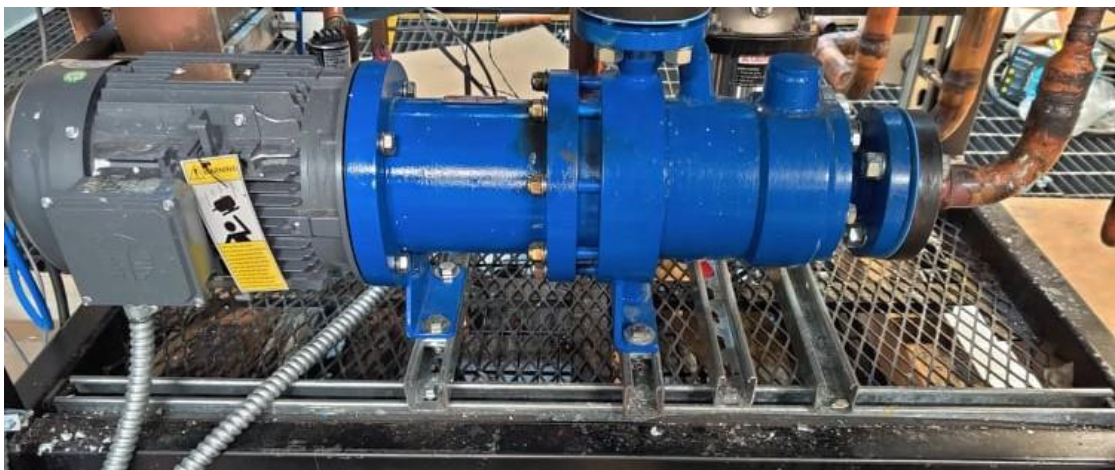
B.4: West side view of the setup



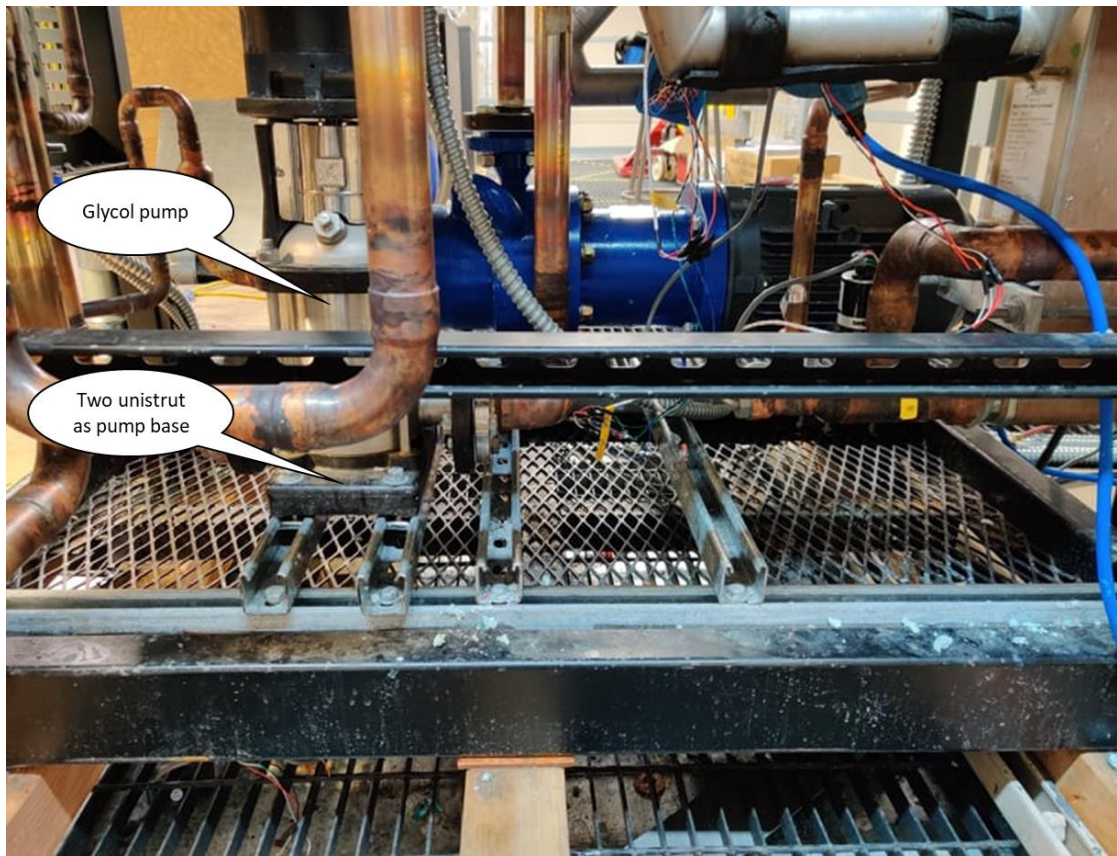
B.5: Pump subframe.



B.6: Each corner of the pump subframe is vertically supported two 2" by 2" natural rubbers (hardness rating – medium soft)



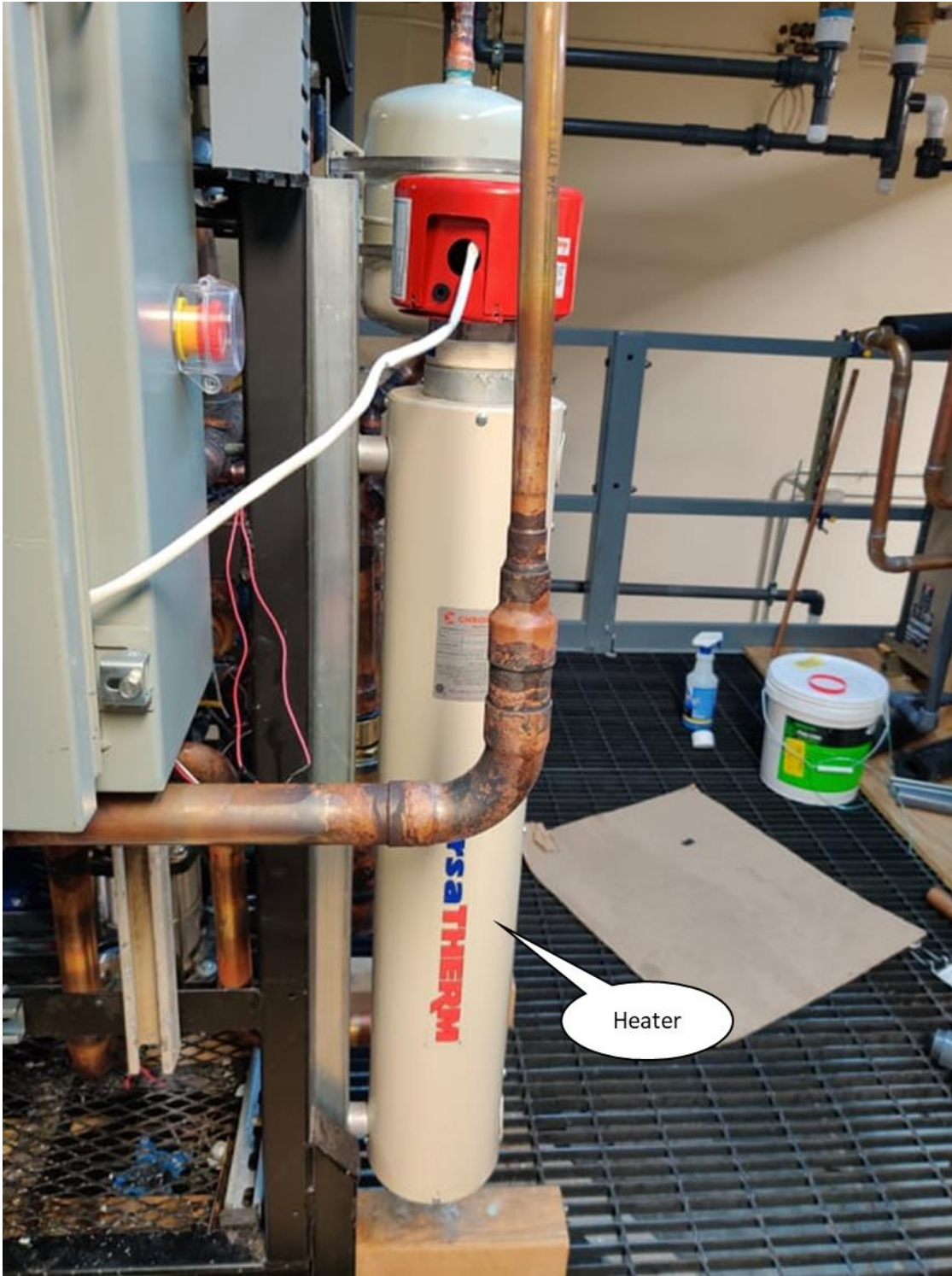
B.7: Refrigerant pump mounted on two pieces of unistrut that are part of the pump subframe.



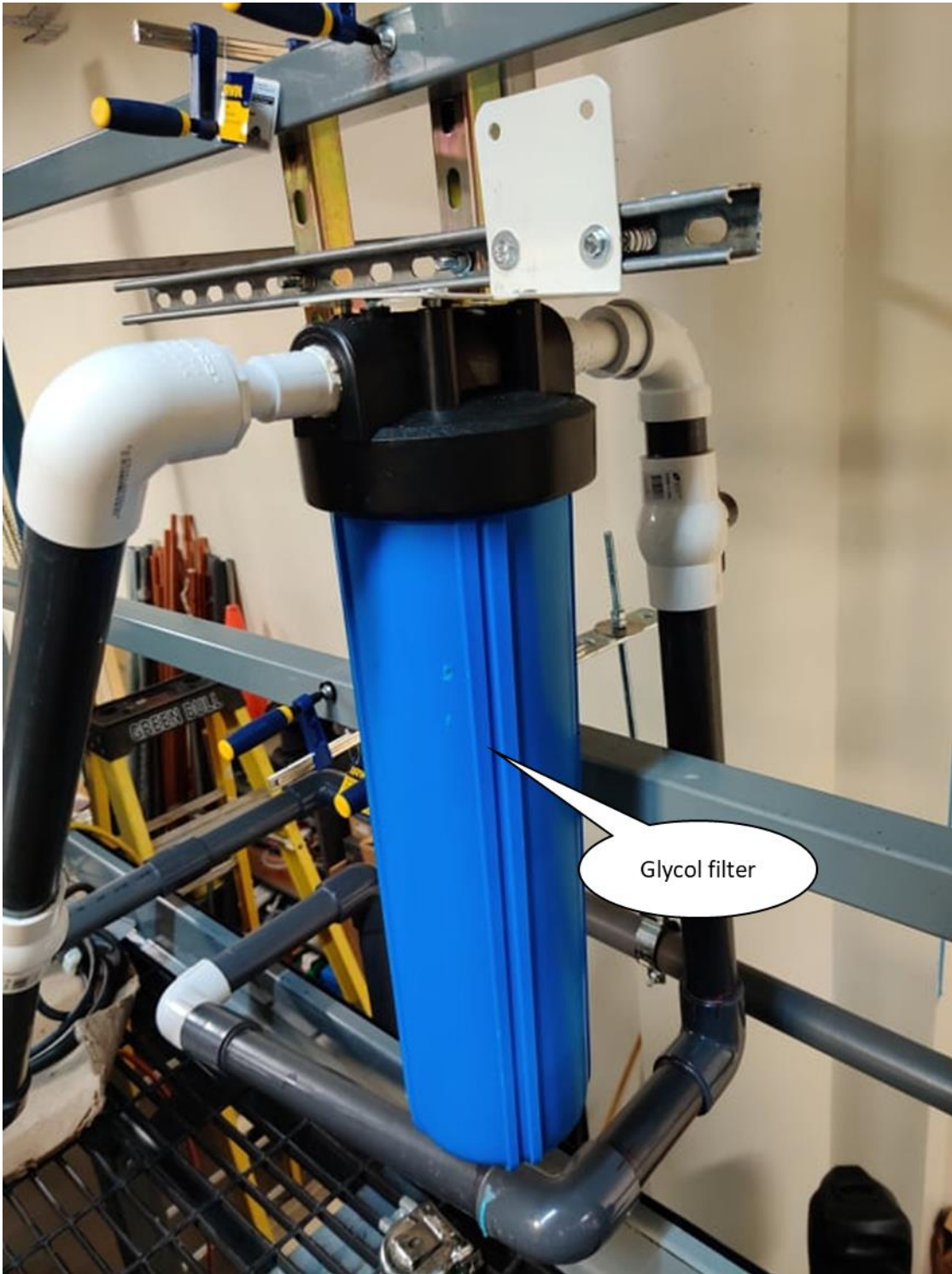
B.8: Glycol pump mounted on two pieces of unistrut that are part of the pump subframe.



B.9: HX attached to the unistrut of the structure with aluminum bar and rubber on both sides.



B.10: Heater mounted on the structure with a vertical unistrut.



B 11: Glycol filter mounted on the railing of the mezzanine on top of the wind tunnel.



B.12: Refrigerant strainer mounted with clamp on a unistrut.



B.13: Refrigerant mass flow meter mounted with clamps.



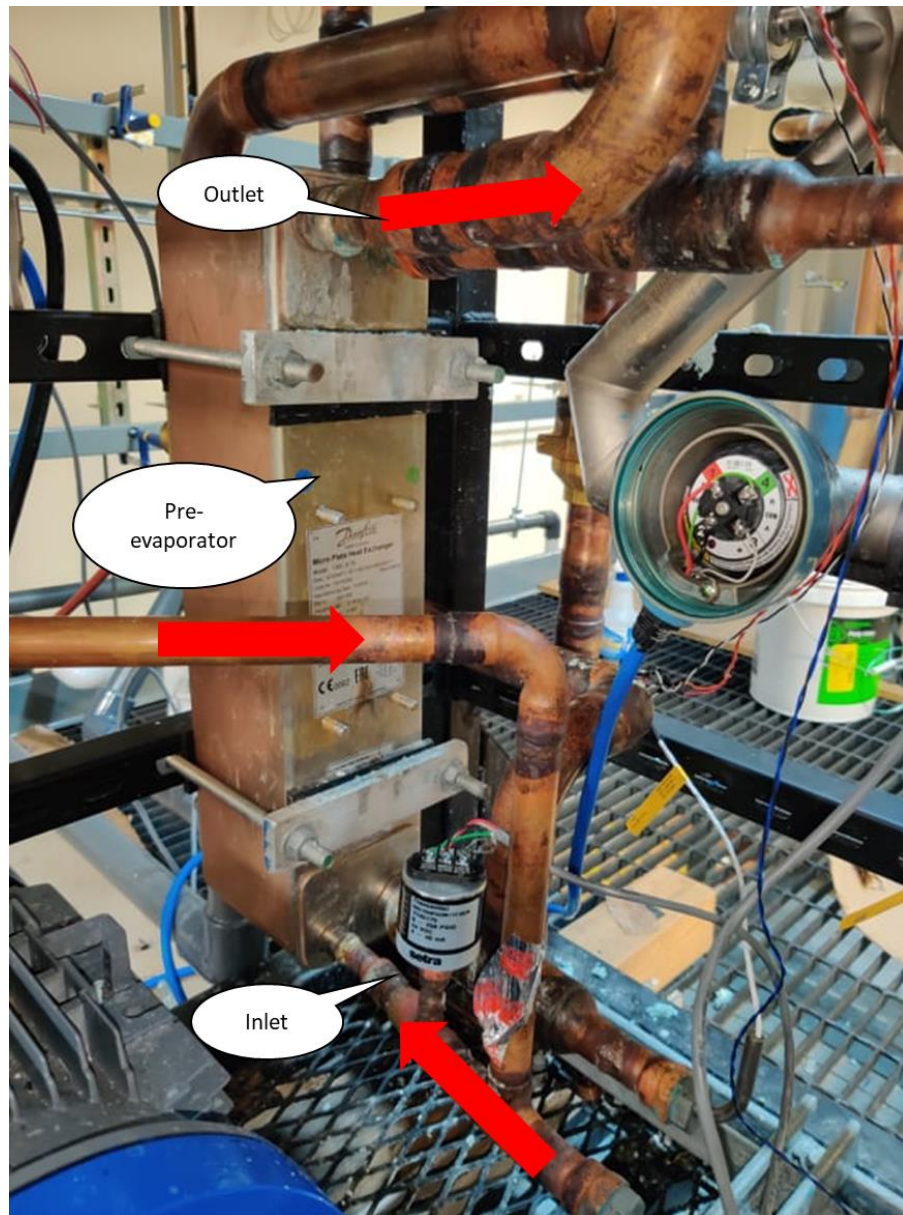
B.14: Transmitters of the mass flow meters mounted on the structure.



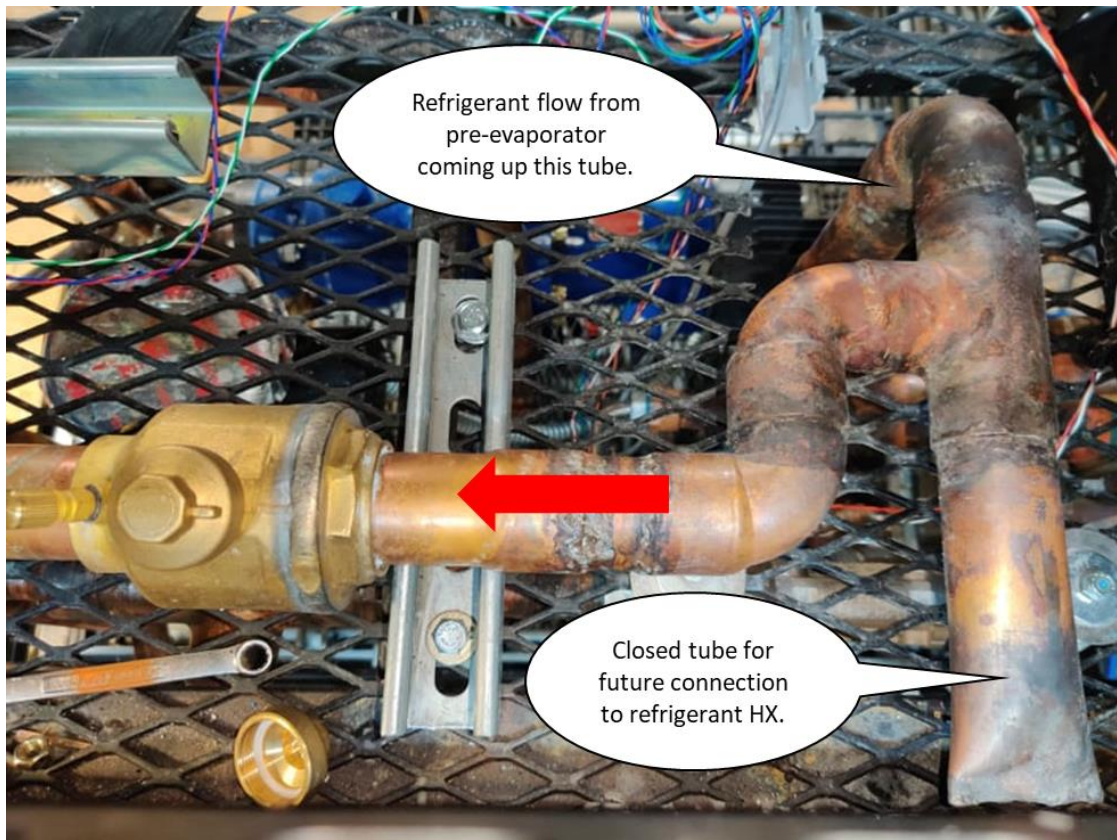
B.15: Glycol expansion tank mounted on the structure with bracket.

APPENDIX C

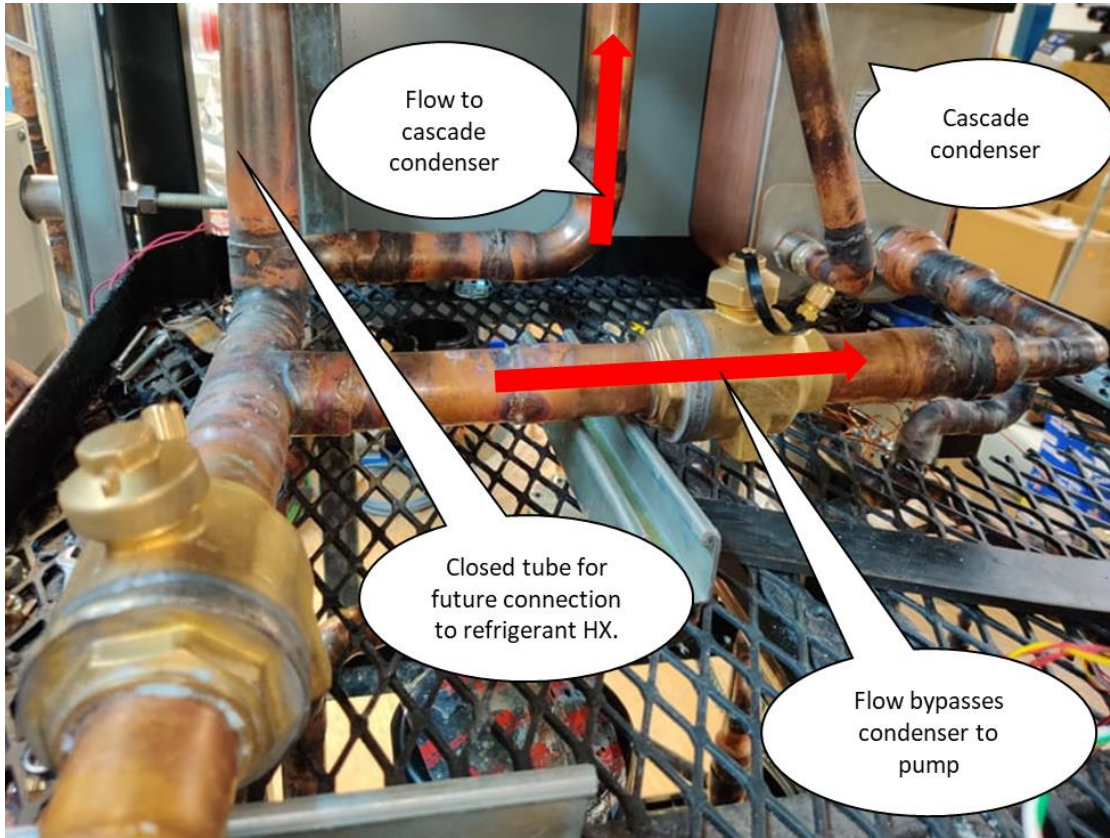
REFRIGERANT FLOW DIRECTION



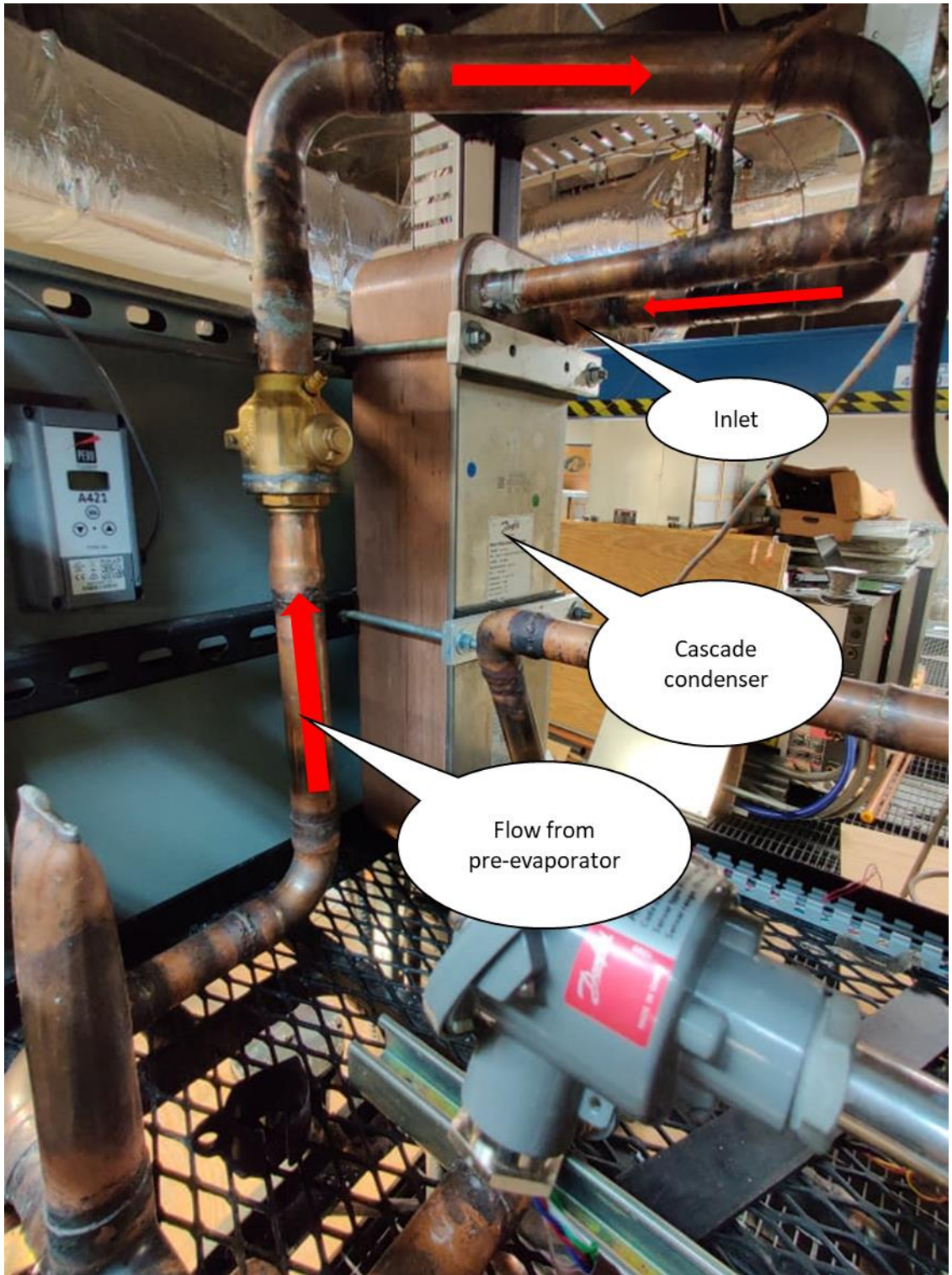
C.1: Flow direction to the inlet of the pre-evaporator.



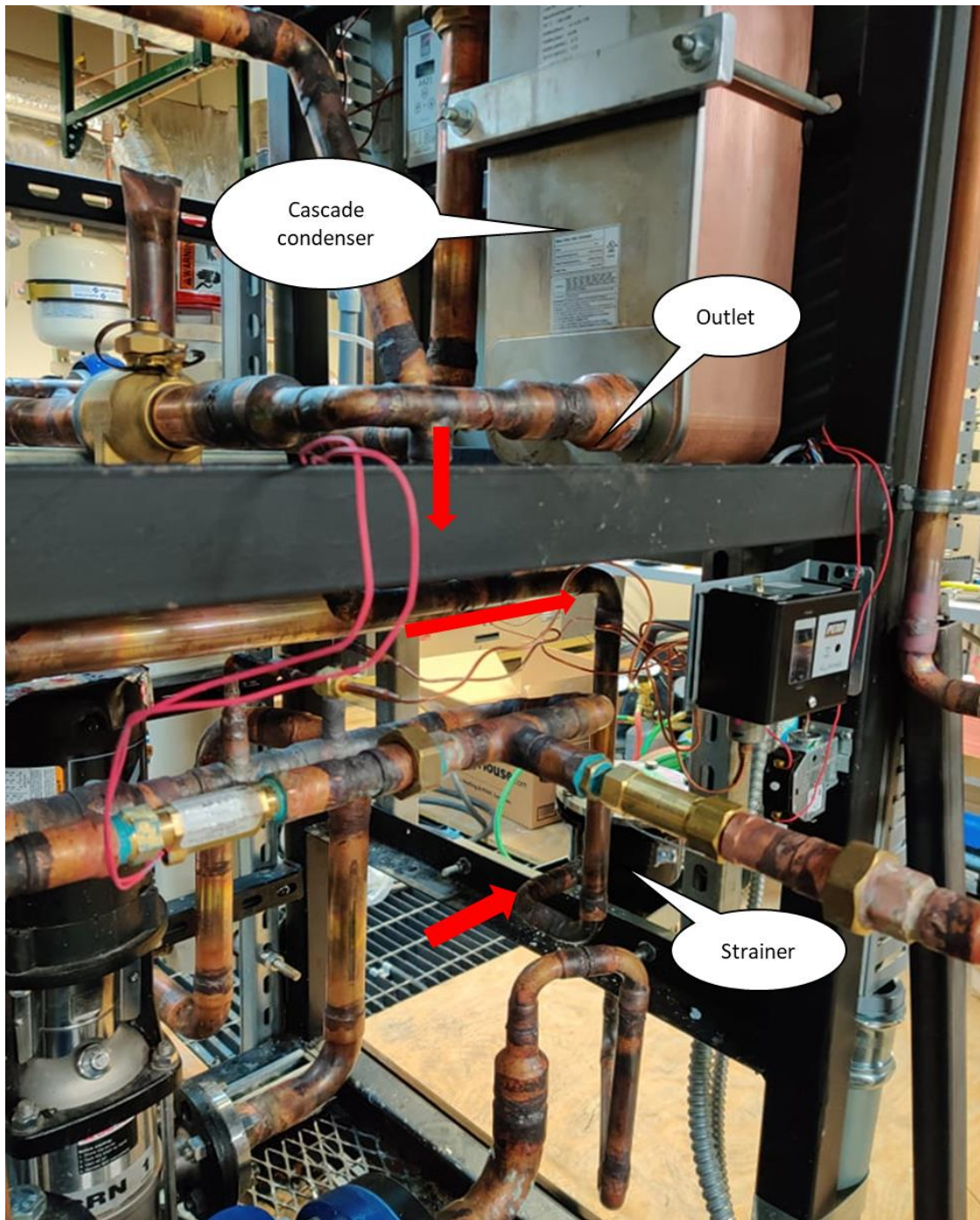
C.2: Flow from the pre-evaporator to the cascade condenser through intermediate valve.



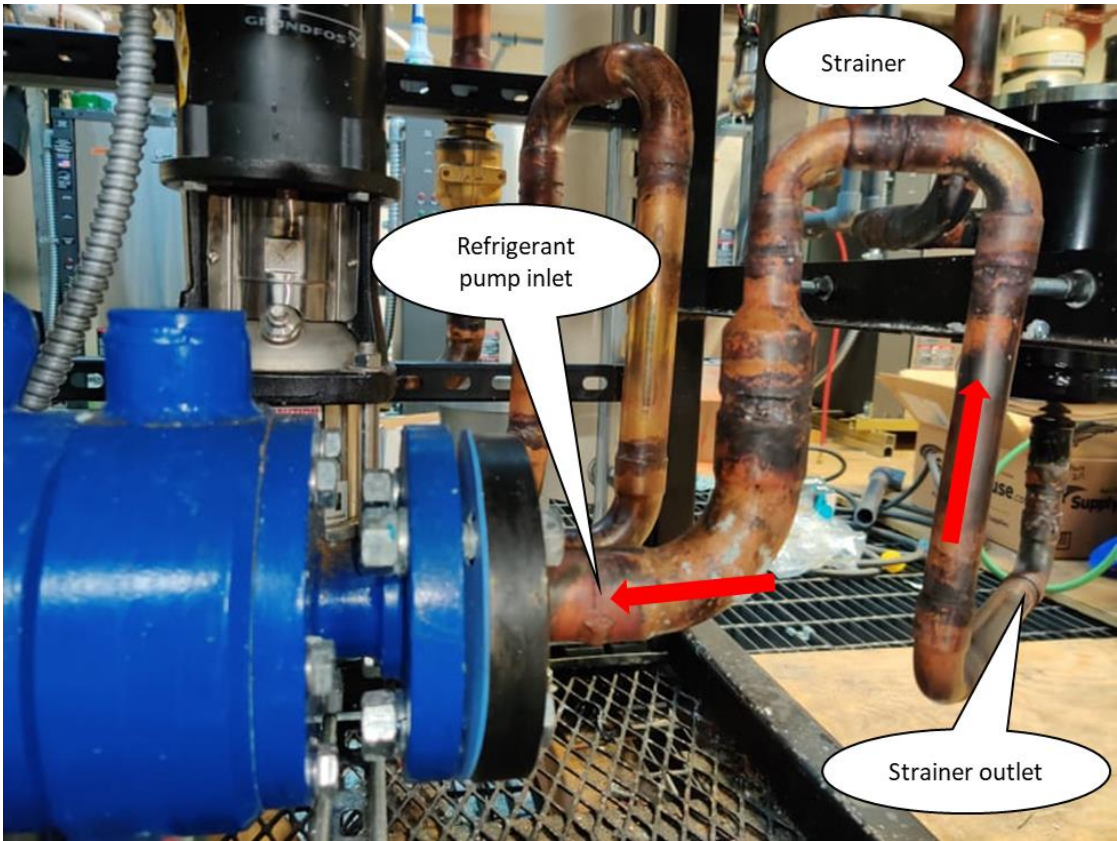
C.3: Flow from the pre-evaporator to the condenser and the bypass.



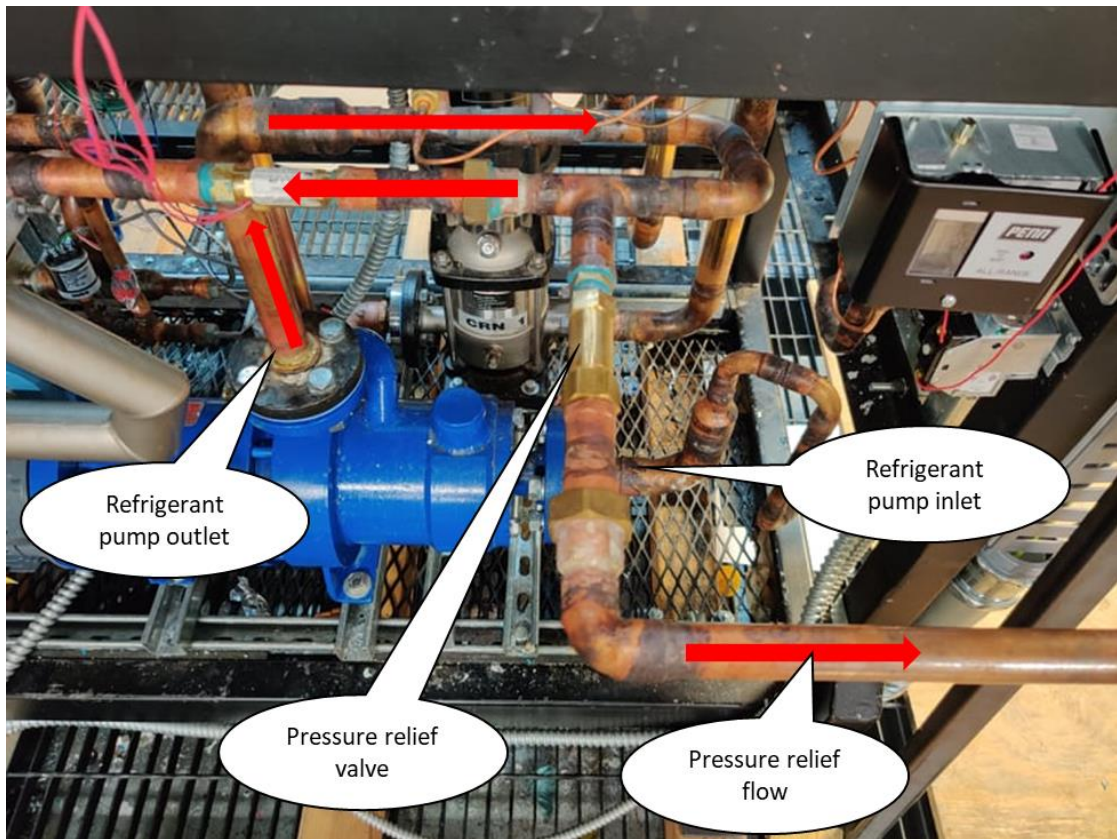
C.4: Flow to the inlet of the cascade condenser.



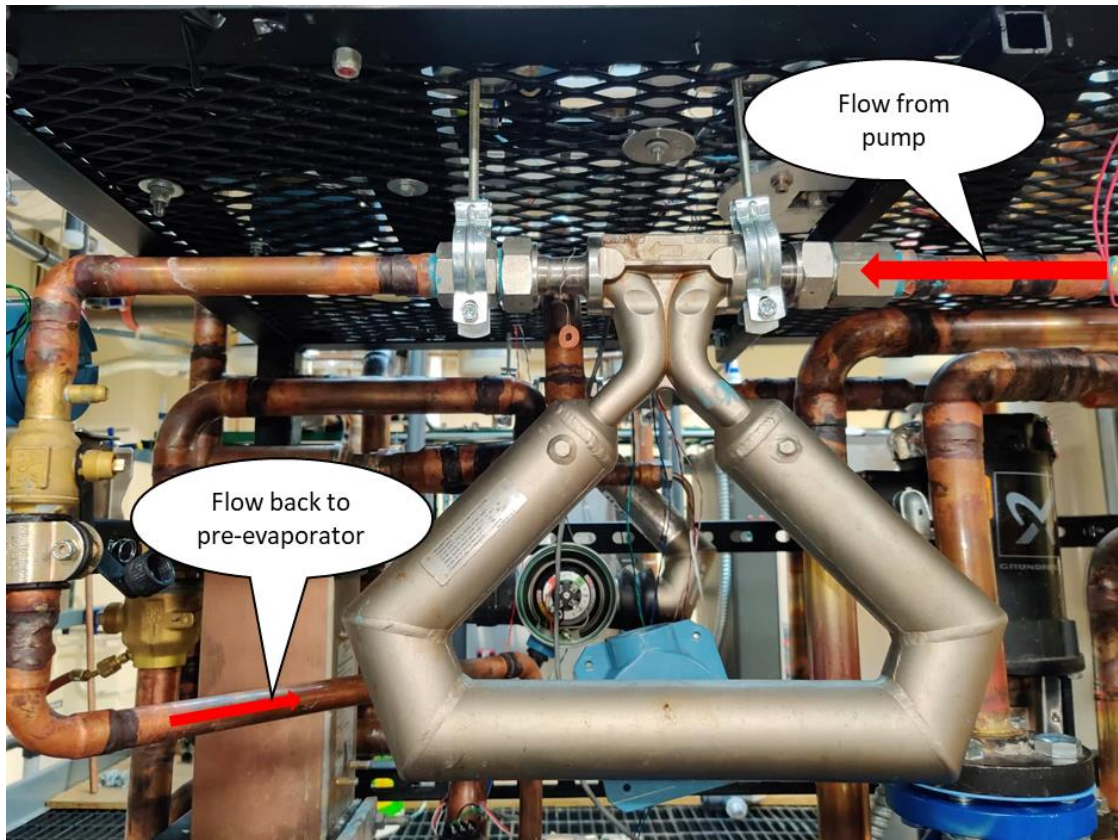
C.5: Flow from the cascade condenser to the strainer.



C.6: Flow from the strainer to the pump.



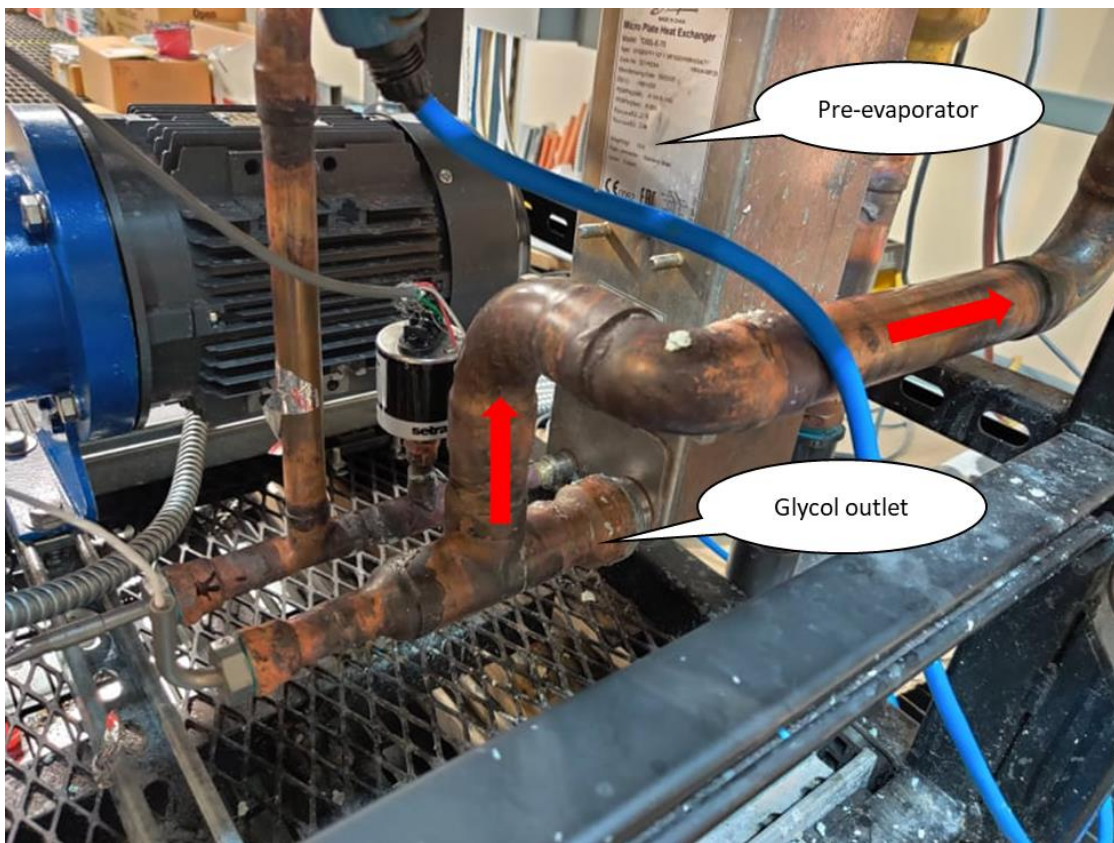
C.7: Flow from pump to mass flow meter with pressure relief in between.



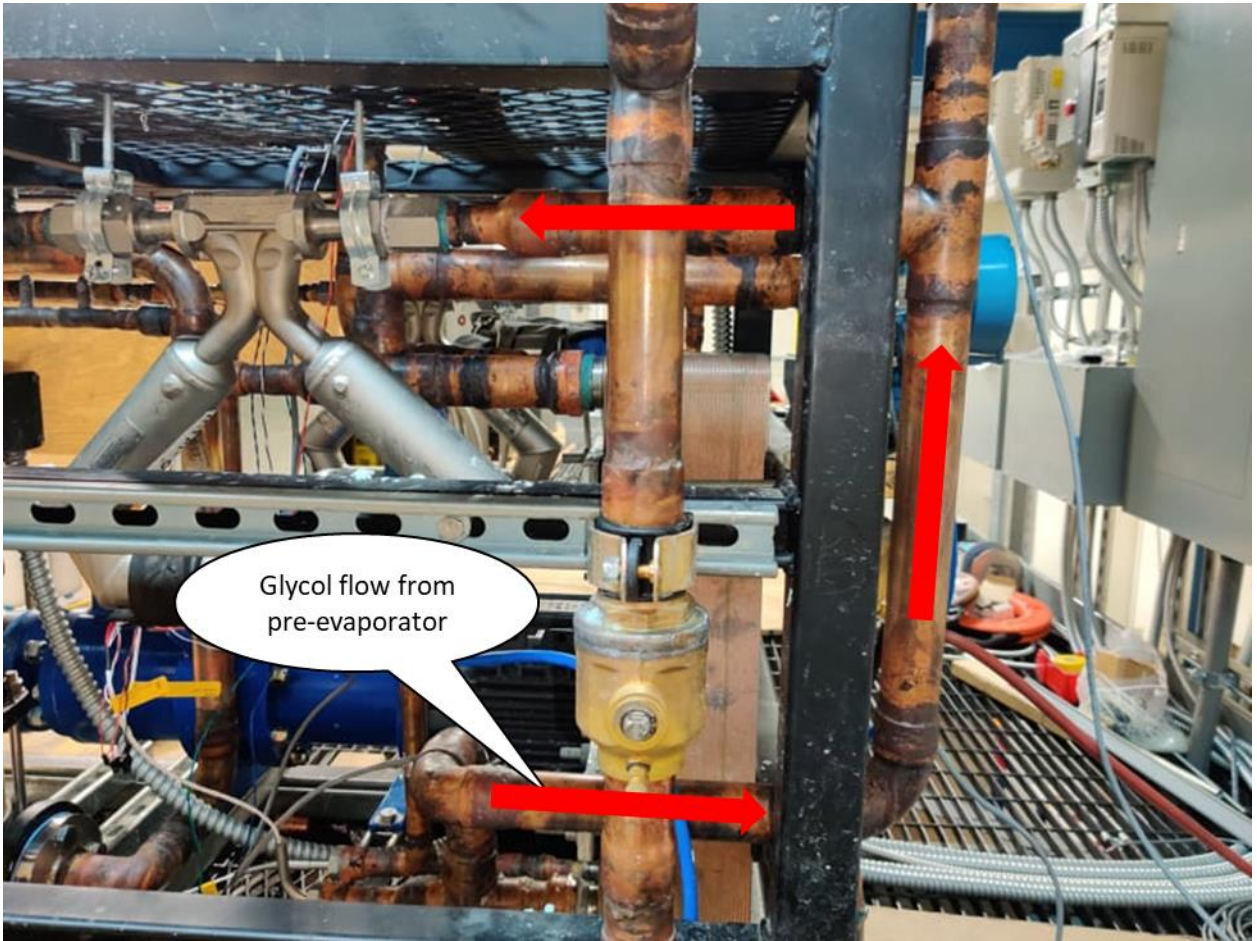
C.8: Flow to and from the mass flow meter.

APPENDIX D

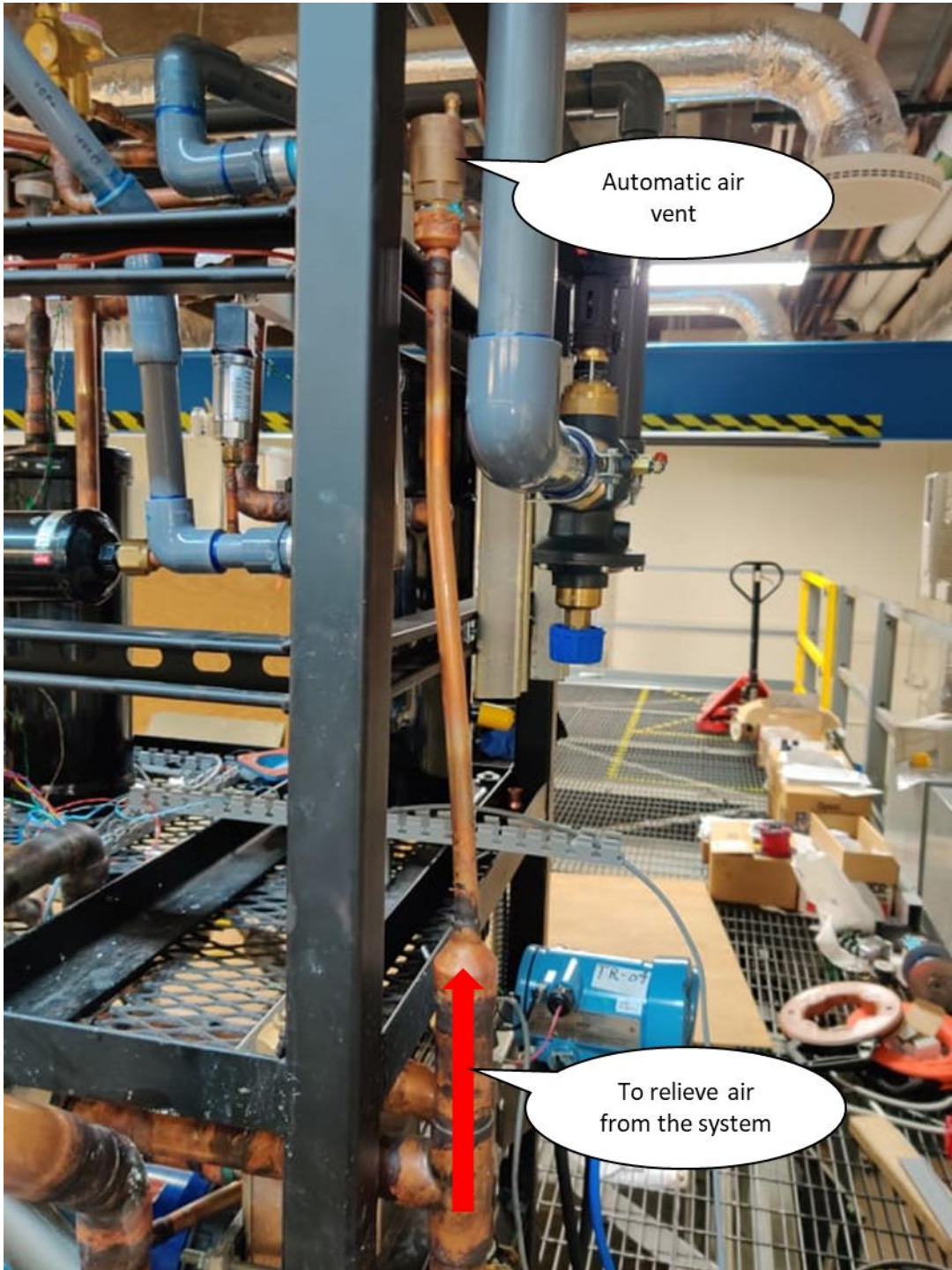
GLYCOL FLOW DIRECTION



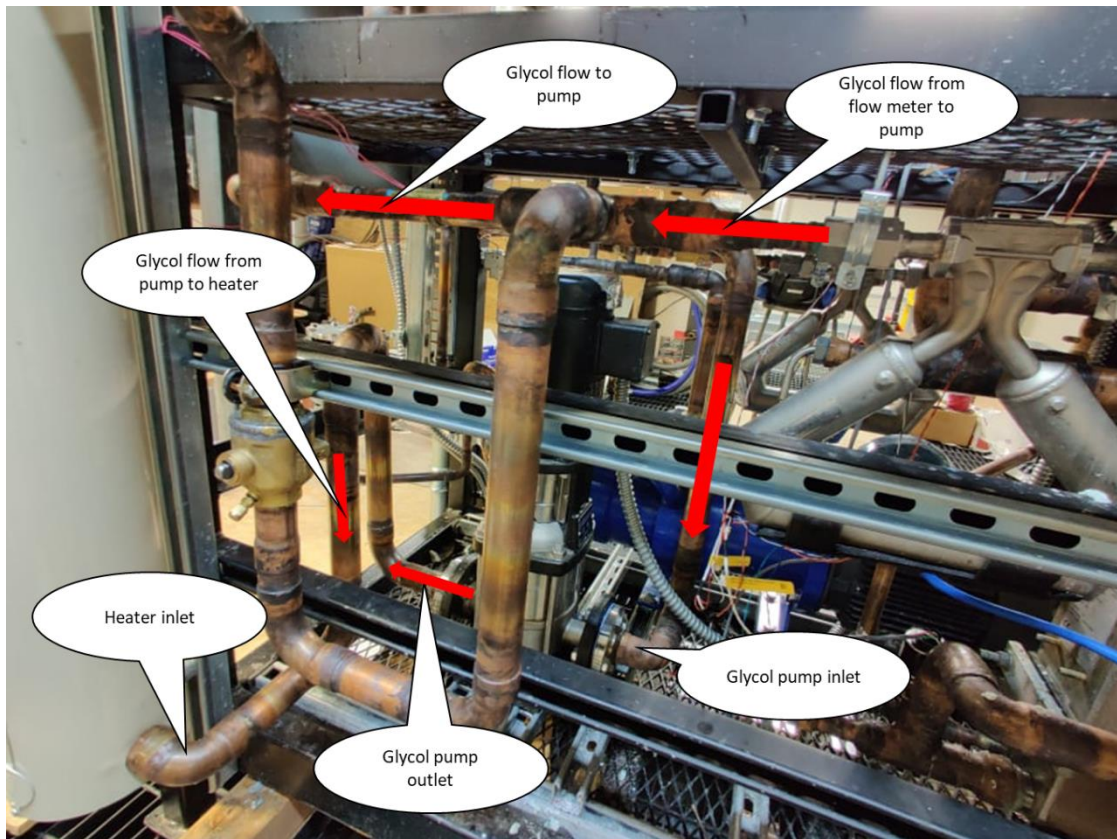
D.1: Flow from the pre-evaporator to mass flow meter.



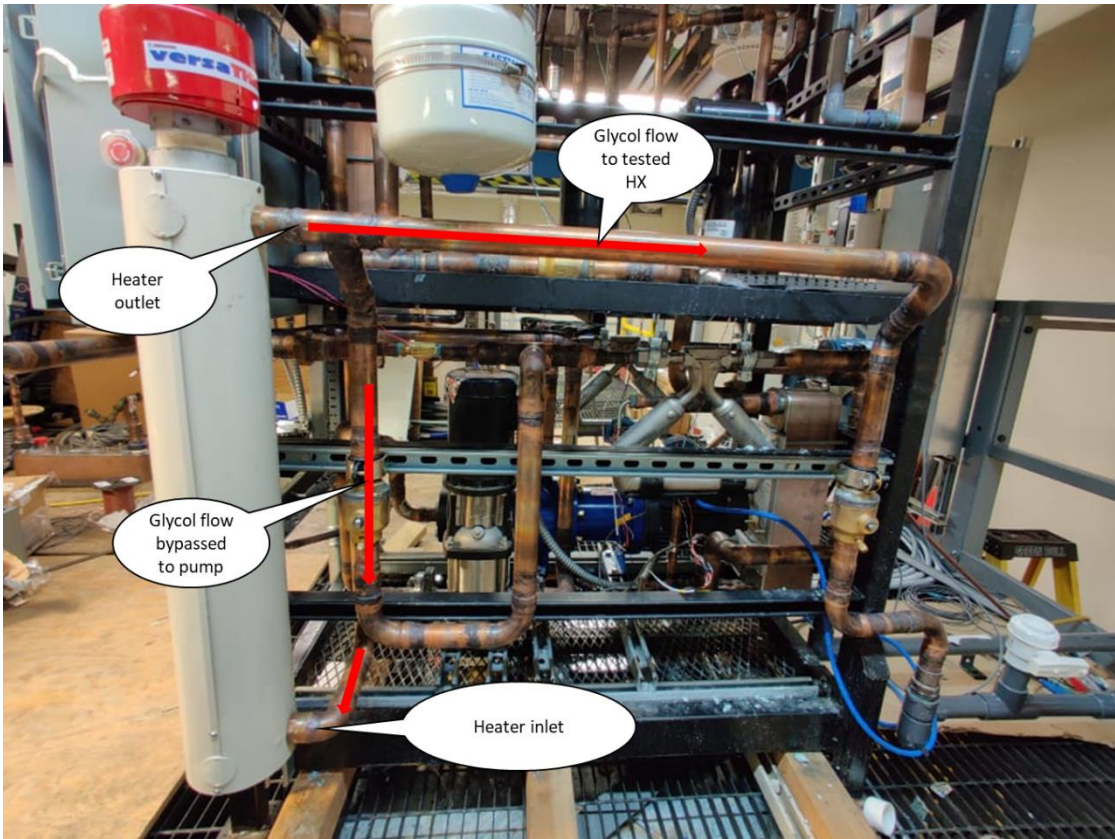
D.2: Complete path of flow from the pre-evaporator to mass flow meter.



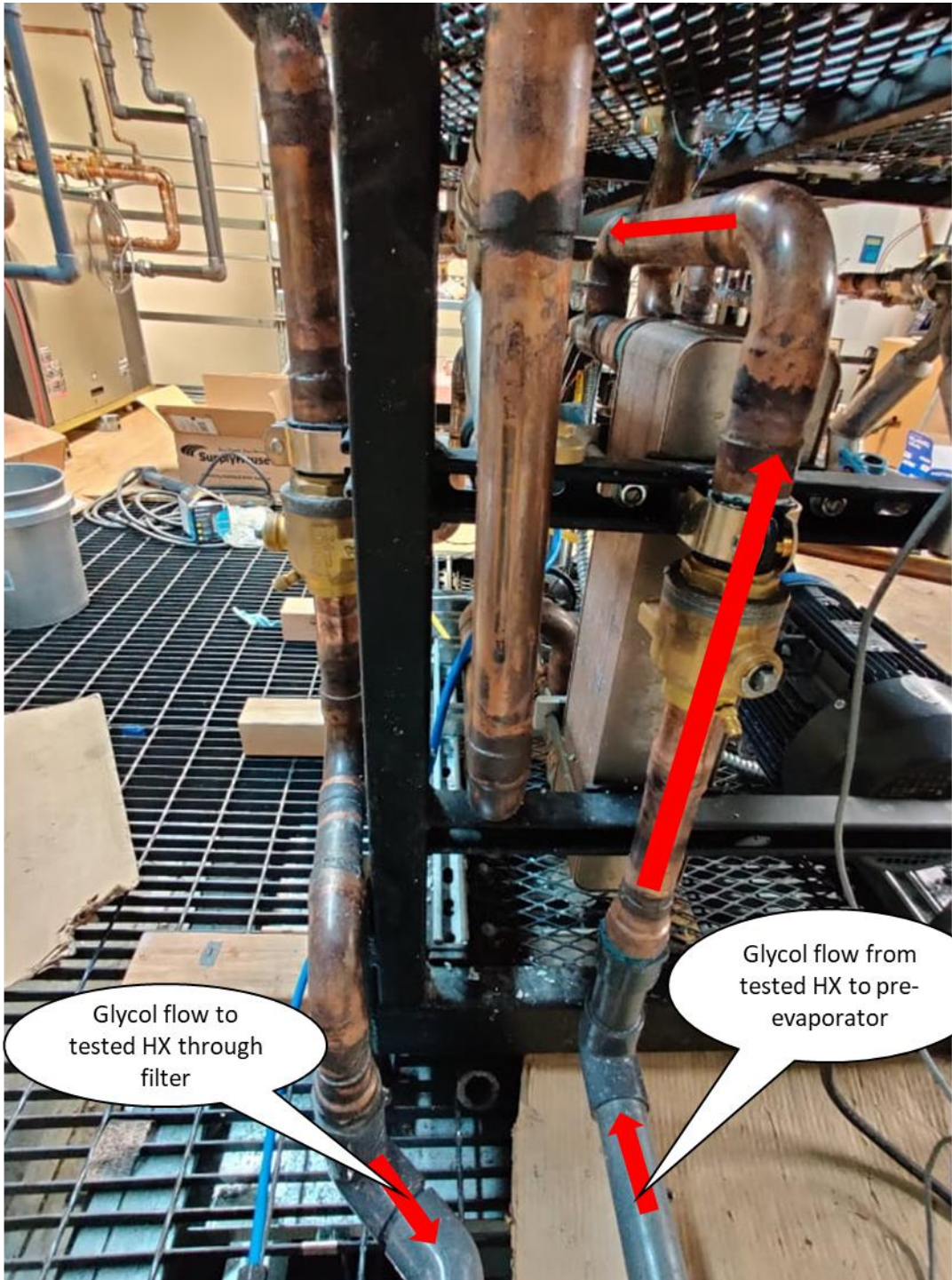
D.3: A branch before the flow meter to release air during charging.



D.4: Flow to the pump and from the pump to heater.



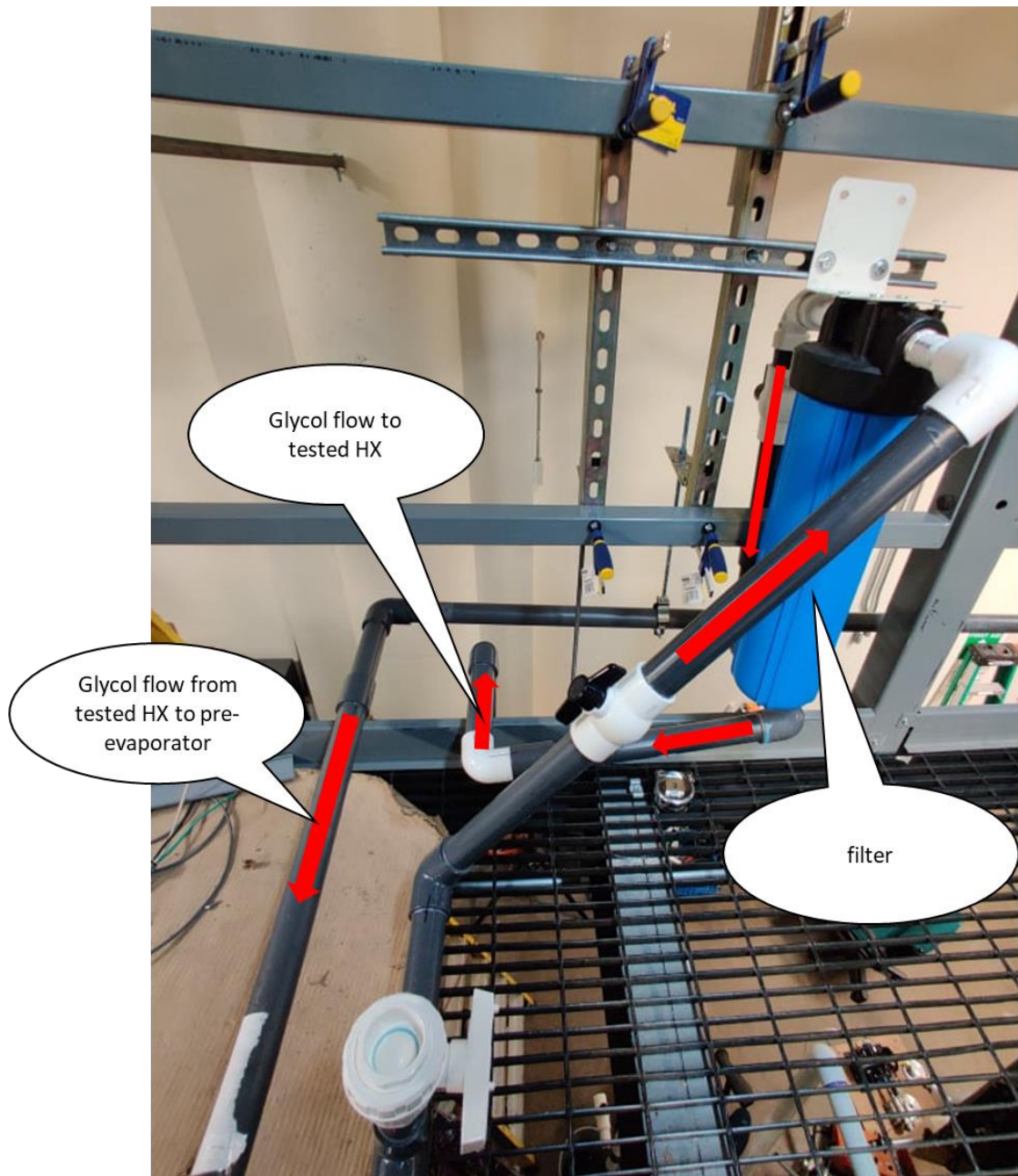
D.5: Flow from heater to the tested HX and bypass to the pump.



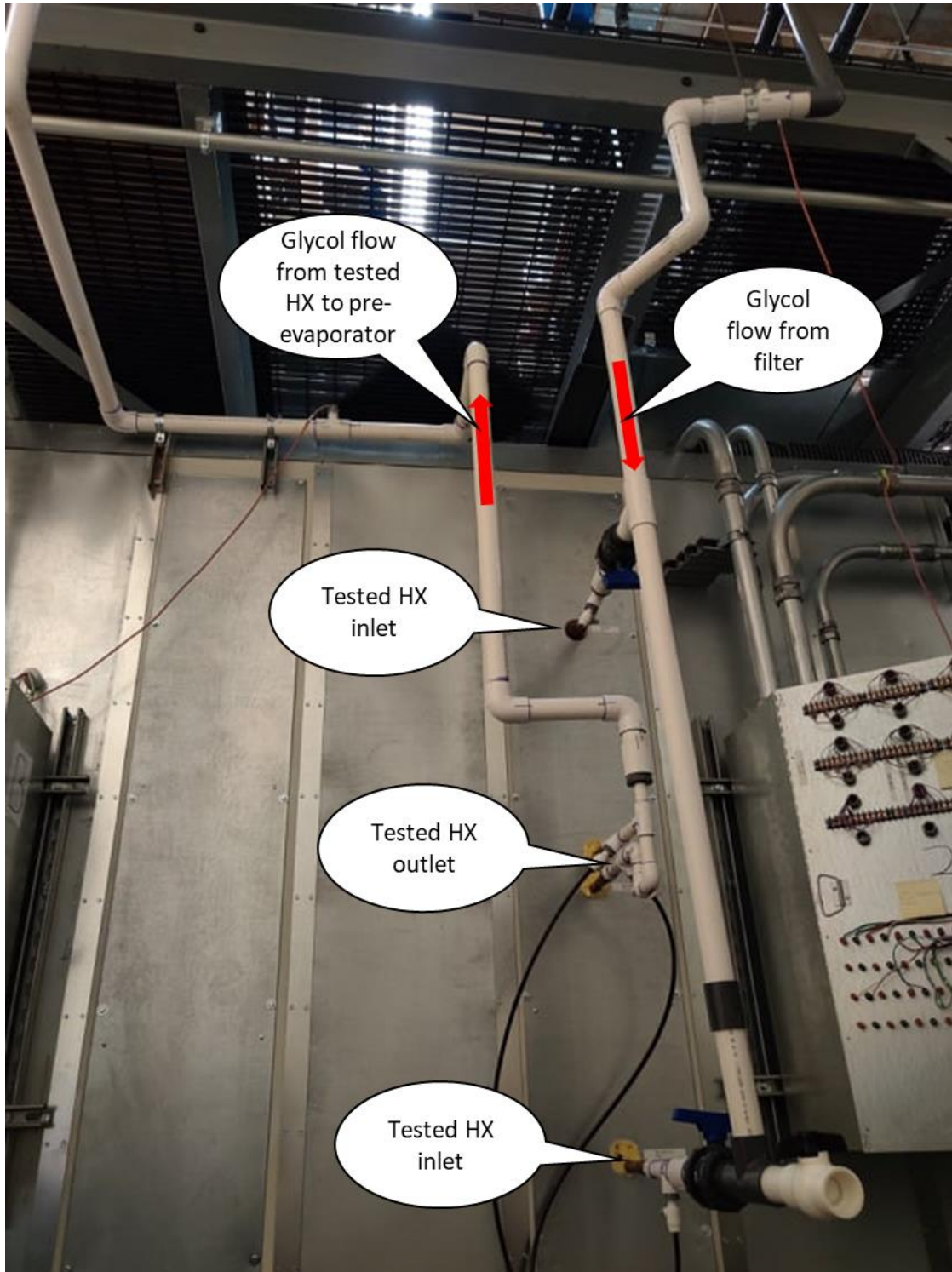
Glycol flow to tested HX through filter

Glycol flow from tested HX to pre-evaporator

D.6: Flow from the heater to the filter and return flow to the pre-evaporator.



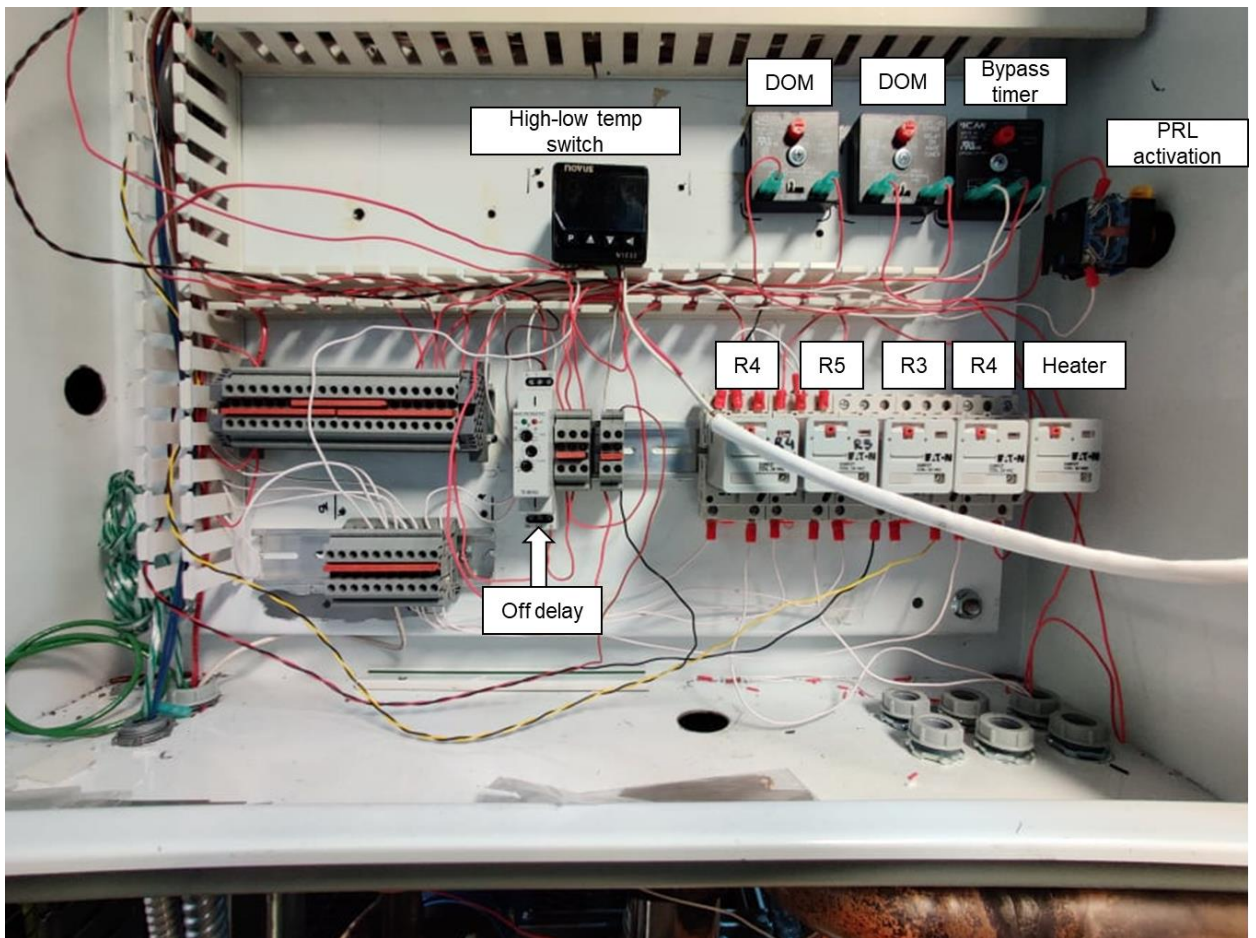
D.7: Flow to and from the filter.



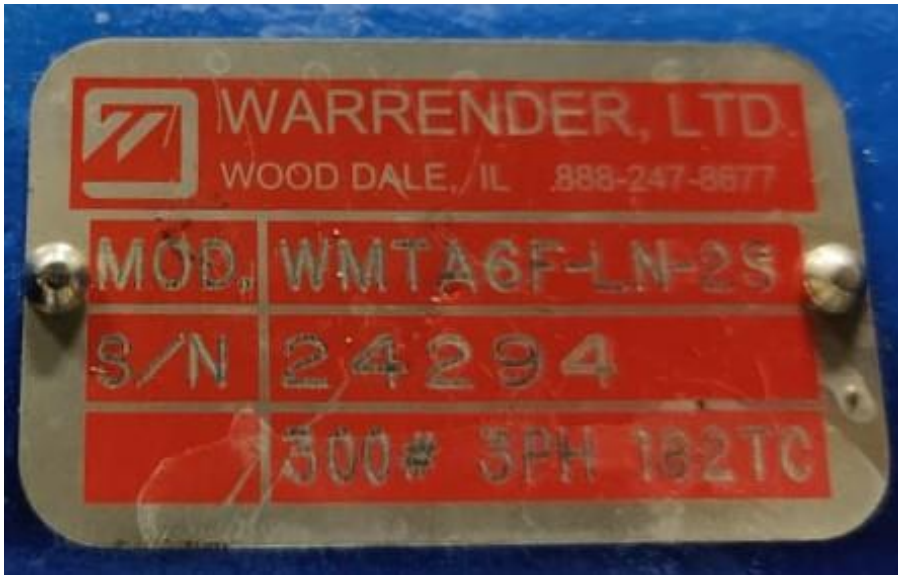
D.8: Flow to and from the tested HX.

APPENDIX E

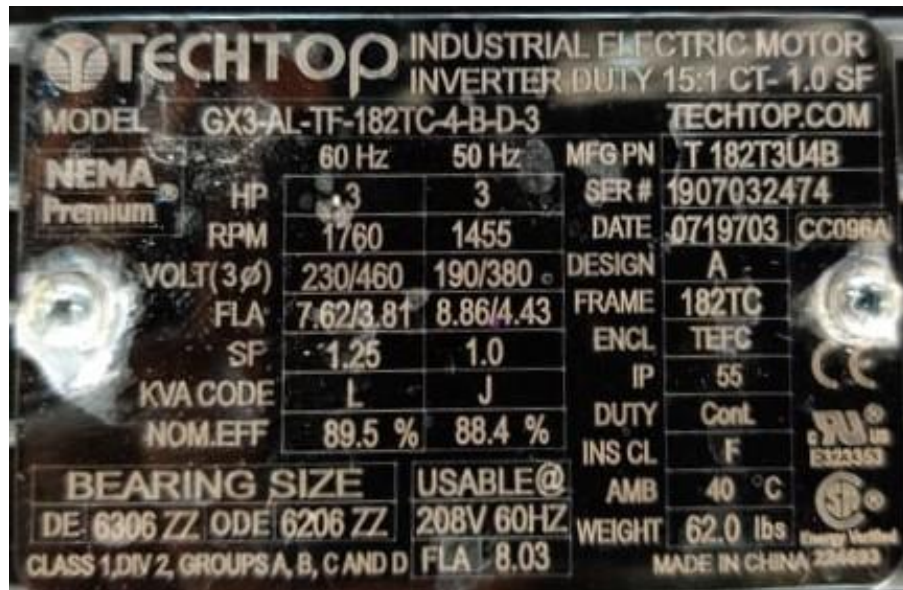
SAFETY CIRCUIT AND NAMEPLATES



E.1: Safety circuit.



E.2: Refrigerant pump's nameplate.



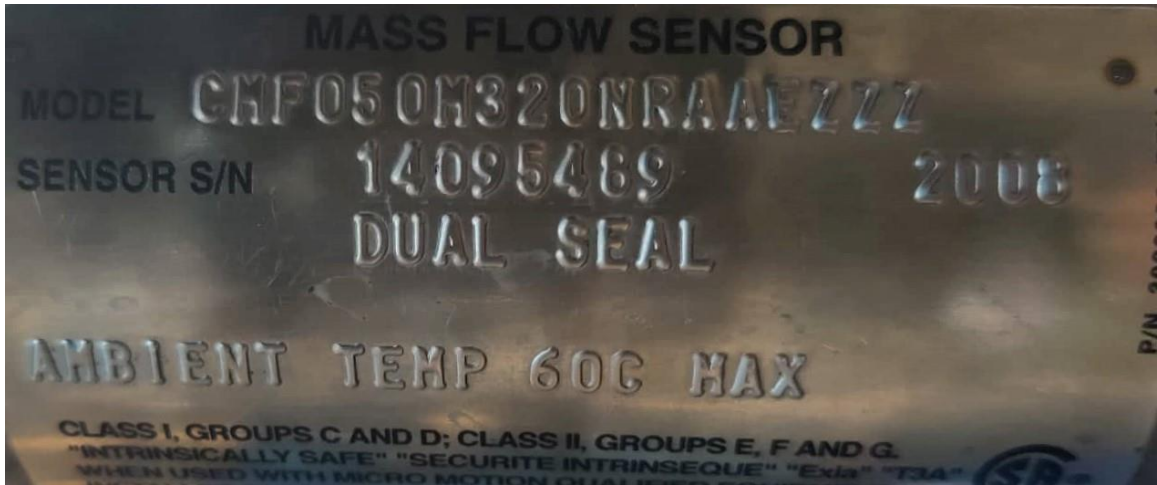
E.3: Refrigerant motor's nameplate.



E.4: Glycols pump nameplate.



E.5: Glycol motor nameplate.



E.6: Mass flow meter nameplate.



E.7: Mass flow transmitter nameplate.



CHROMALOX

Advanced Thermal Technologies

Sales (800)443-2640 www.chromalox.com Service (800)368-2493

PCN	181948	
P/N	156-30476-006	
CATALOG NO.	VTS-30476-E1	
VOLTS 480	CIRCUITS-PHASE	KW 40
MAX V = PLACE VOLTAGE LABEL HERE FROM WIRING DIAGRAM	PLACE CIRCUIT-PHASE LABEL HERE FROM WIRING DIAGRAM	MAX KW = PLACE KW LABEL HERE FROM WIRING DIAGRAM
DATE CODE	253PP	



C US

READ INSTRUCTIONS BEFORE USE

NAMEPLATE P/N 196-304776-003

E.8: Heater nameplate.



E.9: Pre-evaporator nameplate.



E.10: Cascade condenser nameplate.

VITA

A B M Imran Chowdhury

Candidate for the Degree of

Master of Science

Thesis: DESIGN AND CONSTRUCTION OF A PUMPED REFRIGERANT LOOP
FOR COMMERCIAL SCALE LOW-GWP REFRIGERANT HEAT
EXCHANGER TESTING

Major Field: Mechanical and Aerospace Engineering

Biographical:

Education:

Completed the requirements for the Master of Science in Mechanical and Aerospace Engineering at Oklahoma State University, Stillwater, Oklahoma in July, 2021.

Completed the requirements for the Bachelor of Science in Mechanical Engineering at Bangladesh University of Engineering and Technology, Dhaka, Bangladesh in 2017.

Professional Memberships:

ASHRAE